No. 4/2016

HIDRAULICA

HYDRAULICS-PNEUMATICS-TRIBOLOGY-ECOLOGY-SENSORICS-MECHATRONICS

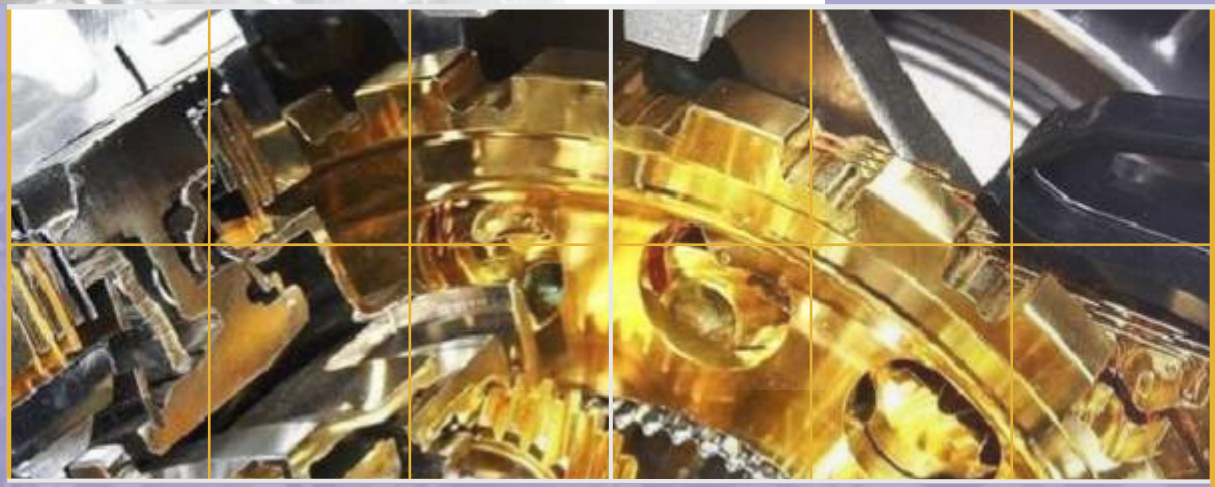

http://hidraulica.fluidas.ro

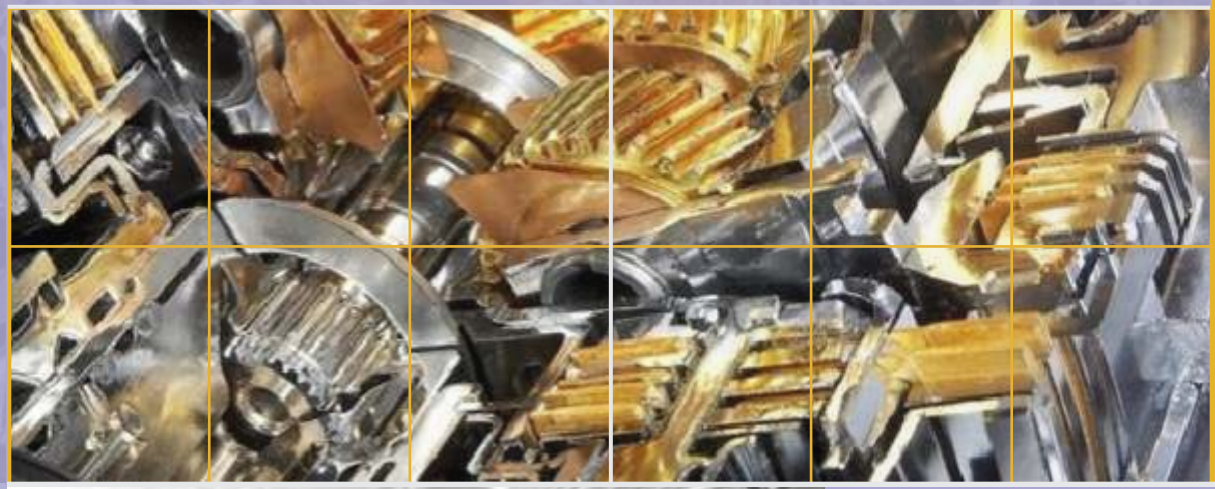

ISSN 1453 - 7303
ISSN-L 1453 - 7303

CONTENTS

Published by:
Hydraulics and Pneumatics Research Institute, Bucharest-Romania
Address: 14 Cuţitul de Argint, district 4, Bucharest, 040558, Romania
Phone: +40 21 336 39 91; Fax:+40 21 337 30 40; e-Mail: ihp@fluidas.ro; Web: www.ihp.ro
with support from:
National Professional Association of Hydraulics and Pneumatics in Romania - FLUIDAS
e-Mail: fluidas@fluidas.ro; Web: www.fluidas.ro

HIDRAULICA Magazine is indexed by international databases:

ISSN 1453 – 7303; ISSN – L 1453 – 7303

EDITORIAL

Repetitio in integrum

Ph.D.Eng. Petrin DRUMEA
DIRECTOR OF PUBLICATION

Lately there is much excitement on plagiarism in all areas involving an activity that should produce something new. I will not deal with troubles in the fields of writing books and elaborating PhD theses, but I will stop over the issue of duplicative ideas in scientific research papers, issue that we, the editorial team of HIDRAULICA magazine, had to face, too.

There are two directions that I think are incorrect and that the magazine does not accept when we detect them in some papers submitted for publication.

The first unacceptable direction is that in which an author takes the basic idea from an article written by a specialist and puts it down on paper in different words, bringing nothing new from the scientific point of view, nor does he/she states that he/she is presenting an important idea which belongs to someone else.

The second unacceptable direction is that in which an author reiterates the idea of an earlier own paper, several times in multiple materials, without bringing anything new, not even in the interpretation of results. This reiteration which I called "Repetitio in integrum", many times difficult to detect, causes great harm to scientific research activity. It is hard to understand how a person can produce 25-30 papers within a year, most of which addressing about the same topic, without repeating and bring some novelty, at least as interpretation of certain phenomena.
Equally hard to understand is how someone who does not have access to a laboratory or does not enter a laboratory for years can write dozens of times about an applied research topic, bringing new stuff.

Of course taking ideas from other authors is possible, but only in the event that updates are made, either experimental or theoretical.

We found ourselves sometimes in a situation where our reviewers agreed to the publication of certain materials which they detected as having no character of novelty simply because they came from regions where these topics were addressed for the first time, and thus allowed us to enlarge the spreading area of our magazine. Even in such cases the stringency that we have required was for the material to be presented in a new form and similar materials be enlisted as paper references.

Experimental and Numerical Investigation of the Flow Past a Thin Circular Airfoil with Mid-Chord Slot

Assist. Prof. PhD Eng. **Andrei DRAGOMIRESCU**[1], Prof. PhD Eng. **Carmen-Anca SAFTA**[2], Assoc. Prof. PhD Eng. **Marius STOIA-DJESKA**[3]

[1] University Politehnica of Bucharest, Department of Hydraulics, Hydraulic Machinery and Environmental Engineering, andrei.dragomirescu@upb.ro

[2] University Politehnica of Bucharest, Department of Hydraulics, Hydraulic Machinery and Environmental Engineering, carmen-anca.safta@upb.ro

[3] University Politehnica of Bucharest, Department "Elie Carafoli" of Aerospace Science, marius.stoia@gmail.com

Abstract: *Results of an experimental and numerical study of the flow past thin, circular arc cambered airfoils with a narrow slot at mid-chord are presented in this paper. The purpose of the study was to investigate the aerodynamic characteristics of this type of airfoils from the point of view of using them in the aerodynamic structure of a small wind turbine. The experimental study was carried out in a closed (return-flow) wind tunnel. Drag forces were measured at different Reynolds numbers for airfoils having slots of different widths, placed at a constant angle of attack of 90°. The numerical study was extended to similar airfoils intended to be used for the guide vanes of a small cross-flow wind turbine. The results of the study show that the usage of mid-chord narrow slots could significantly reduce the aerodynamic loads on the guide vanes of the wind turbine.*

Keywords: *slotted airfoil, aerodynamic loads, wind turbine, guide vanes, CFD*

1. Introduction

The development of the boundary layer was intensively studied for decades due to the fact that the viscous shear stresses that appear inside it and its separation are crucial for determining lift and drag of wings. Different techniques to control the boundary layer were developed to increase the lift or to decrease the drag [1]. Boundary layer control is applied for phenomena of transition from a laminar boundary layer to a turbulent one or in the case of boundary-layer separation [2]. Both in case of transition and of separation suction can be applied as a method of boundary layer control. A very simple, yet very effective suction control is by using properly placed slots that link the pressure side of a wing to its suction side. The pressure difference drives the fluid through such a slot towards the suction surface. The additional fluid flow injected in this manner at a specific position on the suction surface can delay or even cancel the boundary layer separation, thus improving the lift of the airfoil. Such slots are usually placed either close to the leading edge or close to the trailing edge of the wing.
In this study it was aimed actually not at increasing but at decreasing the lift of an airfoil in order to decrease the loads on the guide vanes of a cross-flow wind turbine having a runner similar to those studied by Dragomirescu [3] and Dragomirescu et al. [4]. Preliminary experimental tests showed that by placing the slot at mid-chord could reduce the aerodynamic loads on the airfoil. A numerical study was subsequently carried out in order to get a better insight into the flow around the airfoil and to extend the experimental results.
In the following, the experimental and numerical studies are presented. Obtained results are discussed and, based on them, conclusions are drawn.

2. Experimental Setup

The experimental study was performed in a subsonic wind tunnel with return-flow and with an open test section (Fig. 1). The wind tunnel is powered by a fan driven by a variable DC motor, so that the maximum air velocity provided in the test section (without any blockage) is of about 30 m/s. Upstream of the test section, the flow is directed into a setting chamber containing screens for

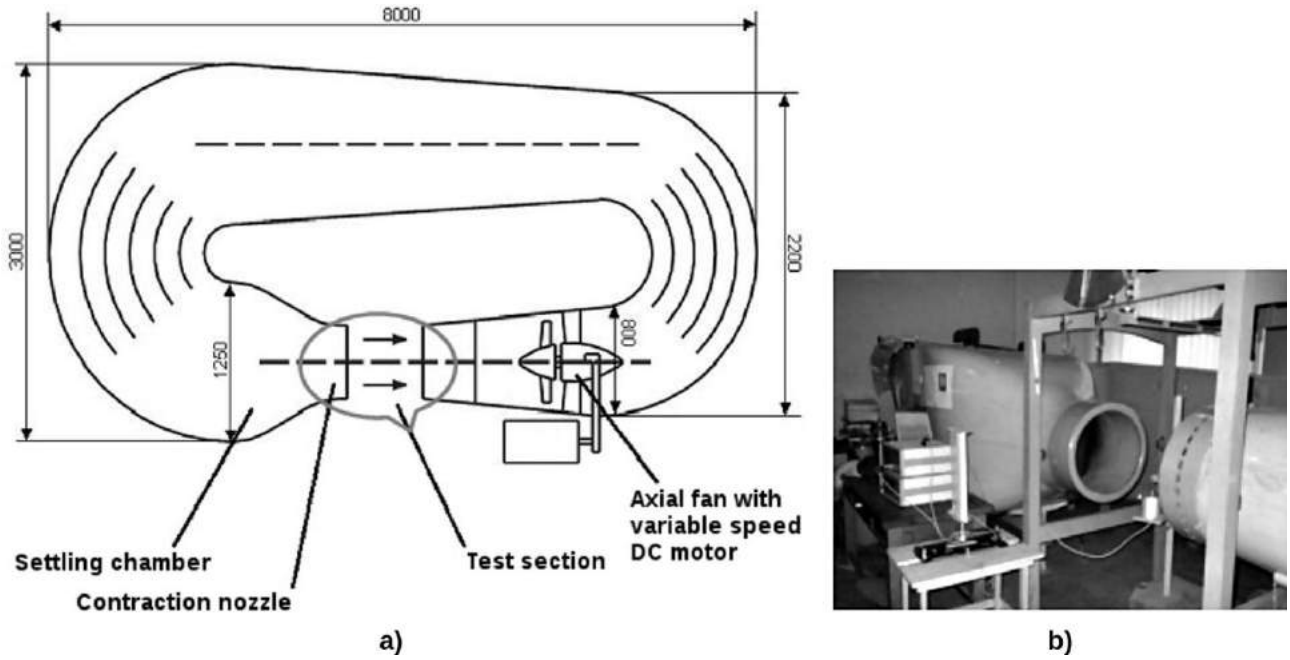

Fig. 1. Experimental installation: a) sketch of the subsonic wind tunnel in "Nicolae Tipei" Laboratory at Department "Elie Carafoli" of Aerospace Science and b) photo of the test section.

reducing turbulence and a contraction nozzle downstream to further reduce turbulence and to accelerate the flow to test velocity. The flow in the open test section is nearly uniform with low turbulence levels.

In this wind tunnel, different arc-shaped thin airfoils with slots at mid-chord were tested. The geometry of the airfoils is presented in Fig. 2. Chord length and breadth of airfoils were kept constant at 45 mm and 60 mm respectively. The slots had a constant length of 50 mm, while their width, *b*, was changed from 0 mm (i.e. no slot) to 6 mm, 8 mm, 10 mm, and 12 mm. The airfoil without slot (with *b* = 0 mm) will be further referenced as *normal airfoil*.

The methodology of testing consisted in measuring drag forces on the airfoil by using a three-component force sensor placed beneath the test section. As it can be seen in Fig. 3, the experimental airfoil (1) is fixed through the support link (3). The force sensor (2) is of type HM 170.40 GUNT [5]. The sensor is connected to an electronic amplifier with digital displays for lift, drag, and aerodynamic pitching moment. A graduated scale allows setting the airfoil at the desired angle of attack.

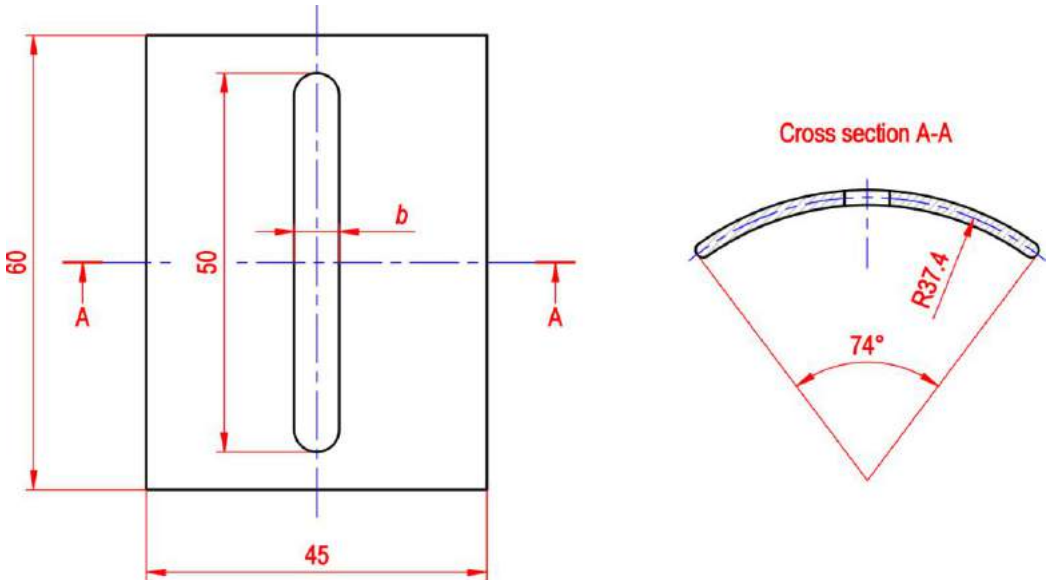

Fig. 2. Sketch of the experimentally investigated airfoil with mid-chord narrow slot.

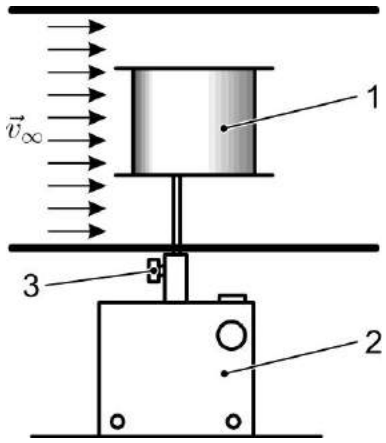

Fig. 3. Assembly of tested airfoil on force sensor.

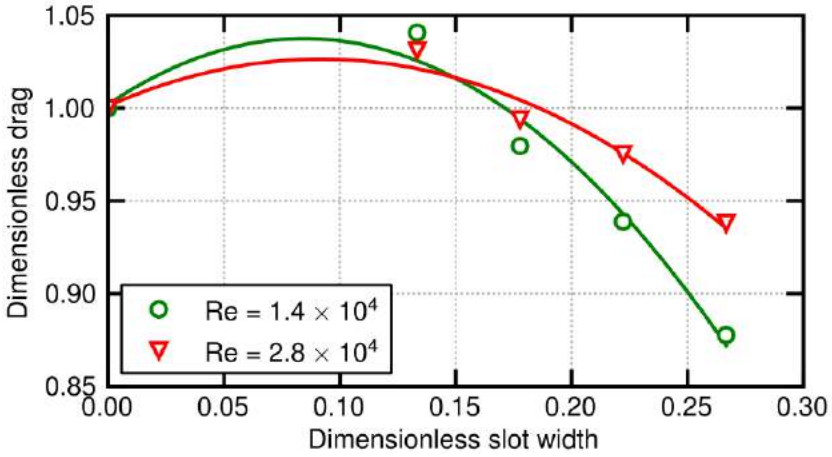

Fig. 4. Variation of dimensionless drag depending on dimensionless slot width.

The experiments aimed at finding the variation of drag force depending on slot width at different air velocities, i.e. at different Reynolds numbers. The angle of attack was kept constant, $\alpha = 90^0$. Measurements were carried out at air velocities v_∞ of 5 m/s and 10 m/s, for which the Reynolds numbers are of about 1.4×10^4 and 2.8×10^4 respectively. The Reynolds numbers were calculated based on the chord length of 45 mm and on the air kinematic viscosity that at test conditions has the value of 1.581×10^{-5} m^2/s.
The experimental results are summarized in Fig. 4 in form of variations of dimensionless drag force depending on dimensionless slot width. At each Reynolds number the reference force is the drag measured on the normal airfoil. The reference length is the chord length. The results obtained suggest that for very narrow slots the drag increases slightly. However, as the dimensionless slot width increases above 0.15, the drag starts to decrease. This decrease becomes less steep as the Reynolds number increases.

3. Numerical Simulations

In order to get an insight into the flow past the circular arc airfoil, numerical simulations were performed for different Reynolds numbers and angles of attack both for the slotted airfoil and for the normal airfoil. The airfoils studies were designed to be used in a cascade of guide vanes for a cross-flow wind turbine having the runner diameter of 1.2 m. At entry and exit of the cascade the blade angles are of 90° and 16° respectively. The outer and inner diameters of the cascade are of 1.79 m and 1.38 m respectively. Fig. 5 presents the resulting slotted airfoil and its dimensions. The chord length is of 235 mm. The slot is placed at mid-chord and has a width of 3 mm. Its axis is

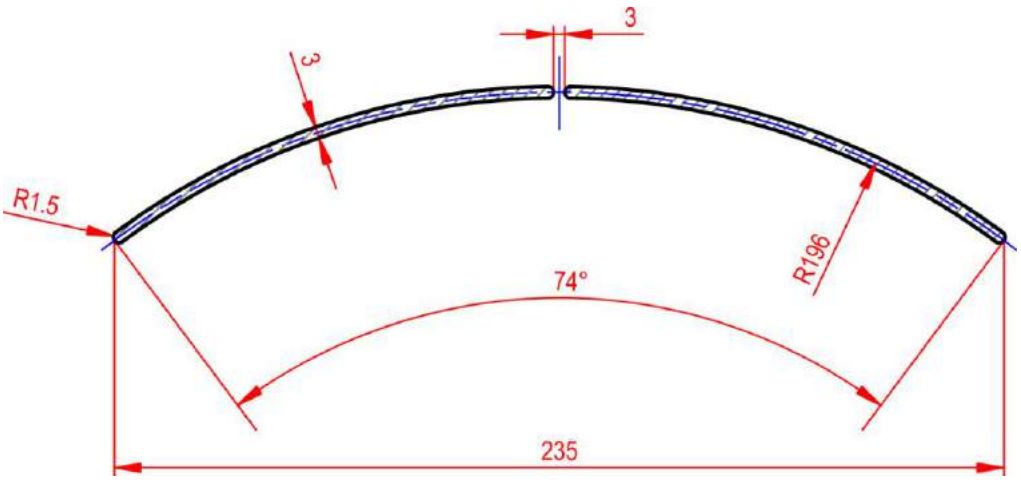

Fig. 5. Sketch of the airfoil with narrow slot, studied by numerical simulations.

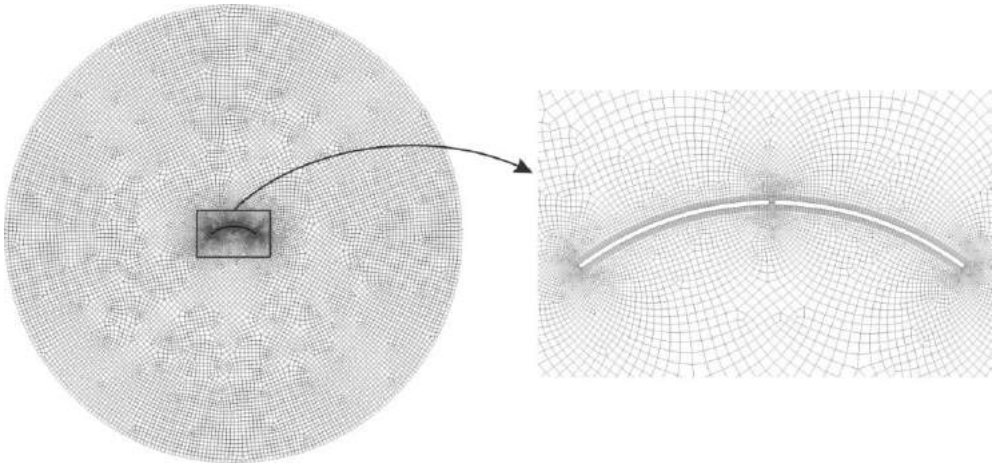

Fig. 6. Computational domain and mesh.

perpendicular to camber line. The normal airfoil has similar geometry and dimensions, except that it has no slot.

For both airfoils the numerical simulations were performed on the two-dimensional computational domain presented in Fig. 6. The domain is circular and has a diameter of 2.4 m, which is roughly ten times higher than the chord length. The airfoils were placed in the middle of this domain. The domain was meshed using quadrilateral cells that form an unstructured grid. Boundary layer-type cells were used close to the airfoils. The resulting grid is also presented in Fig. 6.

The working fluid is air at the reference pressure $p_0 = 10^5$ Pa and the reference temperature $T_0 = 293.15$ K. The air was considered an ideal gas having a constant dynamic viscosity of 1.824×10^{-5} Pa s.

As it will be detailed later, the Reynolds numbers of the flow past the airfoils are relatively large. Additionally, it was desired to catch the effect of the vortices that detach behind the airfoils, in case that these vortices appear. Therefore, the air flow was treated as unsteady and turbulent, being described by the continuity and the Reynolds averaged Navier-Stokes (RANS) equations. The closure equations for the turbulent stresses were provided by the Reynolds Stress Model (RSM) with standard wall functions. This turbulence model was chosen because it is considered to be one of the most elaborate turbulence models, having a great potential to give accurate predictions for complex flows [6].

Numerical simulations were performed for two velocities v_∞ of the free air stream and different angles of attack α of the airfoils. In order to easily change the angle of attack without changing the geometry and re-meshing the computational domain, the outer boundary was treated as a pressure far-field boundary. Consequently, gauge pressure, Mach number, flow direction and turbulent quantities were required as boundary conditions. The gauge pressure was set at 0 Pa. The velocities of the free air stream and the corresponding Mach numbers imposed at the boundary are summarized in Tab. 1. The table also presents the Reynolds numbers calculated based on airfoil chord length. As turbulent quantities, the turbulent kinetic energy, k, and the turbulent dissipation rate, ε, in the atmospheric boundary layer were specified. Their values are also presented in Tab. 1. The values of k and ε were calculated and corrected according to the formulas and remarks presented by Richards and Norris [7]. The aerodynamic roughness required to calculate k and ε was estimated at 1 based on the study of Grimmond et al. [8]. On the airfoils the usual no-slip condition was imposed.

The equations describing the flow, together with their boundary conditions, were integrated in space and time with the finite volume method implemented in the commercial code Ansys Fluent.

TABLE 1: Simulation parameters

v_∞ (m/s)	Ma	Re	k (m^2/s^2)	ε (m^2/s^3)
3	8.7×10^{-3}	4.60×10^{4}	824	72
10	2.9×10^{-2}	1.53×10^{5}	9158	1337

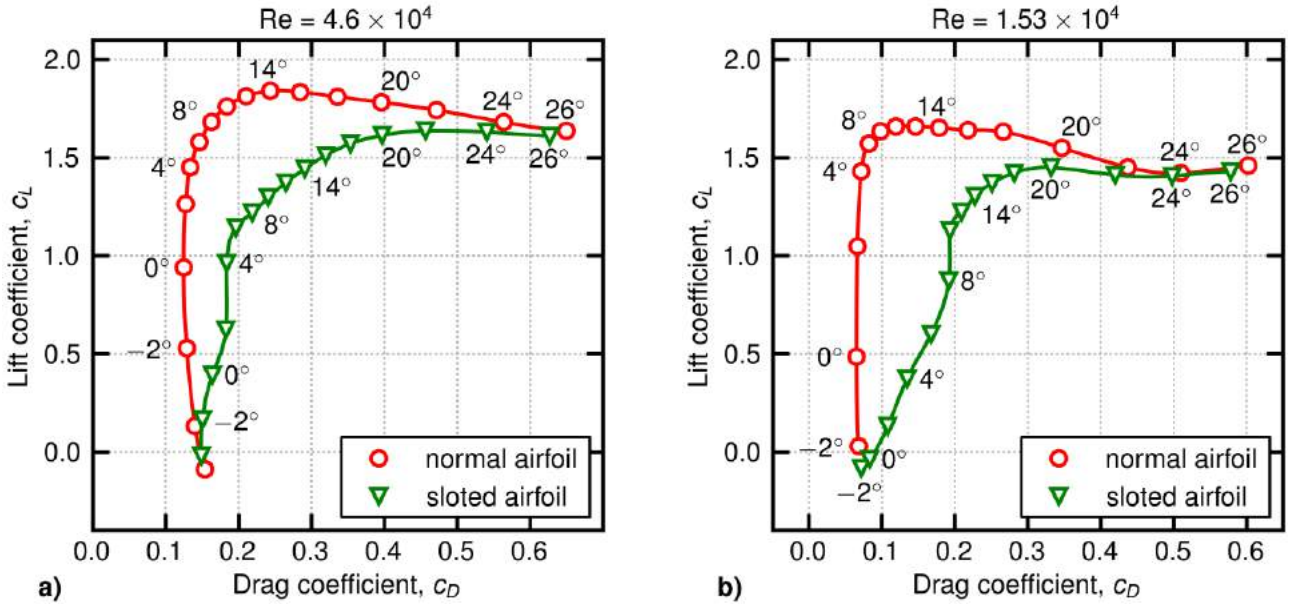

Fig. 7. Comparisons of polar diagrams obtained numerically for both normal and slotted airfoil at a) Re = 4.6×10^4 and b) Re = 1.53×10^5.

Since only quadrilateral cells were used to mesh the computational domain, the QUICK scheme was chosen to discretize the flow equations in space. The discretization in time was accomplished with the first order implicit unsteady formulation.

For each airfoil, the first simulation was performed for the angle of attack of 0°. Subsequent simulations were carried out for angles of attack up to 26° and down to -4°. At each new simulation, the angle of attack was changed by 2° with respect to the previous simulation. The initial guess of each new simulation was the last converged solution of the previous simulation. Each simulation was advanced in time with a time step of 0.002 s until a stabilization of the lift and drag coefficients around an average value was observed for at least 30 s of the simulation time. At each time step, the convergence criterion was the drop in all scaled residuals below 10^{-4}.

The numerical results are summarized in Fig. 7 in form of polar diagrams of the normal and slotted airfoils at the two Reynolds numbers considered. It can be seen that, at low angles of attack, the slotted airfoil has a significantly lower lift than the normal airfoil. In the same time, the drag of the slotted airfoil increases. However, the drag remains about one order of magnitude lower than the lift. Therefore, in terms of absolute values, the decrease in lift is more important than the increase in drag. This behavior can be explained based on the pressure fields and flow configurations around the airfoils. Fig. 8 presents pressure fields and streamlines obtained for the angle of attack

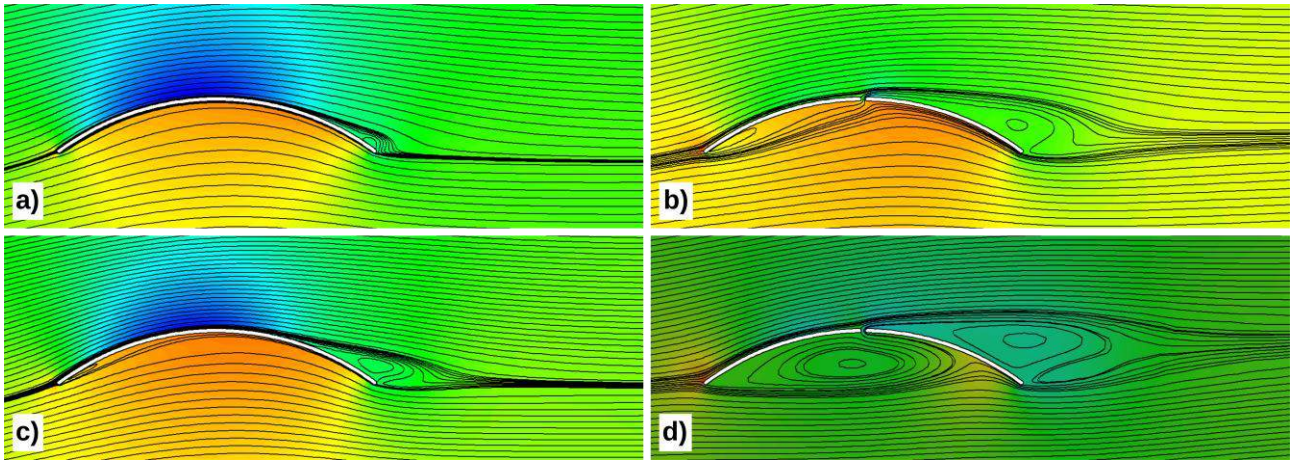

Fig. 8. Streamlines superimposed on pressure fields at α = 4°: a) normal airfoil, Re = 4.6×10^4, b) slotted airfoil, Re = 4.6×10^4, c) normal airfoil, Re = 1.53×10^5, d) slotted airfoil, Re = 1.53×10^5.

$\alpha = 4°$. It can be seen that, for both Reynolds numbers considered, the differences in pressure between pressure side and suction side of the slotted airfoil are clearly lower than in case of the normal airfoil. Hence, the lift of the slotted airfoil is lower. Additionally, the results suggest that the slot placed at mid-chord, with its axis perpendicular to camber line, favors the boundary layer separation, causing larger vortices both behind the slotted airfoil and below it, which could explain the increase in drag.
It is expected that the results presented in Fig. 7 and 8 will change to some extent when the airfoils will be arranged in a cascade. To assess the change, further research is required.

4. Conclusions

Experiments and numerical simulations show that circular arc-shaped airfoils with mid-chord slot have significantly lower lift and only slightly higher drag when compared with the un-slotted airfoils. The drag can be easily controlled by changing the slot width. Such airfoils can be used in applications where the decrease of the loads on wings or blades is desired in order to lower structural loads. A practical application is a cascade of guide vanes used to direct the air flow at appropriate absolute velocity angles towards the runner of a cross-flow wind turbine. This study can be extended in order to assess the influence of the cascade on the behavior of the slotted airfoils.

References

[1] H. Schlichting, K. Gersten, "Boundary Layer Theory", Springer, Berlin, 2000;
[2] A.L. Braslow, "A history of suction-type laminar-flow control with emphasis on flight research", Monographs in Aerospace History, No. 13, NASA History Division, Washington, 1999;
[3] A. Dragomirescu, "Performance assessment of a small wind turbine with crossflow runner by numerical simulations", Renewable Energy, 36, 2011, pp. 957–965;
[4] A. Dragomirescu, C.A. Safta and V. Serban, "A new type of crossflow runner for a small wind turbine", The 14th World Renewable Energy Congress – WREC2015, Bucharest, 2015;
[5] GUNT, Electronic 3-Component Measurement System, Technical book HM 170.40, 2002;
[6] Ansys Inc., "Ansys Fluent Theory Guide, Release 14.0", Canonsburg, 2011;
[7] P.J. Richards, S.E. Norris, "Appropriate boundary conditions for computational wind engineering models revisited", Journal of Wind Engineering and Industrial Aerodynamics, 99, 2011, pp. 257–266;
[8] C.S.B. Grimmond, T.S. King, M. Roth and T.R. Oke, "Aerodynamic roughness of urban areas derived from wind observations", Boundary-Layer Meteorology, 89, 1998, pp. 1–24.

Study of Surface Roughness for Steel Parts Cut with Abrasive Water Jets

PhD. Eng **Sandor RAVAI-NAGY**[1], PhD. Eng. **Nicolae MEDAN**[2]

[1]Technical University of Cluj-Napoca, North University Center Baia Mare,
Ravai.Nagy.Sandor@cunbm.utcluj.ro

[2]Nicolae.Medan@cunbm.utcluj.ro

Abstract: *Today, abrasive water jet technology is used into a full scale production process such us contour cutting, drilling, milling, turning, threading. The purpose of this paper is to determine the surface roughness for two type of steel (S235JR and S355JO) cutting with abrasive water jet (AWJ) cutting machine - Bystronic ByJet Pro L, varying the traverse speed and abrasive flow rate parameters.*

Keywords: *Abrasive water jet, surface roughness, contour cutting*

1. Introduction

First water jet cutting machines was used in the1970s for cutting wood and plastics material [3] and first abrasive water jet cutting machine was commercialized in 1980s, when was considering as a pioneer in the area of unconventional processing technologies [6]. Today, abrasive water jet technology is used into a full scale production process such us contour cutting, drilling, milling, turning, threading, cleaning. Abrasive water jet machines is used in the processing of different type of materials such as titanium, steel, brass, aluminium, stone, glass and composites [2].
In abrasive water jet process, the work piece material is removed by the action of a high-velocity jet of water mixed with abrasive particles based on the principle of erosion of the material upon which the water jet hits [5]. Abrasive water jet machining has few advantages such as high machining versatility, small cutting forces, high flexibility and no thermal distortion [1].
An abrasive water jet is a jet of water that contains some abrasive material like: aluminium oxide, silicon carbide, sodium bicarbonate, dolomite and/or glass beads with varying grain sizes.
The main parts of any abrasive water jet cutting machine are: the hydraulic pump, which provides pressured water, an amplifier, in which the pressure of water is increased and the cutting head, where the water is mixed with abrasive from the system [4].

2. Experiment setup

2.1 The abrasive water jet cutting machine

The experiments were conducted using an abrasive water jet (AWJ) cutting machine - Bystronic ByJet Pro L, presented in Figure 1.

Fig. 1. Abrasive water jet cutting machine used: Bystronic ByJet Pro L

This abrasive water jet (AWJ) cutting machine is a computer controlled machine (CNC).

2.2 Type of material and geometry for cutting parts

Were used for cutting contour two types of steel for general use: S235JR and S355JO.
The design of obtain pieces is presented in figure 2. It was realized two pieces, one for each type of material. The thickness of the pieces is 10 mm.

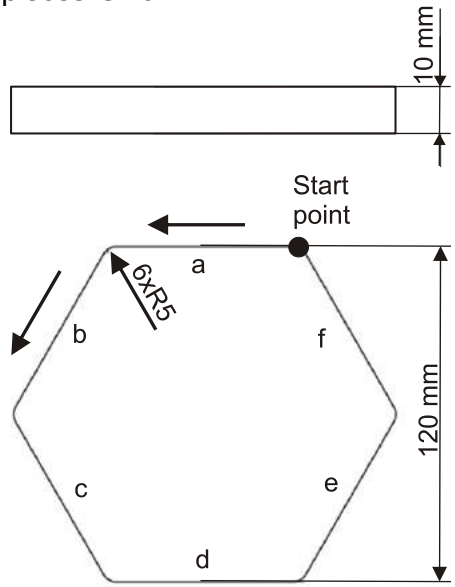

Fig. 2. Design of cutting pieces and order of cutting for established process parameters

2.2 Setting up the process parameters

To cut pieces were used the values of process parameters presented in table 1.

TABLE 1: Process parameters.

Processing regime	Position on piece	Water jet pressure [bar]	Traverse speed [mm/min]	Abrasive flow rate [g/min]
1	a	3600	213	342
2	b		112	342
3	c		260	342
4	d		254	600
5	e		132	600
6	f		312	600

For each face of the hexagon corresponding a certain set of the parameters (corresponding with the values define in table 1). For each fillet zone it was changed the processing regime.
The abrasive material used was GMA Garnet 80 Mesh (300 - 150µm). This type of granulation is recommended to standard industrial applications. Interior diameter of sapphire nozzle was 0.28 mm.

2.3 Achievement the measurements

After cutting the pieces, was measurement the roughness R_a for each face of the pieces.
For each side of the hexagonal pieces was made measurements of surface roughness from two directions, one perpendicular to the direction of displacement of the cutting water jet and one parallel to the direction of displacement of the cutting water jet. For each direction were established three lines of measurements evenly distributed along the length and width respectively cutting surfaces (figure 3).
The device used to measure the surface roughness was Time Group Inc. TR200.

To get the value of surface roughness was measured that roughness on a length of four mm for each area measurement (according to the methodology of measurement established in measurement scheme shown in figure 3). In this way they were obtained six values of surface roughness R_a for each side of machined pieces.

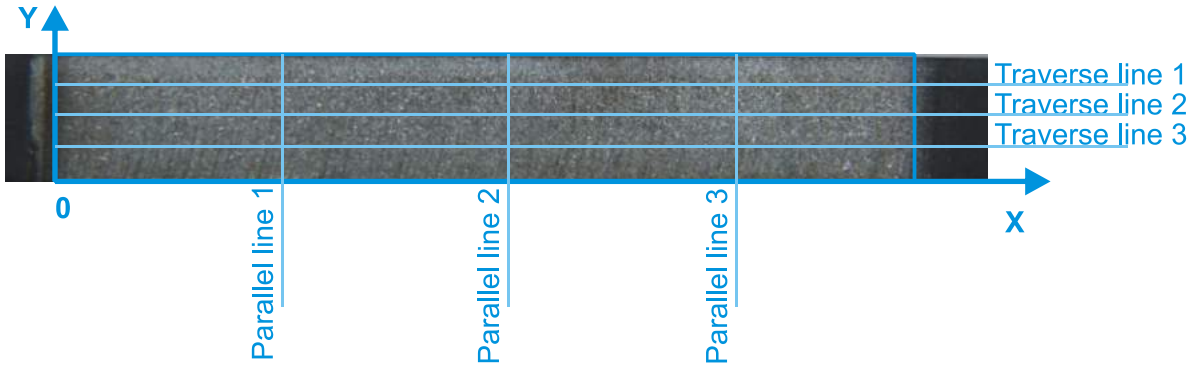

Fig. 3. The scheme of the measurements for each side of the pieces

3. Results

In the following are presented the values obtained for surface roughness corresponding to the two types of materials used and for the six process parameters used (table 1).

3.1 Values of surfaces roughness for S235JR steel piece

In the table 2 are presented the values of roughness surfaces for direction perpendicular to the cutting direction.

TABLE 2: Results of surface roughness R_a perpendicular to the cutting direction for S235JR material.

Measured position on face	Processing regime					
	1	2	3	4	5	6
	Position on piece					
	a	b	c	d	e	f
	Surface roughness Ra [µm]					
Traverse line 1	4.026	3.677	4.175	3.155	2.624	2.768
Traverse line 2	4.371	3.814	6.224	3.682	2.736	4.984
Traverse line 3	6.154	3.496	9.973	6.634	2.810	5.165

In the table 3 are presented the values of surfaces roughness for direction parallel to the cutting direction.

TABLE 3: Results of surface roughness R_a parallel to the cutting direction for S235JR material.

Measured position on face	Processing regime					
	1	2	3	4	5	6
	Position on piece					
	a	b	c	d	e	f
	Surface roughness Ra [µm]					
Parallel line 1	3.234	2.732	3.587	2.957	2.496	3.252
Paralle line 2	2.972	2.380	4.051	3.144	2.423	2.695
Paralle line 3	2.187	2.595	3.177	3.071	3.106	3.214

On the basis of values obtained from tables 2 and 3 of the surfaces roughness value achieved by the graphs of the two directions for S235JR material, graphs shown in figures 4 and 5.

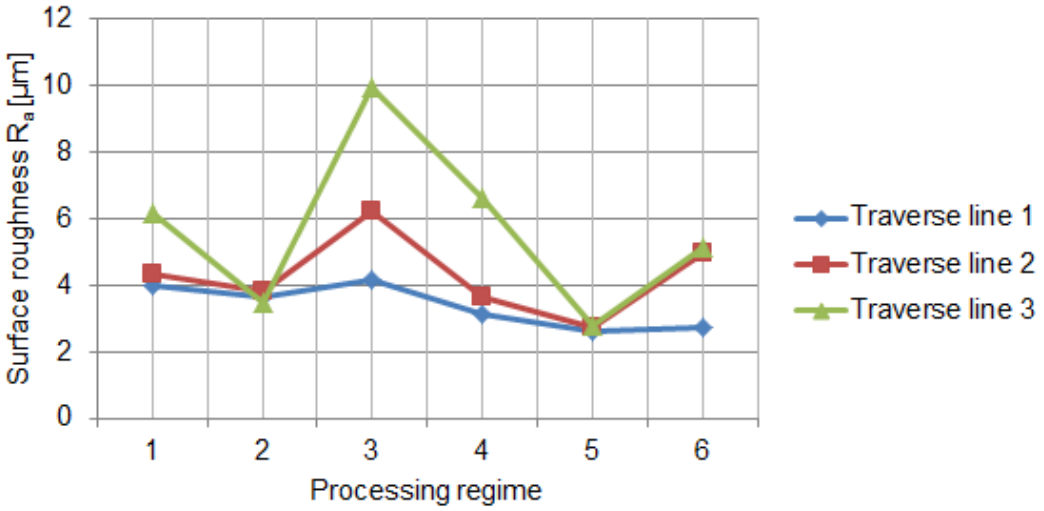

Fig. 4. Surfaces roughness Ra [µm] for perpendicular direction for S235JR steel

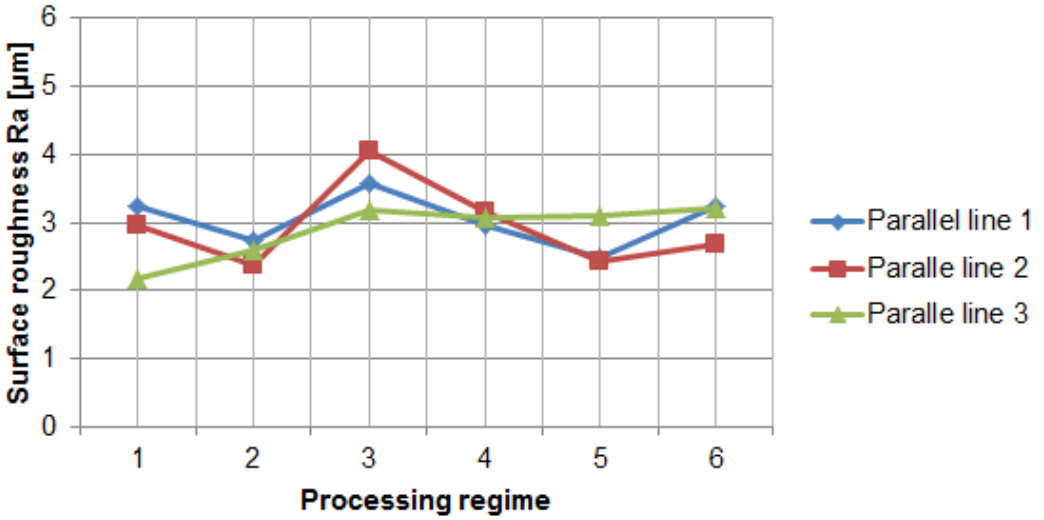

Fig. 5. Surfaces roughness Ra [µm] for parallel direction for S235JR steel

3.2 Values of roughness surfaces for S355JO steel piece

In the table 4 are presented the values of roughness surfaces for direction perpendicular to the cutting directions.

TABLE 4: Results of surface roughness R_a perpendicular to the cutting direction for S355JO material.

Measured position on face	Processing regime					
	1	2	3	4	5	6
	Position on piece					
	a	b	c	d	e	f
	Surface roughness Ra [µm]					
Traverse line 1	3.966	2.735	3.024	3.558	2.652	3.275
Traverse line 2	4.520	3.136	3.773	4.957	3.905	3.629
Traverse line 3	5.317	4.318	6.254	9.061	2.795	6.958

In the table 5 are presented the values of roughness surfaces for direction parallel to the cutting directions.

TABLE 5: Results of surface roughness R_a parallel to the cutting direction for S355JO material.

Measured position on face	Processing regime					
	1	2	3	4	5	6
	Position on piece					
	a	b	c	d	e	f
	Surface roughness Ra [µm]					
Parallel line 1	3.086	1.819	1.274	3.015	2.052	3.111
Parallel line 2	2.887	2.909	1.638	2.655	2.224	3.172
Parallel line 3	2.407	2.368	1.573	3.195	2.178	3.147

On the basis of values obtained from Tables 4 and 5 of the surfaces roughness value achieved by the graphs of the two directions for S355JO material, graphs shown in Figures 6 and 7.

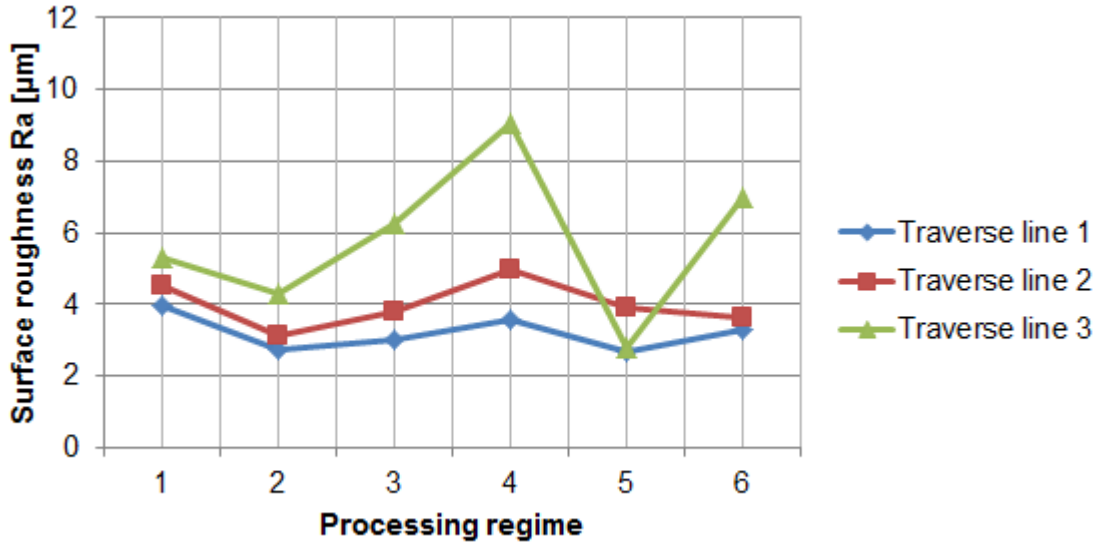

Fig. 6. Surfaces roughness R_a [µm] for perpendicular direction for S355JO steel

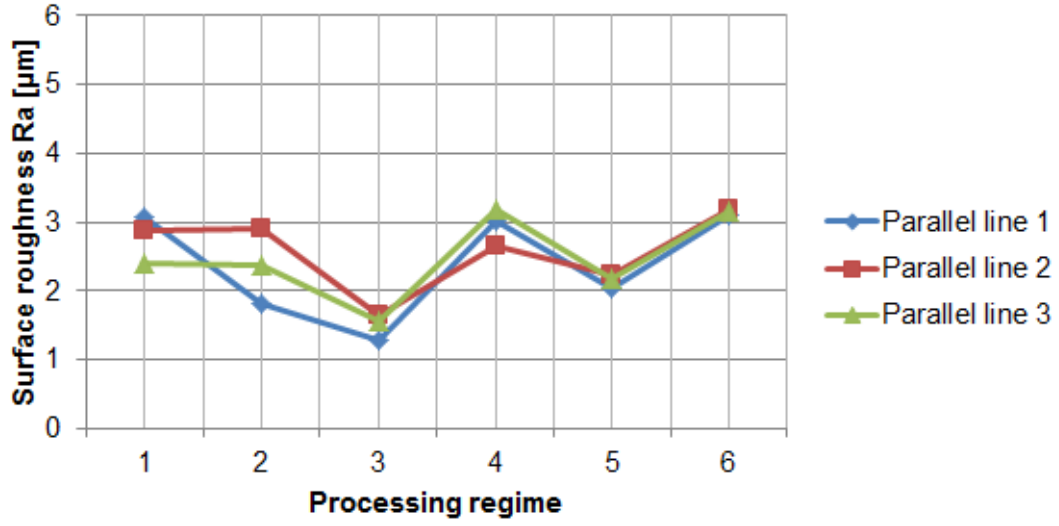

Fig. 7. Surfaces roughness R_a [µm] for parallel direction for S355JO steel

3. Conclusions

In this work was measured surface roughness R_a obtained after cutting contour for two types of steel for general use: S235JR and S355JO. Contour cutting was performed using an abrasive water jet cutting machine Bystronic ByJet ProL. For each type of material was cut one piece that has six sides. For each side was used a different processing regime.
Process parameters that have been modified are traverse speed and abrasive flow rate. Water jet pressure was fixed at 3600 bar. The abrasive material used was Garnet 80 mesh (300-150 µm).
The values of surface roughness R_a depends by:

1) Type of steel used. For S355JO steel the values of surface roughness are lower than S235JR steel. This is because the chemical composition chemical composition of the two steels is different.

2) Values of process parameters. When the traverse speed is lower the values of surface roughness is lowers. When the abrasive flow rate is bigger the values of surface roughness is lowers. So, the values of surface roughness are directly proportional with the abrasive flow rate and inversely proportional with the traverse speed.

3) The place where the surface roughness is measured.

   a) The values of surface roughness are lower for traverse line 1 location and increase when the measurements are made for traverse line 2. The values are the biggest when the measurements are made for traverse line 3. This is because the energy of the abrasive water jet decreases with increasing the cutting depth.

   b) Considering the values of surface roughness for parallel lines measurements, the values are range between 1 µm to 4 µm. These values are not relevant considering the fact that measurements are made in the direction of cutting contour.

References

[1] U. Caydas, A. Hascalik, "A study on surface roughness in abrasive waterjet machining process using artificial neural networks and regression analysis method", 2008, "Journal of Materials Processing Technology", Volume 202, pp. 574–582;

[2] J. Kechagias, G. Petropoulos, N. Vaxevanidis, "Application of Taguchi design for quality characterization of abrasive water jet machining of TRIP sheet steels", 2012. "The International Journal of Advanced Manufacturing Technology", Volume 62, pp. 635–643;

[3] R. Kovacevic, M. Hashish, R. Mohan, M. Ramulu, T.J. Kim, E.S. Geskin, "State of the art of research and development in abrasive waterjet machining", 1997, "Transactions of ASME. Journal of Manufacturing Science and Engineering", Vol. 119, pp.765-785;

[4] I L. Marcu, C. Ciupan, S, "Alternating Flow Hydraulic Generator for Water Jet Cutting Systems", "Hidraulica" (No. 1/2016) Magazine of Hydraulics, Pneumatics, Tribology, Ecology, Sensorics, Mechatronics, ISSN 1453 – 7303, pp.61-66;

[5] K. Metin, K. Erdogan, E. Omer, "Prediction of surface roughness in abrasive waterjet machining of particle reinforced MMCs using genetic expression programming", 2011, "The International Journal of Advanced Manufacturing Technology", Volume 55, pp. 955–968;

[6] M.C. Selvan, N.M. Raju, H.K. Sachidananda,"Effects of process parameters on surface roughness in abrasive waterjet cutting of aluminum", 2012, "Frontiers of Mechanical Engineering" Volume7, Issue 4, pp. 439–444.

About Wind Turbine Power Estimation and Measurement

Prof. Em. PhD. Eng. **Mircea BĂRGLĂZAN**[1], Assoc. Prof. PhD. Eng. **Teodor MILOŞ**[2]

[1] Politehnica University of Timişoara, mbarglazan@yahoo.com

[2] teodor.milos@gmail.com

Abstract: *Power of wind turbine offers various values if there are calculated with different formulas. The reason consists from different models considered and the influence of various factors. The article tries to compare and conclude about the relevance of these factors and influences on the true values. Also there are given characteristic curves measured on a wind power plant designed from Politehnica University of Timisoara.*

Keywords: *Wind turbines, parameters and characteristic curves, analytical and numerical values for power, measurements data.*

1. Introduction

In the subtle play between the energy available in the atmospheric ocean and the harvesting possibilities of it by industrial applications and human using are a lot of enhancing and perturbing factors and parameters.
This situation makes that from the design power to the developed power of a realized wind power plant to occur differences. The sources of these discrepancies are in the wind characteristics and the wind aggregate peculiarities. The wind is an air flow with rapid change in value and direction in turbulent regime and with gusts. Wind's energy is harnessed by wind power plants in which the fluid mechanic energy is transformed in stereo-mechanic energy and then in electric energy through a chain of machines and conversion equipments.
In the following chapters there are given formulas and values for aerodynamic, stereo-mechanic and electric powers associated with different physical models and measurement. The efficiency of wind turbines is smaller than that of the electrical machines and convertors and for this reason it is important to investigate them.

2. Ciugud wind aggregate plant power

The wind power plant Ciugud (Alba County) was designed for a stereo-mechanical power of 5 kW. The wind turbine Ciugud is a horizontal axial rapid wind turbine (HAWT) type. The measured parameters of the wind aggregate operation through a SCADA system are given in [1]. The kinetic power of the wind, "P_1", and the maximum theoretical power of the wind turbines for different aerodynamic models, "P_2" and "P_3", and various diameters of the runners in function of air density, "ρ", swept area, "S", and mean wind velocity, "v", from [2], [3], [8] are given with the formulas:

$$P_1 = \frac{1}{2} \cdot \rho \cdot S \cdot v^3 \tag{1}$$

$$P_2 = \frac{16}{27} \cdot \rho \cdot S \cdot v^3 \tag{2}$$

$$P_3 = \frac{8}{27} \cdot \rho \cdot S \cdot v^3 \tag{3}$$

The results for air density ρ = 1.2 kg / m^3, wind mean velocity v_0 = 8.5 m/s, diameters D and number of blades z are given in Table 1.

TABLE 1

z	D	S	P_1	P_2	P_3	Observations
-	[m]	[m^2]	W	W	W	runner
5	5	19.63495409	7234.989708	8574.802617	4287,401308	Ciugud - A
3	7	38.4845	14180.57614	16806.60876	8403.304378	Ciugud - B

The maximum aerodynamic power, "P_4", from statistical data in function of the similitude coefficient, "K_P", from [2]:

$$P_4 = K_P \cdot D^2 \cdot v^3 \tag{4}$$

Numerical results are calculated in Table 2:

TABLE 2

D	K_P	P_4	Observations
[m]	-	[W]	-
5	0.15	2302.96875	Slow machine
	0.2	3070.625	Rapid machine
7	0.15	4513.81875	Slow machine
	0.2	6018.425	Rapid machine

The maximum power, "P_5", extracted from the wind turbine in function of the runner radius, "R", and power coefficient, "C_P", with the formula from [3] is:

$$P_5 = C_P \cdot \frac{\rho}{2} \cdot \pi \cdot R^2 \cdot v^3 \tag{5}$$

Power coefficients are given in [1] and [3] and the results are offered in Table 3.

TABLE 3

R	C_P	P_5	Observations about C_P
[m]	-	[W]	The source
2.5	0.45	3255.74536	[4] Fig. 5.14
	0.37699	2727.518769	[1] graphic, page 427
	0.3	2170.496912	[3] page115
	0.47	3400.445162	[3] page115
3.5	0.45	6381.260921	[4] Fig. 5.14
	0.37699	5345.936788	[3] page115
	0.3	4254.173947	[3] page 115
3.5	0.47	6664.872518	[3] page115
2.5	16/27 x0.47	2015.078611	[3] page 45
3.5	16/27x0.47	3949.554077	[3] page 45

Analytic aerodynamic power of the wind turbine runner neglecting the finite extension of the blades is:

$$P_6 = \frac{z \cdot \omega \cdot \rho}{2} \cdot \int_{r_o}^{R_o} \left\{ C_L\left[i(r)\right] \cdot v - C_D\left[i(r)\right] \cdot \omega \cdot r \right\} \cdot \sqrt{\omega^2 \cdot r^2 + v^2} \cdot b(r) \cdot r \, dr \qquad (6)$$

where:

$\omega = \frac{\pi \cdot n}{30}$ - angular velocity of the runner

b (r) - blade chord,

R_0 , r_0 , - maximum and minimum radius of the blades,

C_L , C_D , - lift and drag coefficients of the airfoils.

The rated speed of rotation for Ciugud wind turbine is:

$$n_0 = 120 \quad rev / \min$$

the blade chord in function of radius for Ciugud - A:

$$b(r) = 0.48333 - 0.1111 \cdot r \qquad (7)$$

and for Ciugud – B:

$$b(r) = 0.95 - 0.17 \cdot r \qquad (8)$$

The lift and drag coefficients of an airfoil depends from airfoil's geometry and a lot of other parameters. Using for the blade airfoils the same family namely NACA 4415 (d/l = 15 %) in tip (outside) zone, NACA 4418 (d/l = 18 %) in middle zone and NACA 4421 (d/l = 21 %) in hub zone in an interval for angles of attack between i = 0^0 ….. 15^0, the coefficients are independent of the maximum thickness "d/l" and equal with:

$$C_L\left[i(r)\right] = C_L(i) = 0.0685 \cdot i + 0.302 \qquad (9)$$

$$C_D\left[i(r)\right] = C_D(i) = 0.0002857143 \cdot i^2 + 0.0028282571 \cdot i + 0.01414286 \qquad (10)$$

These relations were obtained from the mean experimental characteristics of the airfoils [7]. Approximate analytic values of the power are obtained from relation (6) considering constant values along the blade and taking into account the values of the centre of the blade with the radius r_x. The data from [6] for Ciugud - B are in Table 4:

TABLE 4

		r_0	r_x	R_0
r	**[m]**	1.5	2.5	3,5
b	**[m]**	0.695	0.525	0.355
i	**[^{0}]**	8.93	7.54	6.65

Neglecting the resistant term from the integral rel. (6) because:

$$C_D\left[i(r)\right] \cdot \omega_0 \cdot r \; \square \; C_L\left[i(r)\right] \cdot v_0 \qquad (11)$$

With these approximations rel. (6) becomes:

$$P_6 = \frac{z \cdot \rho \cdot \omega_0}{2} \cdot C_L\left(i_x\right) \cdot v_0 \cdot b_x \cdot \int_{r_0}^{R_0} r \cdot \sqrt{\omega_0^2 \cdot r^2 + v_0^2}\, dr =$$
$$= \frac{z \cdot \rho \cdot \omega_0}{2} \cdot C_L\left(i_x\right) \cdot v_0 \cdot b_x \cdot \frac{\left(\omega_0^2 \cdot R_0^2 + v_0^2\right)^{3/2} - \left(\omega_0^2 \cdot r_0^2 + v_0^2\right)^{3/2}}{3 \cdot \omega_0^2} \quad (12)$$

Here $i_x = i\,(r_x)$ and $b_x = b\,(r_x)$. This solution is calculated for the centre blade values and also for the above mentioned values for air density, wind velocity and runner speed of rotation in Table 5:

TABLE 5

z	R_0	r_0	r_x	b_x	i_x	P_6	Observations
-	[m]	[m]	[m]	[m]	[^{0}]	[W]	Turbine
3	3.5	1.5	2.5	0.525	7.54	14134.91	Ciugud - B
5	2.5	0.8	1.65	0.300015	8.18944395	5637.467	Ciugud - A
5	2.5	1.1	1.8	0.28335	8.46544	5104.375	Ciugud - A

Numeric integration of rel. (6) with different number of intervals, "N", along the runner blade shows the asymptotic limit of the power for Ciugud - B in Table 6.

TABLE 6

N	-	10	50	100	500	1000	5000	10000
P_7	[W]	9203.521	9659.047	9716.872	9763.28	9769.089	9773.746	9774.33

Numerical integration represented in Table 6 gives:

$$P_7 \cong 9773 \quad kW \quad (13)$$

Wind power plant Ciugud with the rated values of the parameters and the known dependence of the airfoils chord in function of runner radius and the angle of attack in function of runner radius:

$$i(r) = 0.2555 \cdot r^2 - 2.4207 \cdot r + 11.99488 \quad (14)$$

For a more precise dependence of the angle of attack in function of blade radius:

$$i\left(r\right) = -12.62158 + 54.51764 \cdot r - 50.827 \cdot r^2 + 22.25471 \cdot r^3 - 4.71721 \cdot r^4 + 0.3900138 \cdot r^5 \quad (15)$$

The power, " P_8", results for two extensions of the blade radius are presented in Table 7:

TABLE 7

N	i	R_0	r_0	P_8	Obs.
-	[^{0}]	[m]	[m]	[W]	Ciugud - B
5000	6.696	3.5	1.5	9771.354	Without hub zone extension
5000	6.696	3.5	0.8	11372.11	with hub zone extension

Through numerical integration in a QBasic program (PUTEREA.BAS) with:

- The angle of attack in function of blade radius by the relation (15);

- The lift coefficient of the profile in function of blade radius by the relation (9);

- The drag coefficient in function of blade radius by the relation (10);

- The chord of the bade airfoils in function of blade radius by relation (7) respectively (8).

The runners Ciugud – A and Ciugud – B have the blade airfoils from the same NACA family and the lift and drag coefficients have the same dependency from the angle of attack by different radiuses. The power "P_9" integration results using the relation (6) solved numerical are given in Table 8.

TABLE 8

$\rho = 1.2$ kg / m^3 ; $n_0 = 120$ rev / min ; $v_0 = 8.5$ m / s ; N = 5000;						
z	**R_0**	**r_0**	**$b(R_0)$**	**$b(r_0)$**	**P_9**	**Observations**
-	**[m]**	**[m]**	**[m]**	**[m]**	**[W]**	**-**
3	3.5	1.5	0.355	0.695	9800.96	Ciugud - A
		0.8	0.355	0.814	11378.05	
5	2.5	1.5	0.20558	0.31668	3034.538	Ciugud - B
		1.1	0.20558	0.36112	3850.07	

3. Power coefficient – solidity performances

Knowing the power coefficient in function of the number of wind runner blades from the literature [4],[5] as in Fig. 1:

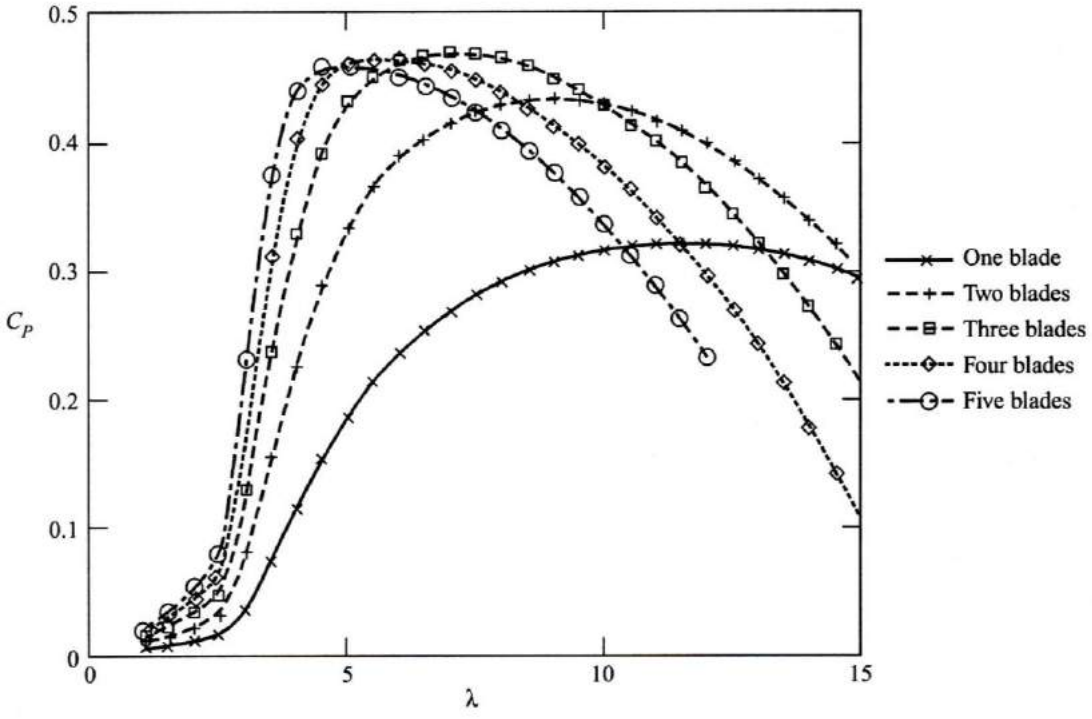

Fig. 1. Power coefficient in function of the number of runner blades of an axial wind turbine

The extracted data from [1] for 18.02.2016 and 30.12.2015 gives the dependence from Fig. 2.

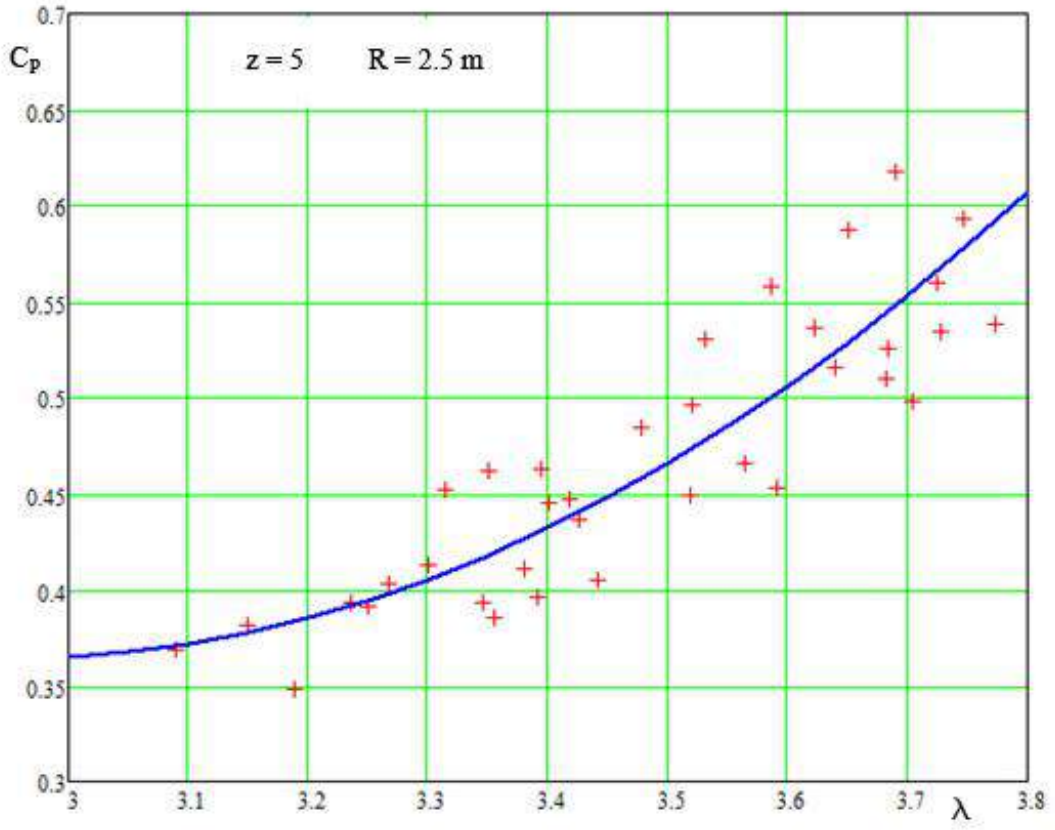

Fig. 2. Power coefficient in function of rapidity for Ciugud - A wind turbine

This correlation of the power with solidity C_P – λ, Fig.2, compared with above given Fig. 1 has the following peculiarities:
- The rapidity of the Ciugud Wind power plant is smaller than the rapidity from literature for the axial wind runner with same number of blades.
- The values of the power coefficients are greater than the values from Fig. 1.

The conclusion from Fig. 2 shows that there are some problems with estimation, for the same rapidity, of the speed of rotation for calculus of solidity.

For the power coefficient I have no explanations.

A better approximation is: $C_P = 62.61622 - 54.25966 \cdot \lambda + 15.636 \cdot \lambda^2 - 1.487106 \cdot \lambda^3$

With $\varepsilon_m = 0.025968$ and $\sum \varepsilon_i^2 = 0.01332$ all for sign "o" in Fig. 2.

Another approximation is $C_P = 32.21472 - 27.86668 \cdot \lambda + 8.04936 \cdot \lambda^2 - 0.765309 \cdot \lambda^3$

With $\varepsilon_m = 0.023025$ and $\sum \varepsilon_i^2 = 0.021515$ all for sign "+" in Fig. 2.

A better approximation for Fig. 3 is: $C_P = -0.10775 + 0.05867376 \cdot \lambda$

With $\varepsilon_m = 0.0020928$ and $\sum \varepsilon_i^2 = 0.000058631$

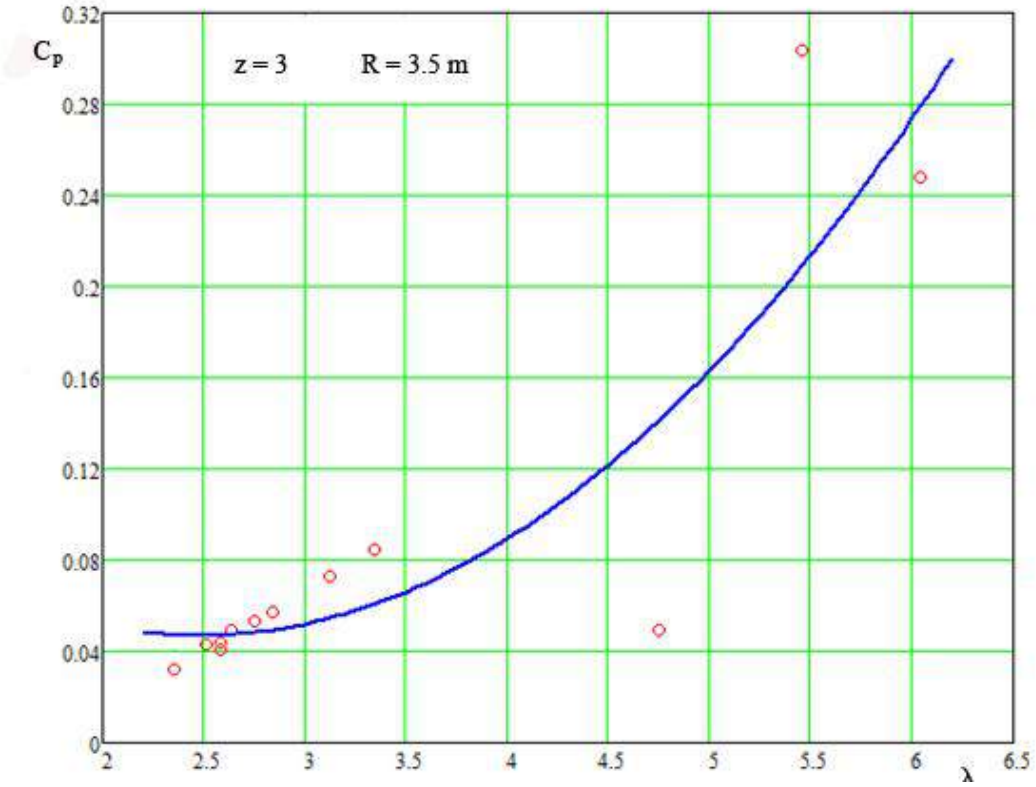

Fig. 3. Power coefficient in function of rapidity for Ciugud – B wind turbine

Power coefficient in function of rapidity for Ciugud - B wind turbine is presented in Fig. 3. The rapidity intervals for Ciugud – A (z = 5) namely in Fig. 2 , λ = 3…4 corresponds with the data from [1] for z = 3…6 , λ = 3 and for Ciugud – B (z = 3) Fig. 3 , λ = 2.5…3.5 corresponds with the data from [1] z =2…4 , λ = 4. The small discrepancy can be explained because the measured data are in a zone of increasing values of the power coefficient in Fig. 2 and Fig.3 and not in the maximum of C_P values.

5. Blade extension and angle of attack function

Wind turbine runner blade for Ciugud – B from type R_0 = 3.5 m to hub r_0 = 1.5 m and for runner blade extension Ciugud – B from type R_0 = 3.5 m to hub r_0 = 0.8 m power is calculated.

The airfoils angle of attack in 28 sections of the runner blade (of Ciugud – B) between tip and hub are approximated polynomial.

Angle of attack "i" in function of runner blade radius "r" is approximated through a:

- Two degree relation (Pol. 2):

$$i = 9.14033 + 0.0190224 \cdot r - 0.2313245 \cdot r^2 \tag{14}$$

With mean error: ε_m = 0.2301 and square error sum $\sum\varepsilon^2$ = 2.305.

- Three degree relation (Pol. 3):

$$i = 5.099766 + 7.08846 \cdot r - 3.823122 \cdot r^2 + 0.5568679 \cdot r^3 \tag{15}$$

With mean error: ε_m = 0.13349 and square error sum $\sum\varepsilon^2$ = 0.83193.

- Four degree relation (Pol. 4):

$$i = -2.31821 + 24.1731 \cdot r - 17.49545 \cdot r^2 + 5.068098 \cdot r^3 - 0.5245616 \cdot r^4 \quad (16)$$

With mean error: $\varepsilon_m = 0.070217$ and square error sum $\sum\varepsilon^2 = 0.20957$.

- Five degree relation (Pol. 5):

$$i = -12.62158 + 54.51764 \cdot r - 50.827 \cdot r^2 + 22.25471 \cdot r^3 - 4.71721 \cdot r^4 + 0.3900138 \cdot r^5 \quad (17)$$

With mean error: $\varepsilon_m = 0.03237$ and square error sum $\sum\varepsilon^2 = 0.041344$.

The comparative results are mentioned in Table 9 with respect of numerical approximation of the extracted power, P_{10}.

TABLE 9

Wind turbine	i	R_0	r_0	P_{10}	Obs.
-	[^{0}[]	[m]	[m]	[W]	
Ciugud - B	Pol. 2	3.5	1.5	9804.595	
	Pol.3			9844.215	
	Pol.4			10429.47	
	Pol. 5			9775.817	
Ciugud - B	Pol. 2	3.5	0.8	11382.93	
	Pol.3			11440.23	
	Pol.4			12078.25	
	Pol. 5			11378.13	

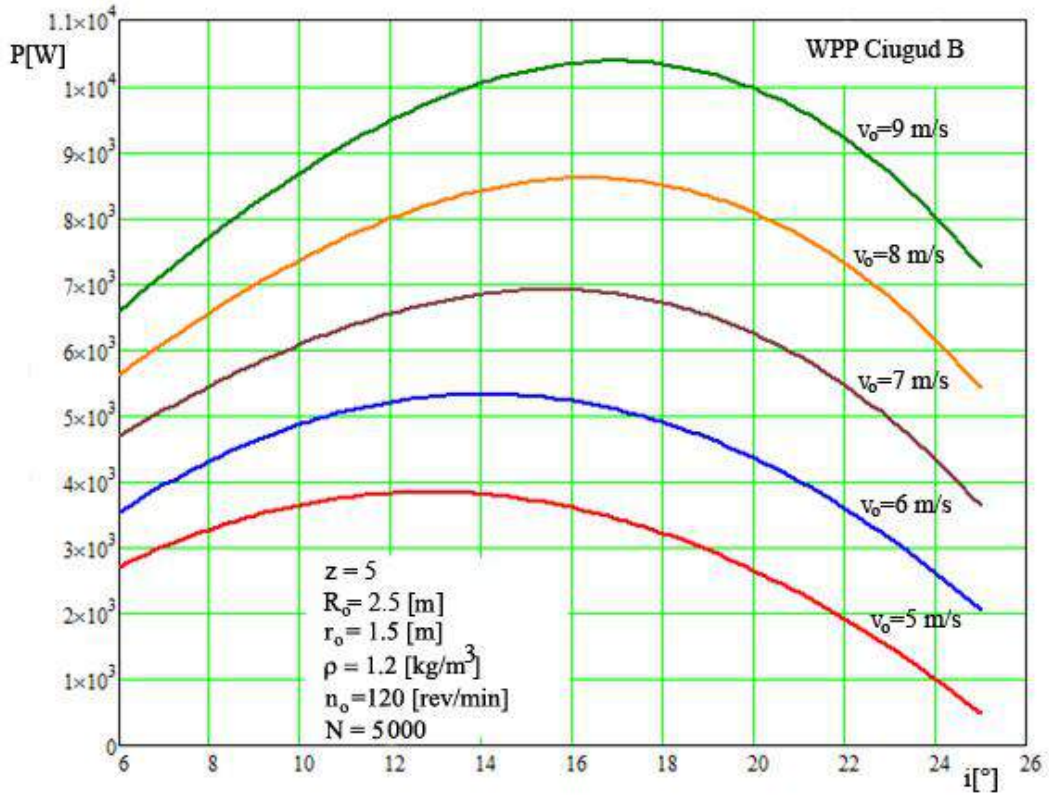

Fig. 4. Extracted power in function of the attack angle by different wind velocities

Runner blades airfoils angle of attack can be modified through blade rotation in respect of blade axis. Because the wind velocity and speed of rotation of the runner remain constant the sum of the angles of attack and stagger angle of the blade remain constant. So the power obtained may be modified. Increasing power is in the same time more close to flutter and the assurance of the operation is decreased. In Fig. 4 the power obtained from Ciugud – B in function of the angle of attack by different wind velocities using the model in QBasic (EXTREM.BAS) for numerical integration of relation (6).
The maximum power and the correspondent angle of incidence gives the degree of protection against stall of the profile respectively blades of the turbine runner.

4. Conclusions

Comparative analysis of the results for different mathematical models of power calculations made to the wind power plant Ciugud establish:

1) The maximum theoretical powers value, for Ciugud – A, $P_3 \approx 4287$ W and for Ciugud – B, $P_3 \approx 8403$ kW, are greater than the designed values of P = 3 kW and respectively P = 5 kW.

2) The maximum aerodynamic power statistical and similitude data are around the designed value as it is seen from Table 2 and Table 3.

3) The analytical power $P_6 \approx 5$ kW and respectively $P_6 = 14$ kW - taking into consideration a two-dimensional model and neglecting a lot of factors and influences – is much greater than the rated values. The simplification to obtain an analytical integral took its toll.

4) The numerical integral is much closer to the reality. The value of power $P_7 = 9794.644$ W obtained after a satisfactory number of 5000 intervals is adequate.

5) The measured parameters of power and rapidity are in a narrow band of values and so the conclusions are hazardous.

6) The blade extension of the runner has a major importance for the extracted power.

7) Higher polynomial approximation of the angle of attack in function of the blade radius introduced little influence on the calculated power.

References

[1] *** Report of Ciugud operation 2013 – 2016;
[2] M. Bărglăzan, "Turbine hidraulice şi transmisii hidrodinamice", ed. Politehnica, Timişoara, 2000;
[3] D. le Gourieres, „Energie eoliene", ed. Eyrolles, Paris, 1980;
[4] E. Hau, „Windkraftanlagen", Springer -Verlag, Berlin, 2014;
[5] T. Burton,..,"Wind Energy Handbook", John Wiley &Sons, New York, 2011;
[6] M. Bărglăzan, "Optimization of axial wind turbine operation", Hidraulica, no. 1 2016;
[7] T. Miloş, F. Gyulai, "CAD technique for blade design of small power wind turbine", Sci. Bull. of Politehnica University Timisoara, 2008;
[8] E. M. Fateev, "Vetrodvigateli i vetroustanovki", OGHIS Moscva, 1948.

Aspects Regarding the Special Hydraulic Distributors Operation

Assistant professor **Fănel Dorel ȘCHEAUA**[1]

[1]"Dunărea de Jos" University of Galați, MECMET Research Center, fanel.scheaua@ugal.ro

Abstract: *At the beginnings of fluid use as an energy carrier medium inside mechanical systems called hydrostatic drives were not many differences between static or mobile drives because the majority of circuit specific components (pumps, motors) were the same. Lately they were developed highly efficient systems adapted for each application type. This has led to the development of a comprehensive array of different devices, specific to each application. Such devices used within the hydrostatic systems are hydraulic distributors necessary to adjust and direct the working fluid through the working circuit different branches. In this paper are described the hydraulic distributors of special construction which have the adjustment and control element of the working fluid a spherical piece centrally positioned within the body. They were designed and analyzed in terms of the operation principle two distributor models having two and three way. The obtained results are presented in terms of velocity and pressure of the working fluid in the fluid region declared and analyzed for each model.*

Keywords*: hydraulic distributor, fluid flow, 3D modelling, computational fluid dynamics (CFD)*

1. Introduction

The hydrostatic drive uses for energy transmission a working fluid of low compressibility. This constitutes the support through which the energy is transmitted between the power source and the working body of a certain machine or equipment. The energy transmission is carried out continuously by circulating the working fluid between the hydraulic circuit components represented by pumps, piping, distributors, motors, or filters.
The phenomenon of the working fluid flow within the circuit on a permanent or impermanent regime, according to the fluid mechanics laws, is always accompanied by energy losses, greatly influenced by the geometric shape of the flow section and flow regime.
The hydraulic distributors represent special devices that are designed to restrict, direct or obstruct the working fluid flow within the hydraulic circuit. The effect of these distributor sequences are having as effect motion or repose of a hydraulic motor acting a technological equipment working body.

2. Special constructive solutions for hydraulic distributor

The role of a distribution and direction device acting on the fluid in the hydraulic circuit is to ensure the achievement of the working program through the bond achieved with the technological process imposed to the installation by the project.
By means of a directional device in the hydraulic circuit are ensured various functions related to connection and disconnection of one or several motors simultaneously or successively connecting or disconnecting of a circuit or several circuits of or from a hydraulic pressure source.
Directing the working fluid to a receiver of the hydraulic circuit is intended to perform various rotational or translational movements at the equipment working body thereof and the overcoming of technological resistances from the driven equipment.
The most used hydraulic distributors are the drawer models used in both stationary and mobile applications. The working principle of this distributor consists of axial displacement of the drawer inside the device body, through which are realized the connection between the ramifications made inside the drawer and device body. The drawer axial movement is performed by axial forces applied to their ends by means of special command systems which can be hydraulic, pneumatic, and electric or combined (electro-hydraulic, electro-mechanical).
The characteristic parameters of a hydraulic distributor are the drawer nominal size, the connections number, the possible working positions, the positioning system on the drawer neutral position and the switching command systems.

An important feature of the hydraulic distributor is the ratio number of connections/number of positions. The representative states of operation represented symbolically are: open, closed, the choice state - number of positions (figure 1).

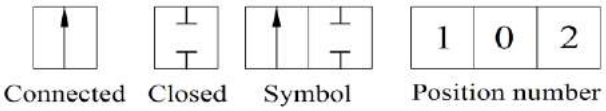

Fig. 1. Symbolization method

In addition to drawer distributors there are special hydraulic distributor models where the distribution of hydraulic fluid is performed by means of a rotational working body, which can be a sphere or a cam.
The distributor models with rotating sphere that may have two or three paths represent a constructive solution used currently in industrial hydraulics. The distribution working body is represented by a sphere provided with internal channels through which the fluid is directed depending on body relative position. At these constructive models the sealing between the sphere and the body is made directly metal on metal, or through the use of special gaskets.
The constructive principle for this particular distributor is shown schematically in figure 2.

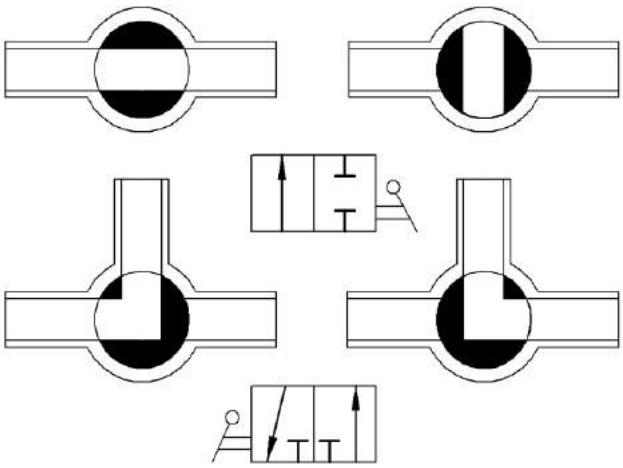

Fig. 2. The principle and symbol of two and three way distributor with spherical rotary piece

For the constructive solution of the two-way distributor shown in Figure 2, the spherical piece has a longitudinal channel through which the fluid can be circulated and according to the relative position to the body can open or close the connection with the working circuit.
The second model presents a constructive solution for the three-way hydraulic distributor which features a spherical piece having an angular channel inside through which is ensured the momentary connection with two of the three distribution lines.
For these constructive distributor types the command is mechanical and can be manually enabled.
Figure 2 presents also the symbolization manner for these devices capable of fluid distribution in a hydraulic circuit.
The required characteristics for the selection of a hydraulic distributor in a particular installation are related to the nominal diameter and the required connection diagram to the hydraulic circuit.
The required diameter can be calculated after being established the limit velocity value regarding the fluid flow through the device in order to have lowest possible load losses: [1]

$$d_n = 10\sqrt{\frac{2Q_c}{3\pi w}} \tag{1}$$

where:
d_n - nominal diameter;

Q_C - fluid flow rate;

w - fluid velocity.

The limit velocity value of the fluid circulated through the distribution devices mounted on the hydraulic circuits is in the range 8-10 m / s.

The real velocity value of the fluid circulated through the distributor can be calculated using the equation: [1]

$$w_r = \frac{200}{3\pi} \quad \frac{Q_C}{d_n^2} \tag{2}$$

In the hydraulic circuit working operation there is a pressure drop across the distributor, which depends on factors such as the flow section shape, the hydraulic fluid nature or temperature. The pressure drop amount can be calculated with the equation: [1]

$$\Delta_p = \xi \frac{\rho}{2} w_r^2 10^{-6} \tag{3}$$

where:

ξ - local losses coefficient;

ρ - circulated fluid density.

3. Hydraulic distributor model analysis

Two distributor models having two and three way, presented in figure 3, have been considered for analysis. Two three-dimensional model assemblies have been constructed for the hydraulic distributors and analyzed using ANSYS CFX in order to emphasize the fluid flow parameters represented by velocity and pressure at the level of fluid region function of spherical piece relative position to the body.

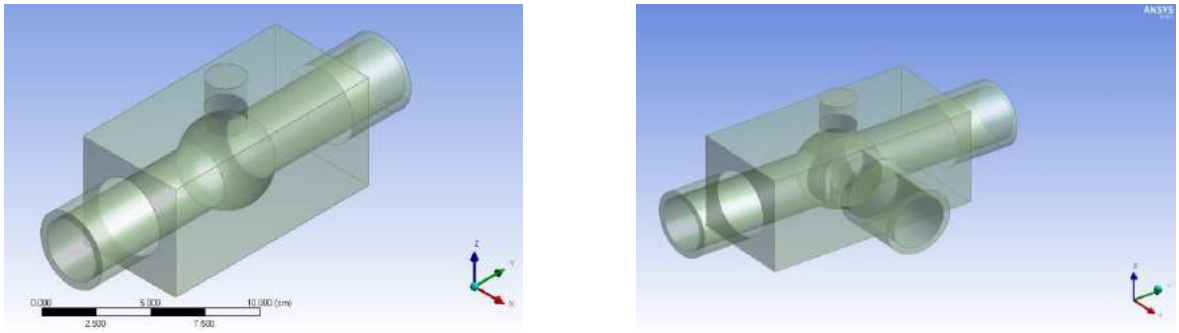

a) Two way distributor model b) Three way distributor model

Fig. 3. Three dimensional hydraulic assembly models

The analysis was performed for each distributor model separately. For two-way distributor model the fluid region was declared within the body having inlet and outlet boundaries and a spherical piece inside capable of rotational motion on OZ axis. The obtained results are shown in Figure 4.

The fluid flow analysis for the three way hydraulic distributor model was carried out from the established initial data for an inlet and two outlets which are sequentially selected by the rotation of spherical distribution piece, positioned within the distributor body.

The results for the three-way distributor model of are shown in Figure 5.

For both models was declared a fluid circulation velocity at the inlet of 10 m/s and the reference fluid pressure across the region being 1 atm.

The working fluid is a hydraulic oil (H60A), having a density of 0.905 g/cm3 and kinematic viscosity at 40 degrees Celsius of 60 cSt. [6]

The rotation of the spherical piece has been declared at 0.5 rad/s, and the total flow analysis was of 3 seconds with a time step of 0.3 s.

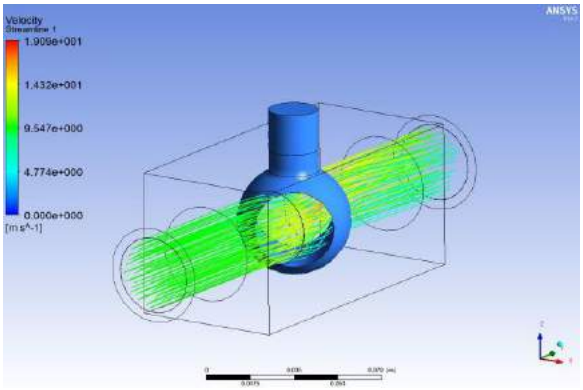

a) Fluid velocity values on streamlines

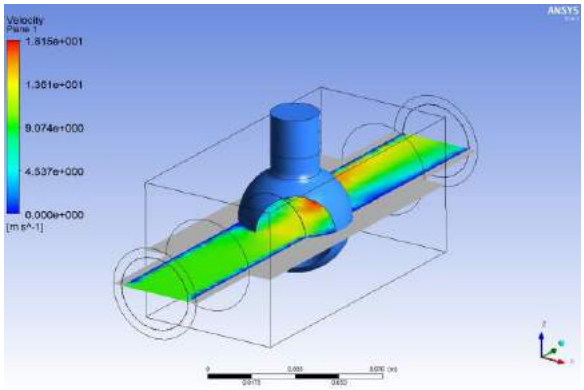

b) Fluid velocity values on XY plane

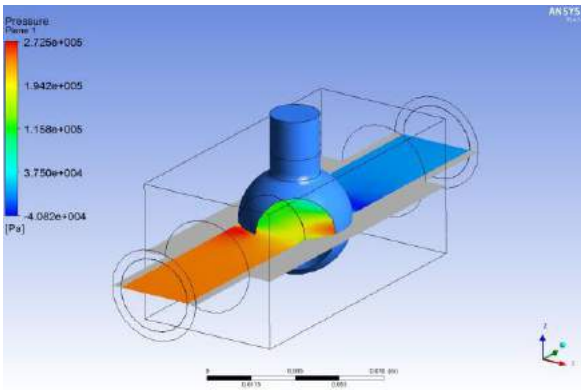

c) Pressure values at half of stroke

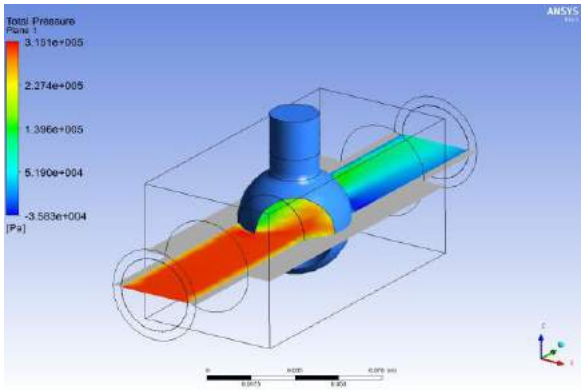

d) Total pressure values at half of stroke

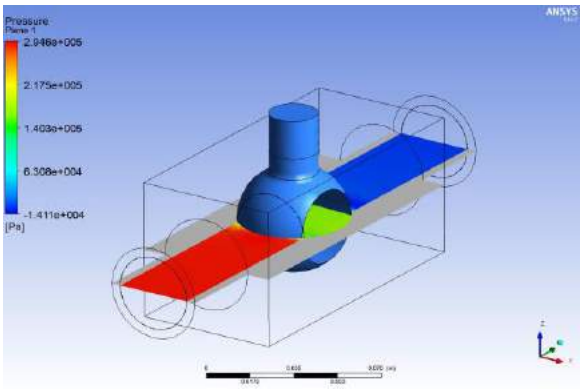

e) Pressure values at maximum stroke

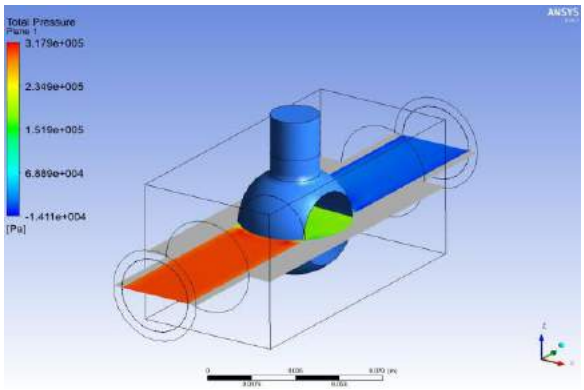

f) Total pressure values at maximum stroke

Fig. 4. The obtained results for the two way hydraulic distributor model

The result values obtained for the working fluid velocity and pressure achieved in the considered fluid region are presented, depending on the spherical piece adjustment position. For the two-way distributor model are shown in Figure 4 the intermediate position set for the spherical piece at half of stroke and at the stroke end, when it is performed the full closure of the flow channel of the working fluid.

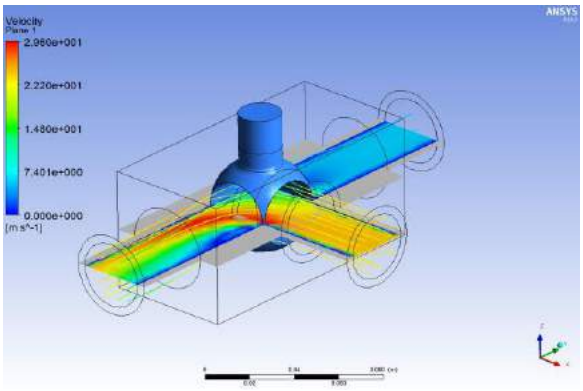

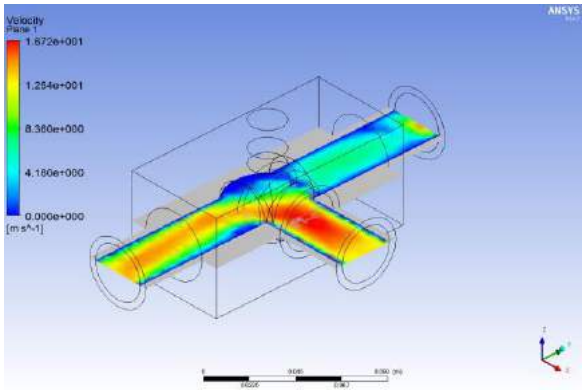

a) Fluid velocity values for circulation on outlet 1

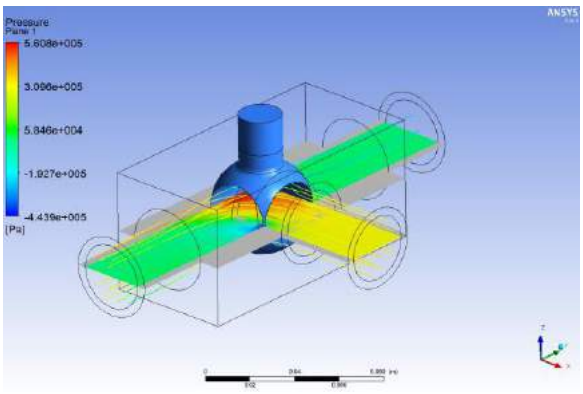

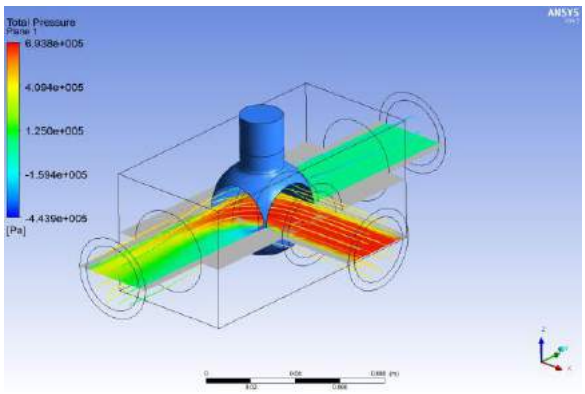

b) Pressure values on the flow outlet 1 c) Total pressure values on flow outlet 1

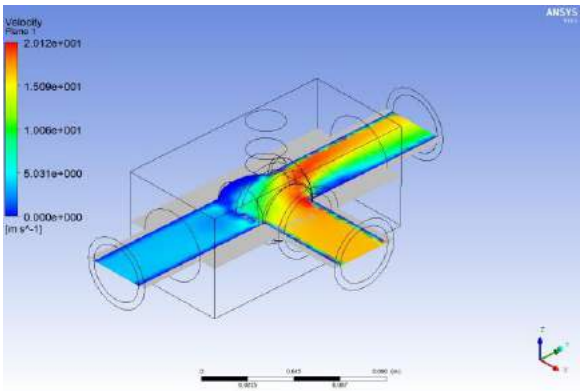

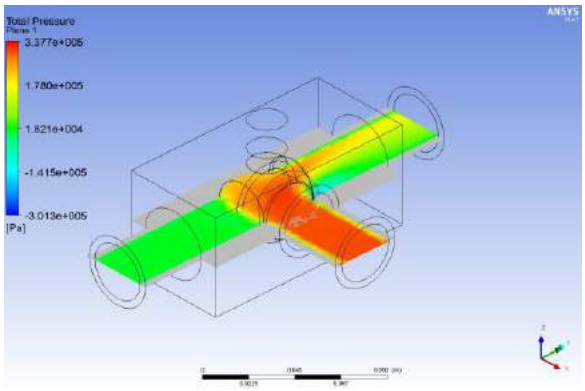

d) The fluid velocity values for outlet 2 e) The total pressure values for outlet 2

Fig. 5. The obtained results for the three way hydraulic distributor model

For the model of the three-way distributor the analysis was performed according to the changing position of the spherical piece within the body so that it can accomplish the sequential connection of the inlet of the working fluid and two outlet ports. The results obtained present the values for velocity and pressure of the working fluid inside the fluid region (Figure 5).

TABLE 1: The diagrams for fluid flow rate and adjusted flow rate values

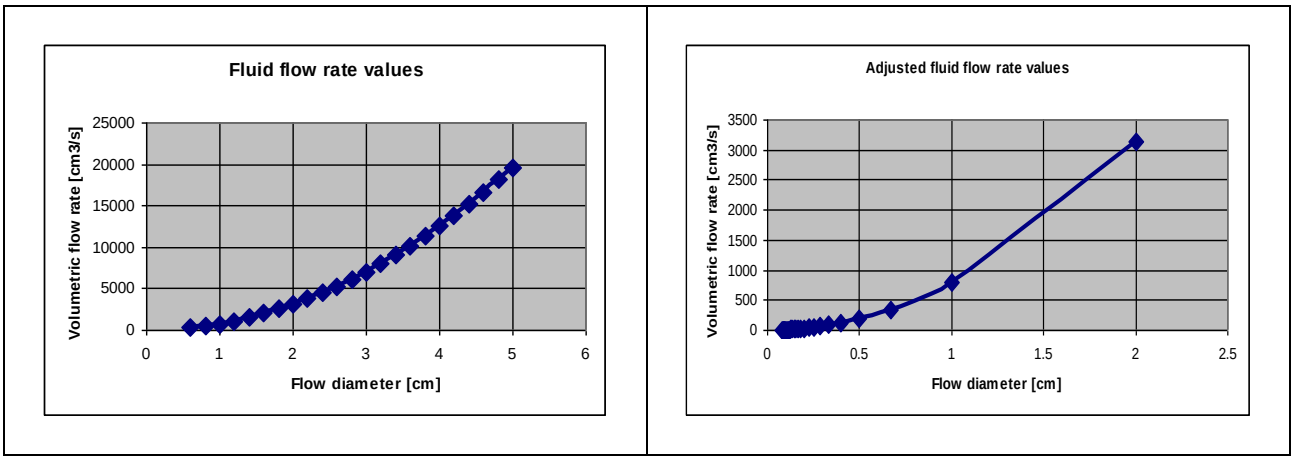

In Table 1 are presented the results diagrams for the theoretical fluid flow rate values according with the orifices diameter of the distributor model. Also are presented the results for the adjusted fluid flow rate obtained at hydraulic distributor model operation. They have been considered the volumetric flow rate values of fluid circulating through the distributor according with the spherical piece control positions which achieves a full stroke.

4. Conclusions

In this paper were presented and analyzed two special constructive solutions for hydraulic distributor. These are in fact directional regulatory elements for the hydraulic fluid flow in a hydraulic circuit which may be used to serve in practice particular installations.
Two distributor assembly models were designed having two and three way, which were analyzed with ANSYS CFX program in order to highlight the operating characteristics.
The results obtained from the carried out analyzes show the values of the working fluid velocity and pressure created in the fluid region for each model, according with the spherical piece position which achieves control and direction of fluid flow inside the distributor body. The working fluid was declared a hydraulic oil (H60A) used in the practice of hydraulic actuations.
Such devices for which they were built and analyzed virtual models are currently used for various applications in industrial hydraulic involving high levels of working pressure up to 300 bar, with a range of nominal diameters from 6 to 50 mm and ability to work in a temperature range between -30 and +150 degrees Celsius. [7]

References

[1] A. S. Axinti, F. D. Șcheaua, "Introducere în hidraulica industrial", Editura Galati University Press, Galați, 2015;
[2] G. Axinti, A. S. Axinti, "Acționări hidraulice și pneumatice", Vol III, Editura Tehnica-Info, Chișinău, 2009;
[3] Al. A. Vasilescu, "Mecanica fluidelor", Ministerul Educatiei și Învățământului, Universitatea din Galați, Galați, 1979;
[4] F. D. Șcheaua, "Functional description of a hydraulic throttle valve operating inside a hydraulic circuit", Hidraulica Magazine, ISSN 1453 – 7303, No. 1, 2016;
[5] F. D. Șcheaua, "CFD Analysis for hydraulic flow rate control device", Journal of Industrial Design and Engineering Graphics - JIDEG, ISSN 1843 - 3766, Volume 11, Issue 1, 2016;
[6] www.ulei hidraulic aditivat H46A/H60A, accessed at 25.11.2016;
[7] www.hrpc-hydraulics.com/products, accessed at 30.11.2016.

Combined Energy Systems for Obtaining Energy from Renewable Sources Used in Isolated Areas

Ph.D. eng. **Corneliu CRISTESCU[1],** Ph.D. eng. **Catalin DUMITRESCU[1],**
Dipl. eng. **Genoveva VRÂNCEANU[1],** Dipl. eng. **Liliana DUMITRESCU[1],**
Res. Assist. **Ana-Maria POPESCU[1]**

[1] INOE 2000-IHP, Bucharest, cristescu.ihp@fluidas.ro

Abstract: *The paper presents some aspects of obtaining energy from renewable sources, especially for remote areas, where we meet, usually, individual users or very limited groups of consumers. In the second part there are presented some solutions for combined systems that use renewable energies, which is a secure path to increase efficiency of their use and supply, throughout the day and even the year, the energy needed for consumption in remote areas.*

Keywords: *Renewable energy, capture technologies, power hydraulics, wind power, photovoltaic technology, hydrostatic transmission, fluid power transmission*

1. Introduction

European Union energy policy by 2020 is based on three core objectives: Sustainability, Competitiveness, Safety of energy supply.
Regarding the production energy from renewable sources, European Union **target** for 2030 is 27 % of total energy consumption, mandatory for the community block.
According to Romania's energy strategy over the period 2007 – 2020, the **general objective** of the strategy in the energy sector is represented by **meeting the energy needs,** both now, and in the medium and long term, by promoting the **production energy from renewable sources**, so the share of electricity produced from these sources in the total gross electricity consumption be 33% in 2010, 35 % in 2015, and 38 % in 2020, [1].
To implement this policy, there has been developed *Planul Naţional de Acţiune în Domeniul Energiei din Surse Regenerabile (PNAER) – 2010 / National Action Plan in the Field of Energy from Renewables – 2010,* which states that energy produced from renewable energy resources is "*clean*" energy, and their exploitation provides an alternative to energy produced from fossil fuels. An important role will be played by **measures to increase energy efficiency** in the public sector, which will have an important role at national level [2].
The concept of **energy efficiency** (or energy consumption optimization) has become, nowadays, one of the main concerns of humanity in the entire world.
Diversifying the energy sources is becoming **an economic and environmental imperative**. These alternative energies are renewable energies. The most popular renewable energy sources are: **solar** energy (direct, photovoltaic and thermal energy), **wind** energy (as a solar energy derivative), **hydraulic** energy (by using the potential and kinetic energy of the water), **geothermal, bio-energy,** etc.
Renewable energy sources can be used both as **centralized sources of energy** and, largely, **decentralized**. Decentralized sources are particularly advantageous, especially for **rural** consumers or those **in remote areas** [3].
Decentralized energy sources are particularly interesting for individuals or for small groups, especially if they are in remote areas.
The issue of choosing a particular **system of energy generation from renewable sources**, especially for natural persons, individuals, or for **consumers in remote areas**, is not a simple issue, as one needs to know very well the **requirements for power consumption**, on the one hand, and on the other hand the **technologies** that are addressed **must be well known** as well, including the thermal parameters, wind speeds, etc, which can result in energy availability, daily or seasonal, which is different for different areas, even if the equipment is the same.

The main systems / technologies for the **use of clean energies** are: **solar** systems (thermal and photovoltaic), **wind** systems / power plants, or **mixed or hybrid systems**, which combines two or more sources of renewables in order to increase energy efficiency and availability.
This is because, apart the clear benefits of renewable sources of energy, they also have downsides, which mainly consist of fluctuation, intermittence, of the basic parameters (temperature, wind speed), their variation both during the day and throughout the year.
From theoretical analysis and practice of **experts in renewable energies**, the use of **combined or hybrid systems** has **clear advantages** compared to the single ones, especially for **remote areas.** Of course, combined or hybrid systems also have the disadvantage of high upfront investment costs [4].

2. Combined systems practiced worldwide

The combined systems provide the opportunity to have energy throughout the day, irrespective of whether one of the sources is unavailable, being possible for another one to be operative and produce energy.
The combined systems which use **the energy of running water** or **geothermal energy** provide nearly **incessantly the energy required**, but such systems are **very expensive**, especially for individual users in remote areas.
Nonetheless, in the world there are many successful attempts to use combined or hybrid systems, confirming the superiority of this type of system in using the renewable sources of energy.
There are already companies that offer **kits for photovoltaic and wind hybrid systems** for **generation of electricity from renewable sources**, which work by using both photovoltaic panels and a wind turbine. Such photovoltaic and wind power hybrid kits are recommended for providing the necessary power in a tourist accommodation facility, housing, hostel, school or medical facility. The photovoltaic and wind power hybrid kits also include inverters, charge controllers and solar accumulators to store electricity which is beyond the consumption needs. The photovoltaic and wind power hybrid kits are also ideal to be used in irrigation systems on agricultural land [5].
In the following, **some examples** are given **of the diagrams of combined or hybrid systems** that use renewable energy to achieve continuous energy.
A **hybrid system** for electricity generation integrates **several energy sources** and it can feed consumers without interruptions, even if one source does not work any longer. The most used hybrid systems are the solar-wind ones, which combine photovoltaic panels and wind generators.

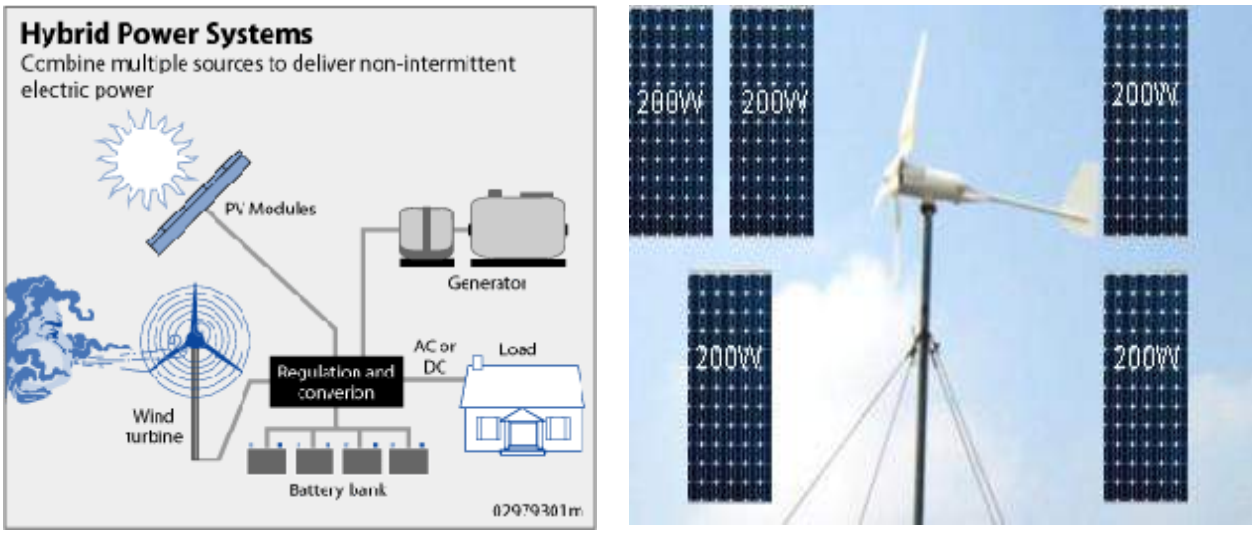

a) Schematic diagram

b) Photovoltaic panels and wind power plant

Fig. 1. Combined system of three types of energy: solar, wind and chemical energy [6].

A combined/ hybrid system of three energy sources, consisting of photovoltaic panels and wind generators, is shown in figure 1 a and b, composed of: photovoltaic panels, wind generator, generator with internal combustion engine, charge controller, inverter and electric accumulators. The advantage of such a system is using multiple sources for electricity production, working both day and night [6], [7].
As solar energy is fluctuating, and the generation capacity of the diesel genesets is limited to a certain range, it is often a viable option to include battery storage in order to optimize solar's contribution to the overall generation of the hybrid system.
Hybrid renewable energy systems (HRES) are becoming popular as stand-alone power systems for providing electricity in remote areas due to advances in renewable energy technologies and subsequent rise in prices of petroleum products.
Other solar hybrids include **solar-wind systems**. The **combination** of **wind** and **solar** has the advantage that the two sources complement each other because the peak operating times for each system occur at different times of the day and year. The power generation of such a **hybrid system** is more constant and fluctuates less than each of the two component subsystems.
The next figures 2 a,b,c and d present some combined/hybrid systems developed worldwide [6].

a) Typical wind and solar hybrid system

b) Hybrid on Žirje, Croatia

c) Hybrid in Leh, India

d) Small wind and solar hybrid system

Fig. 2. Some combined/hybrid systems developed worldwide [6]

A wind-hydro system generates electric energy combining wind turbines and pumped storage. The combination has been the subject of long-term discussion, and an experimental plant, which also tested wind turbines, was implemented by Nova Scotia Power at its Wreck Cove hydro electric power site in the late 1970s, but was decommissioned within ten years [6].
Biomass-wind-fuel cell hybrid system. For example, let us consider a load of 100% power supply and there is no renewable system to fulfill this need, so two or more renewable energy systems can be combined. For example, 60% from a biomass system, 20% from wind system and the remainder from fuel cells. Thus combining all these renewable energy systems may provide 100% of the power and energy requirements for the load, such as a home or business [6].

Suntech Green Energy hybrid systems make optimal use of sunlight and wind speeds - the two main resources readily available in the South Asian sub-continent. When the solar resource is low during the monsoon, the wind is quite strong and vice versa. The resultant hybrid system thus offers an optimal solution at a substantially lower cost. It is ideal for electrification of **remote villages** in India [8].

a) Schematic diagram b) Actual placing of the combined system

Fig. 3. Suntech Green Energy hybrid systems

In figure 4, for a Hybrid Renewable Energy System, there is presented the diagram of economical optimization of wind and solar based hybrid production systems [8].
A ***Hybrid energy*** system usually consists of two or more renewable energy sources used together to provide increased system efficiency as well as greater balance in energy supply.
An example of a hybrid energy system is a **Solar photovoltaic** array of panels, and even **Solar Heat collectors**, coupled with a **Wind Turbine**. Such a system is shown in figure 5 [9].

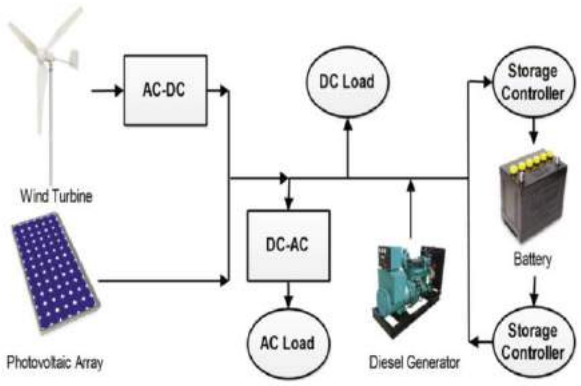

Fig. 4. Diagram of a triple source combined system

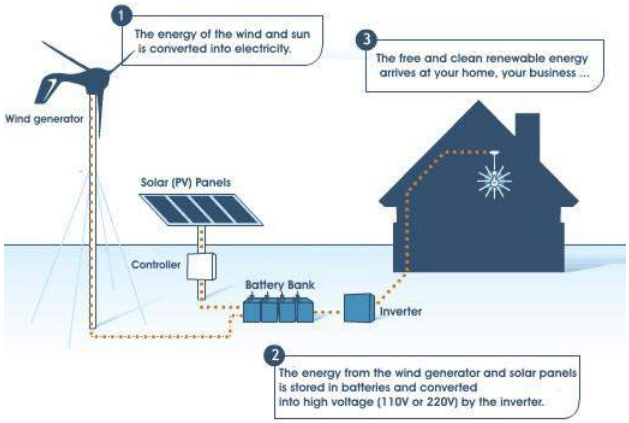

Fig. 5. Solar Heat collectors**,** coupled with a Wind Turbine

This would create more output from the wind turbine during the winter, whereas during the summer, the solar panels would produce their peak output.
The **combination** also **works efficiently with greater energy output** during the day with the Solar panels & collectors, with wind turbine generated energy at night [9].
Figure 6 presents a Hybrid system that uses wind and solar system to support and power a street light; it is an independent system which does not need power supply from the grid (all the power comes from renewable energy: wind & sunshine).
The Hybrid renewable system below, figure 7, is one that again provides electricity from a Wind generator and Solar panels from the sun during the day, and continues to be supported by the Wind energy generator source, coupled with energy stored in batteries at night.

The Hybrid renewable energy system presented in figure 7 may also include a Solar thermal Hot water system that has collected the sun's radiation during the day to heat and store hot water in the boiler for use at night, for a personal home.

Fig. 6. Wind and solar combined system to support and power a street light

Fig. 7. Wind and solar combined system for a personal home

Hybrid energy systems oftentimes yield greater economic and environmental returns than wind, solar, hydro or biomass generation stand-alone systems by themselves [9].

3. Innovative solutions for combined systems

Out below, we will present some new, innovative concepts / diagrams of achieving combined systems that use renewable energies. Figure 8 presents a diagram for use of solar thermal energy system on a **river pontoon**, intended to reduce, to a large extent, the conventional fuel consumption in the existant **power motor-generator**, with which it is **operating in a combined system**.

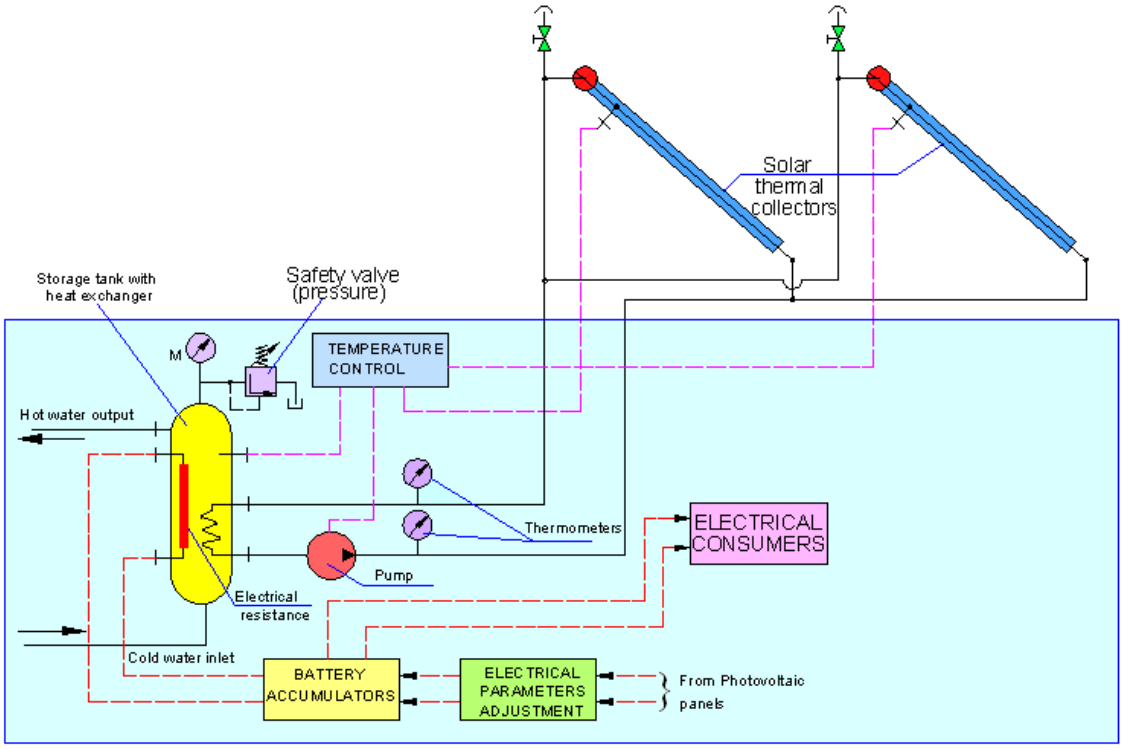

Fig. 8. Diagram/Concept of a combined system of solar energy and power from the motor-generator

Figure 9 presents a concept/diagram of a combined system for energy production from two renewable energy sources, namely: thermal and electrical energy, both from the sun. Thermal energy is produced by using solar thermal panels, flat or vacuum tube panels, while electrical power is supplied by photovoltaic panels / collectors, which operate on the photoelectric phenomenon. For domestic water heating, solar thermal panels contribute directly, and also electricity generated by photovoltaic panels, which, after adjustment of the parameters to the storage system consisting of a battery of electric accumulators, is conveyed to an electrical resistance installed inside the container / tank of hot water. Also from the battery of electric accumulators other electrical consumers (light bulbs, air conditioning, radio, TV set, etc.) are supplied as well.

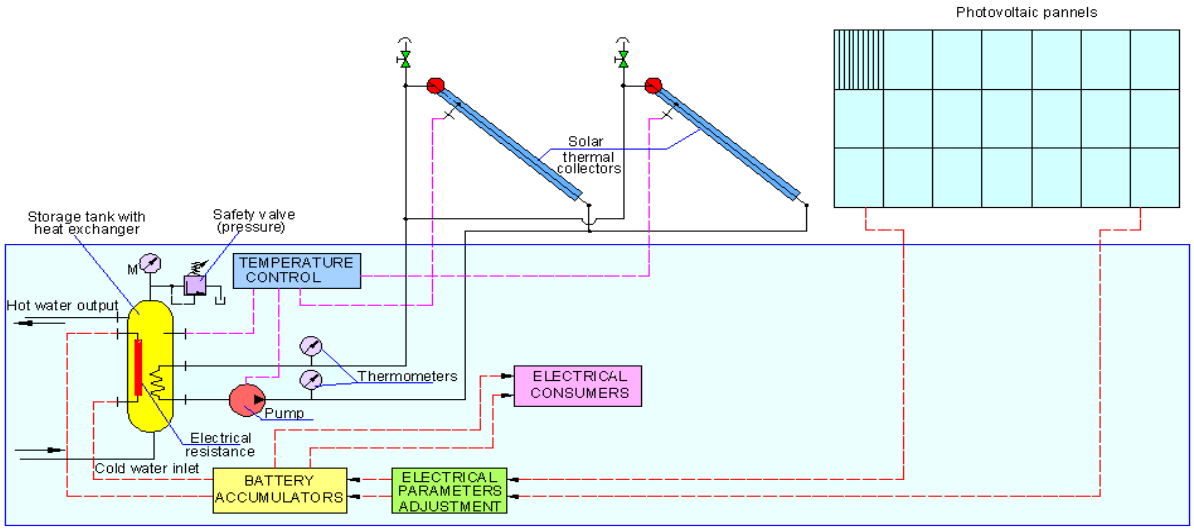

Fig. 9. Solar system combined diagram to obtain heat and electricity from photovoltaic panels

On the **hot water tank**, provided with cold water connections at the bottom and hot water connections at the top, there are installed a **safety valve** and **a manometer** indicating the working pressure, and on the input and output circuits of the **heat exchanger coil** there are provided **sensors and thermometers**, one for the lowest temperature, one for the highest. The system operates with **two circuits**, one for actual use and the other for heat transfer from heat panels / collectors to the water in the tank, by means of a **heat exchanger**, which can be located inside or outside the storage tank.

The fluid circulating through the heater coil releases the heat received from the collector to the cold water inside the heater, and there may be **water / propylene glycol mixture**, in a ratio **40/60** or **45/55**, based on the minimum temperature of the environment, during cold seasons the mixture 45/55 ensuring protection down to -26^{0}C. The fluid in the heat transfer circuit is circulated by means of a **centrifugal pump**, controlled by temperature control system / controller, ensuring the smooth functioning. The controller compares the temperatures provided by the two temperature sensors and activates the circulation pump as long as between the 2 points there is a temperature difference (adjustable) of more than 6...20 K°; when the temperature difference decreases below the set threshold, the pump is switched off and heat transfer ceases.

Another variant of a **combined system** for generation of **heat and electricity**, shown in figure 10, consists in **combination of one renewable energy source from the sun**, in order to **obtain thermal energy**, and a **wind micro/mini power plant**, intended to **supply electrical current** for one consumer or more, in **remote areas**, without the possibility to connect to the national electricity networks.

Figure 10 presents a concept/diagram of a combined system for energy production from **two renewable energy sources**, namely: **thermal** energy and **electrical** energy; the first comes directly from the sun, solar energy, and the second source exploits **wind energy**.

Thermal energy is obtained by using **solar thermal panels**, flat or vacuum tube panels, as in the first variant, while electrical energy is supplied by **a wind micro/mini power plant**.

This combined system requires a significant investment on the wind power plant.

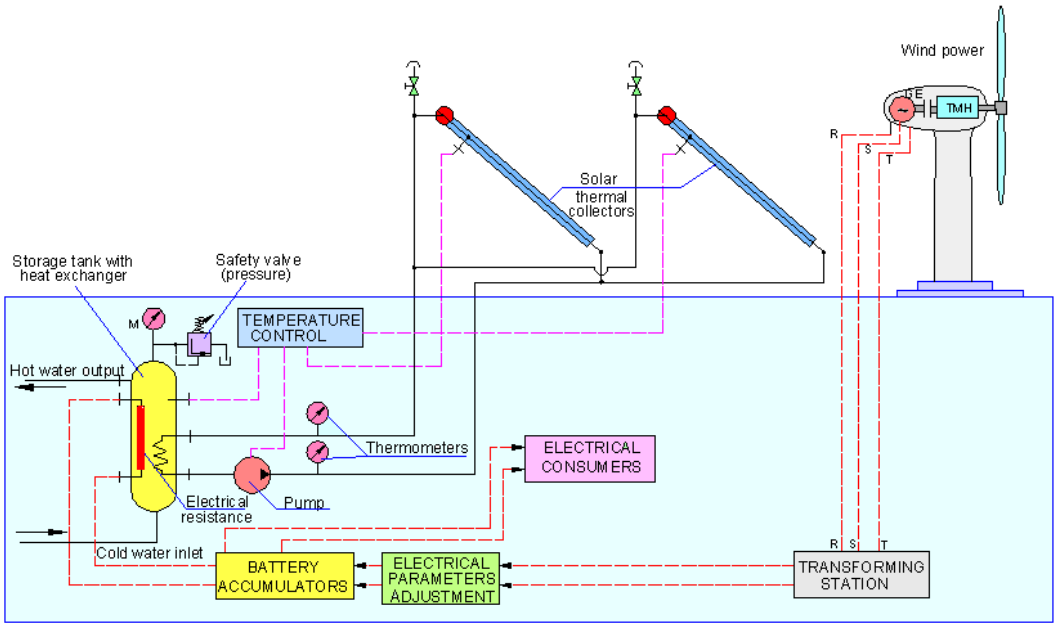

Fig. 10. Combined system for obtaining heat and electricity

Electricity provided by the wind power plant is first converted and then adjusted to the required parameters so that to be possible to **store it in the battery of electric accumulators**.
From the electric accumulators, the current can be used by **usual electrical consumers** or by **heating resistance** installed into the hot water tank, if appropriate.
As for the rest, structure and operation of the combined energy production system are similar.
The system shown in figure 11, below, is similar to that shown in the previous figure, but it integrates **3 energy supply systems**, being further provided with a connection to a **wind micro/mini power plant**, which also has fluctuating functioning, as the wind blows, at higher or lower speeds.

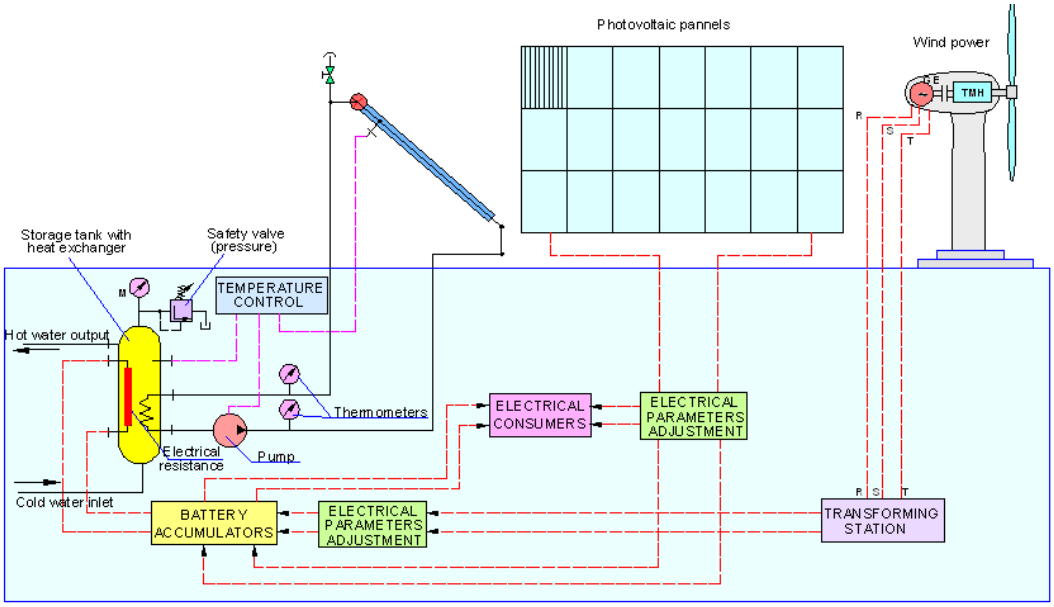

Fig. 11. Solar system combined diagram to obtain heat and electricity from photovoltaic panels and wind power

Combining the **three types of energy** offers increased security to have available at any time of day, the energy needed for a **consumer located in remote areas**.
If alternating, the electric current supplied by the wind power plant is first converted and then adjusted to the required parameters so that to be possible to **store it in the battery of electric accumulators**.

From the electric accumulators, the current can be used by **usual electrical consumers** or by **heating resistance** installed into the hot water tank, if appropriate.
As for the rest, structure and operation of the combined energy production system are similar.
As one can see from the above, developing new technologies for renewable energy storage, conversion and use is a major global activity, and consequently in our country, where the target is to meet the percentage set by the EU in use of renewable energy.

4. Conclusions

The paper has developed on the issue of using renewables at high energy efficiency, namely by means of combined energy production systems for remote areas.
As a synthetic conclusion, it can be said that the use of renewable energy is in full expansion and it includes all forms.
Therefore, the article presented a number of methods and technologies for combined systems, practiced worldwide, including in our country, some still being in a concept phase or experimental phase.
Finally, there are presented some new concepts for development of combined systems that use renewable energy, diagrams which will be the basis of several applied research activities to be developed in our institute.
Developing novel technologies and systems for capture, conversion, storage and reuse of renewable energies represents a new research direction within INOE 2000-IHP Institute [10], [11].

Acknowledgement

Research presented in this paper has been conducted with financial support of Romanian National Authority for Scientific Research and Innovation (ANCSI), under the national research programme NUCLEU-2016, research project titled "Physics of processes for reducing energy losses and developing renewable energy resources by use of high performance equipment", project code 16-40-03-01, Financial Agreement no. 5N/2016.

References

[1] *** Strategia energetică a României pentru perioada 2007 - 2020 actualizată pentru perioada 2011 – 2020. În: http://www.minind.ro/energie/STRATEGIA_energetica_actualizata.pdf;
[2] *** Planul Naţional de Acţiune în Domeniul Energiei din Surse Regenerabile (PNAER) – 2010. In: http://www.minind.ro/pnaer/draft_PNAER_15_06_10.pdf;
[3] G. Mircea, Course: "Conversia neconvenţională a energiei electrice. Introducere",.In: http://mircea-gogu.ro/pdf/Curs%20Conversia%20neconventionala%20a%20energiei%20electrice/Introducere.pdf;
[4] *** E-SOLAR : De ce trebuie să ținem cont atunci când instalăm un sistem fotovoltaic sau/și eolian? In : http://www.esolar.ro/sfaturi-utile/ce-sistem-de-energie-alternativa-alegem-fotovoltaic-eolian-sau-unul-hibrid.html;
[5] *** E-SOLAR: Kituri hibride fotovoltaice si eoliene - Hybrid photovoltaic and wind kits. In: https://www.esolar.ro/tehnologie-solara-fotovoltaica/kituri-hibride-fotovoltaice-si-eoliene.html;
[6] ***Wikipedia. Solar hybrid power systems. In: https://en.wikipedia.org/wiki/Solar_hybrid_power_systems;
[7] *** Sisteme hibride – Hybrid systems. In: http://www.sunnyway-solar.ro/sisteme%20hibride.html;
[8] *** Suntech Green Energy hybrid systems. In: http://http://enarchgroup.com/ees/hybridenergy.php;
[9] *** Hybrid Energy.EcoPlanetenergy. In: http://www.ecoplanetenergy.com/all-about-eco-energy/overview/hybrid/;
[10] C. Cristescu, C. Dumitrescu, I. Ilie, L. Dumitrescu, "Increasing energy efficiency of the solar thermal panels through the use of hydraulic tracking systems", In: Proc. of International Multidisciplinary Scientific Geo-Conference SGEM-2014, 17 – 26 June, 2014, Albena Co., Bulgaria, Vol.: „Energy and clean technologies", pp. 291–298, ISBN 978-619-7105-15-5, ISSN 1314-2704, DOI: 10.5593/SGEM2014/B41/S17.038;
[11] C. Cristescu, C. Dumitrescu, R. Rădoi, G. Vrânceanu, C-tin Chirita, "Capturing and storage the energy recovered from hydraulic drive systems of mobile machinery and equipment", In: CD Proc. of 22nd International Conference on Hydraulics and Pneumatics HERVEX – 2016, November 9-11, 2016, Baile Govora, Romania, pp. 105-114, ISSN 1454 – 8003.

Aspect about Design of Experiment (DOE) to Study the Impact Forces Produced by Water Jets Used in Sewage Cleaning

PhD. Eng. **Nicolae MEDAN**[1]

[1] Technical University of Cluj-Napoca, North University Center Baia Mare, Nicolae.Medan@cunbm.utcluj.ro

Abstract: *The purpose of this paper is to present the steps necessary to make a design of experiment with application to study the impact forces produced by water jets used to cleaning the sewage system. The functioning of the cleaning sewer is dependent on certain process parameters, which can vary, causing variations of the impact forces. The research method used is that of the full factorial design of experiment. In the first part of the experimental research the Taguchi method shall be used to determine the percentage of influence of parameters involved in the process.*

Keywords: *Design of experiment, impact forces, water jet*

1. Introduction

Throughout history, as the first cities emerged, the issue of managing the rain and waste water consequently occurred. This has proven to be a real challenge. The first evidence of the sewerage systems being used goes back as early as the 4th century BC. As of the 19th century, together with the development of the modern sewerage systems, emerged the issue of cleaning and maintaining them. At first „primitive" methods were used for sewer cleaning, such us: different types of flush sewers, "pills" (round wooden balls pushed downstream by the sewage), bucket on wheels or a disk pulled through the pipe. When a sewer was entirely stopped up, a "sewer rod" was pushed into the obstruction. Early rods used short lengths of pipe or wood, which were assembled together and forced through the obstruction.
As of the middle of the 20th century, simultaneously with a higher reliability of the high pressure pumps, was used high pressure water jet-based equipment for sewer cleaning. Such equipment is also currently being used. Also, have been developed water jet and abrasive water jet cutting machine which are used into a full scale production process [6].
The main components of the equipment used for sewer cleaning are the high pressure pump and the cleaning heads. They generate water jets at the necessary working pressure. There are more types and sizes of cleaning heads based on the purpose of the activity in question (the diameter of the sewer to be cleaned, the type of material deposited, the type of obstruction) and based on the characteristics of the pumps (the provided pressure and water flow).
At the outlet of the cleaning head nozzles water jets under pressure appear, which generate impact forces. By means of these impact forces the cleaning of the sewers takes place.
Phenomena that occur in the cleaning water jets are complex. Adler [1] describes mechanisms occurring at the impact of a jet with a surface. Leach et al [3], Leu et al [4] and Guha et al [2] analysed pressure distribution along centreline of the water jet. A number of papers have studied the influence of nozzle geometry on water jet [5].
In the water jet cleaning process a series of parameters are involved [7]. These parameters can be divided into two major groups, namely: 1) target parameters which shall be defined according to the contact area between the water jet and the surface to be cleaned and 2) process parameters.
The aim of this paper is to present the design of experiment (DOE) to study the impact forces, which are dependent on certain process parameters (these process parameters can be set by the operator of equipment for cleaning and maintenance of sewer systems).

2. Management of experimental research

To carry out an experimental research, it is recommended to follow a series of steps [8]:

1) recognition of and statement of the problem;
2) selection of the response variable;

3) choice of factors (process parameters), levels, and ranges;
4) choice of experimental design;
5) performing the experiment;
6) statistical analysis of the data;
7) conclusions and recommendations.

2.1 Recognition of and statement of the problem

After completing field of bibliography, can be formulated the research question is formulated as follows: study pressure water jets used in cleaning head sewerage systems, in order to produce effects depending on certain parameters involved in the process.

2.2 Selection of the response variable

Given the geometry of cleaning heads, in sewer system we deal with the issue of force (generated by pressure water jets) in two directions:

a) dislocation and release of deposits from the work area by pushing into outlet space (behind the cleaning head) through free water jets (cleaning heads);

b) use of water jet force for training the cleaning head and creating impact force of head in order to fracture, dislocation and breakage deposits (pointed heads, wire rope and chain scrapers, gliding heads).

Given the phenomena occurring under cleaning head sewer system, response parameter studied is the impact forces produced by pressure water jets.

2.3 Choice of factors involved in the process (process parameters)

For cleaning sewer, the parameters involved in the cleaning sewer process were identified in the references [7]. These parameters can be divided into two broad categories:

1) target parameters for deposit removal. This parameters which shall be defined according to the contact area between the water jet and the surface to be cleaned (deposit thickness, cleaning with, mass removal, cleaning rate);

2) process parameters, which can be divided into two groups. The first group refers to hydraulic parameters (work pressure p, volume flow Q, nozzle diameter D). The second group is the performance parameters (stand-off distance x, traverse rate v_t and impact angle α).

Parameters directly involved in determining the impact forces of pressure water jets are the process parameters (figure 1).

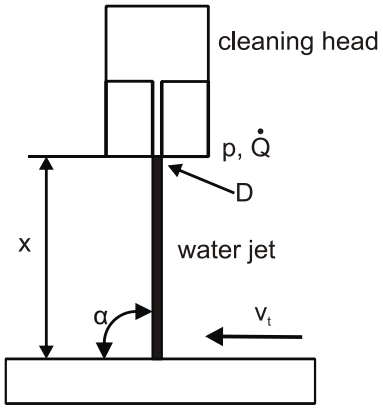

Fig. 1. Process parameters [7]

Because is studying the impact forces generated by the stationary jet it is eliminated the parameter traverse rate v_t. Volume flow Q is an indirectly parameter in the sense that it is determined by the operating pressure p of the jet and the nozzle diameter D.

It is necessary to study four parameters namely: p water pressure at the outlet of the nozzle, D nozzle diameter, x stand-off distance (between the nozzle and impact surface) and the angle α (between water jet and impact surface).

After determining the process parameters it is necessary to choose their values.
Usually, the pressure of water jets are used varies between 120-180 bar pressure to prevent the damage of the sewer pipes. The pressure p is established between 100 and 200 bars with an increment of 20 bars.
It is studying the impact forces in the sewers with a maximum diameter of 400 mm.
The stand-off distance x has been fixed at the values from x=25 mm to x=200 mm, with a step of 25 mm.
For working pressure and diameter sewer previously set, manufacturers recommend cleaning head with nozzle diameter D between 0.3 and 3 mm. As a result nozzle diameter D was set to values of D = 1 mm, 1.5 mm and 2 mm.
For cleaning heads used for sewers with diameters up to 400 mm, the usual value of the impact angle α is 75^0 [9]. If impact angles α decrease below 60^0 it leads to a drop in of the impact forces. Impact angle α was set to values α=60^0, 75^0 and 90^0. Table 1 presents the experimental domain established.

TABLE 1: Experimental domain

Parameter	Abbreviation	Values
Nozzle diameter D[mm]	A	1, 1.5, 2
Pressure p [bar]	B	100, 120,140,160,180,200
Impact angle α [^{0}]	C	60, 75, 90
Stand-off distance x [mm]	D	25, 50, 75, 100, 125, 150, 175, 200

2.4 Choice of experimental design

Type of experiment is used full factorial design. For this four established parameters and there levels, result a number of 3x6x8x3 = 432 experiments.
In order to achieve a statistical analysis of the results, each experiment requires a number of 3 to 7 replications [8]. For statistical analysis of the data, shall be conducted seven measurements for each experiment. It follows a number of measurements required 432x7 = 3024.
At a simple calculation, allocating just 10 minutes for each measurement and given preparation and end times for each day on which measurements are made, result a number of 120 days.
Considering this, in the first part of experimental research Taguchi method shall be used to determine the percentage of influence of parameters involved in the process (screening).
Further, based on the results from Taguchi method will be used full factorial design to study the impact forces.

2.5 Performing the experiments

In order to measure the impact forces, a stand for generating pressure water jets, as well as a device to measure the impact forces were designed and built.
Schematic diagram of the stand to generate a pressure water jet is shown in figure 2.

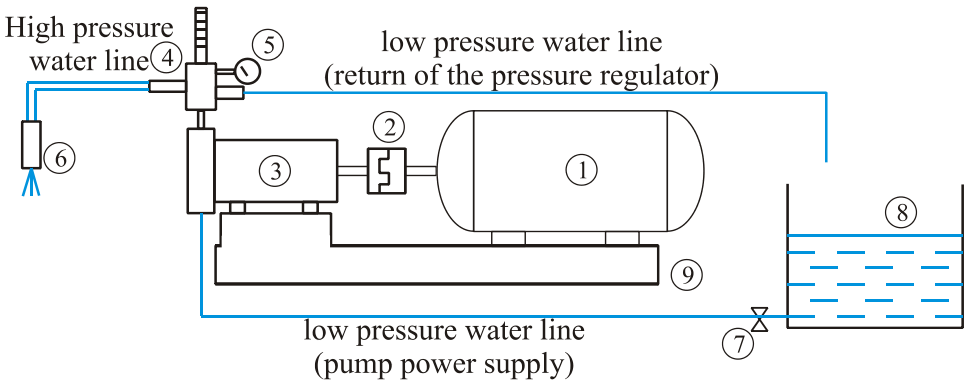

Fig. 2. Schematic diagram of the stand to generate pressure jet

Component parts of stand: (1) electric motor (2) flexible coupling; (3) high pressure pump, 4) pressure regulator, 5) pressure gauge, 6) nozzle, 7) tap water, 8) water tank, 9) chassis.
Water coming out of the high pressure pump (3) goes into the pressure regulator (4). Through it adjusts the pressure and flow of water in the path of the high pressure water. This pressure corresponds to the one at the outlet of nozzle.
In figure 3 is presented the stand to generate pressure jet.

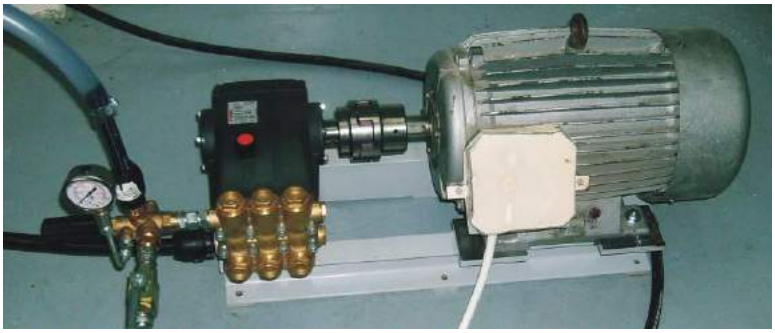

Fig. 3. Stand to generate pressure water jets

In figure 4 is represented the device for the measurement of the impact force of the water jet and a flat and rigid surface.

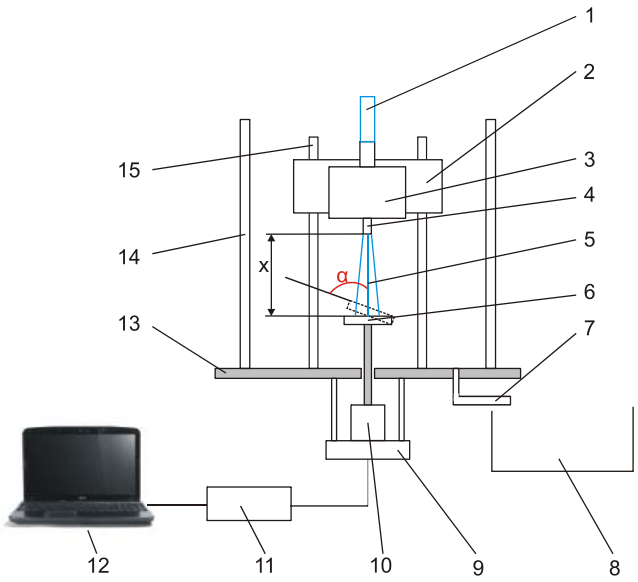

a) Diagram of the device b) Device realized

Fig. 4. Diagram of the device for the measurement of the impact force of the water jet

The main component parts of the device are:1) high-pressure water hose, 2) support nozzle, 3) nozzle block, 4) nozzle, 5) water jet, 6) flat and rigid target plate, 7) collection path water, 8) scaled container for measurement of the flow of water jet, 9) piezoelectric sensor mounting, 10) piezoelectric sensor, 11) data acquisition Personal Daq/3000, 12) computer for the processing of data; 13) support plate, 14) acrylic tube, 15) rods for adjusting distance x.
From the high pressure water hose (1) the water comes at a certain pressure p desired. A water jet (5) is generated at the outlet of the nozzle (4) that strikes the target plate (6), which it located at a certain distance x in front of the nozzle. The jet (5) generates an impact force at a time when it meets the target plate (6). This force produces axial movement of the target plate. This movement is converted into an electric signal by the piezoelectric sensor (10). Electrical signals are collected by data acquisition Personal Daq/3000 (11), which forwards data to a computer (12) using

DaqView soft processes. Thus, accurate data is obtained.
Using the Taguchi method was determining the percentage of influence of parameters involved in the process (screening). For each of the four parameters set (table 1) will use two values, the smallest and greatest value to determine their influence and interactions between them over the impact forces. In figure 5 are presented the results.

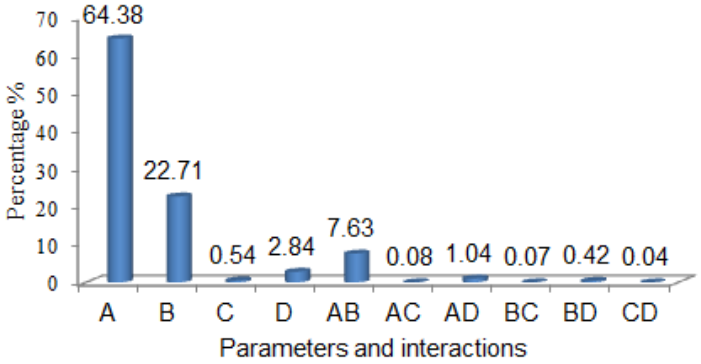

Fig. 5. The percentage of influence of parameters and their interactions

In conclusion, after screening using Taguchi method result, for experimental domain established, only three factors have an important contribution to the impact forces: diameter D, pressure p and angle α.
In the next step, are established the experimental domain to determine the impact forces using the full factorial design (table 2).

TABLE 2: Experimental domain for full factorial design

Parameter	Abbreviation	Values
Nozzle diameter D[mm]	A	1, 1.5, 2
Pressure p [bar]	B	100, 120,140,160,180,200
Impact angle α [^{0}]	C	60, 75, 90
Stand-off distance x [mm]	D	25

For those 3 parameters established (table 2) (after screening using Taguchi method), a number of 3x6x8x1 = 144 experiments results. With seven measurements for each experiment, result a number of 1008 measurements, three times less than was previously established (before carrying out screening using the Taguchi method).

2.6 Statistical analysis of the data
An important role in an experimental research has statistical analysis of the data. Statistical analysis of experimental data obtained certifying that the values are real values of the process studied they are not affected by the system errors or measurement errors.
Statistical analysis of the experimental data consists of:

1) verifying the aleatory character of data. This will be performed using the Young test;
2) To verify the normality of the experimental data distribution will be used Shapiro-Wilk normality test. This test is used for data sets that do not exceed 50 values. In the present case the each data sets have a number of seven values;
3) Identifying data affected by aberrant errors can be accomplished by applying the Romanowski test. This test for identifying data affected by aberrant errors having applies for a number of up to 20 data.

After performing statistical analysis of the data can proceed to modelling the experimental data in order to obtain those mathematical models which best describe the process. With the results of

values of impact forces, for the experimental domain established can be determined an equation who described the impact forces according to the values of process parameters involved.
In figure 6 are presented the chart stages planned in the design of experiment to study the impact forces of water jet.

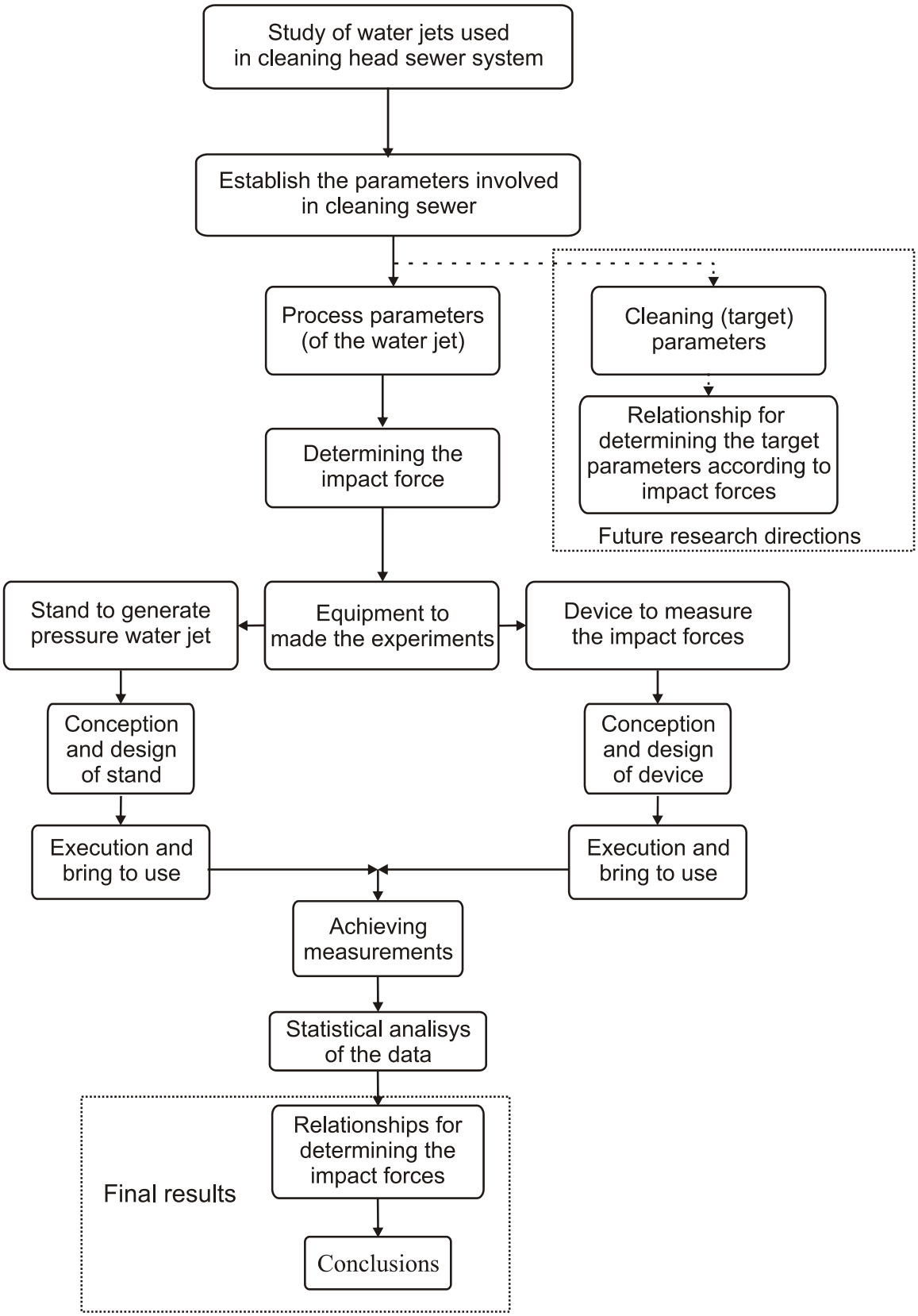

Fig. 6. Chart stages planned in the design of experiment to study the impact forces of water jet.

3. Conclusions

To carry out an experimental research, it is necessary to follow a series of stages, broadly presented in scientific literature. An experimental research aims to obtain results which then can be used to improve the study process.
In the present work was performed the study of impact forces produced by water jets used in cleaning sewer system.
In order to realised the experiments it was necessary to designed and built a stand for generating pressure water jets and a device to measure the impact forces.
The impact forces are depending on certain process parameters. In first stage were determined four process parameters: p water pressure at the outlet of the nozzle, D nozzle diameter, x stand-off distance (between the nozzle and impact surface) and the angle α (between water jet and impact surface). For experimental domain established was necessary a number of 432 experiments. In order to achieve the statistical analysis of experimental data obtained for each experiment was made seven measurements. Result a number of 3024 measurement.
In the first stage of research was used Taguchi method to determine the influence of parameters.
Result that only three parameters have an important contribution to the impact forces: diameter D, pressure p and angle α.
Next, it is used full factorial design to determine the values of impact forces. In this stage it was necessary to make 1008 measurements.
So, using Taguchi method to realise a screening of process, the number of necessary measurements decreased from 3024 to 1008, resulting savings of time and money.
An important part of the design of experiment is represented by statistical analysis of the data obtained.
A direction of further research is to study the cleaning (target) parameters, to determine relationship between these and impact forces.

References

[1] W. F. Adler, "The Mechanics of Liquid Impact", Treatise on Materials Science and Technology, 1979, pp. 127-183;
[2] A., Guha, R. M., Barron, R. Balachandar, "An Experimental and Numerical Study of Water Jet Cleaning Process", Journal of Materials Processing Technology, pp. 610-618, 2011;
[3] S. J., Leach, G. L. Walker, "Some Aspects of Rock cutting by High Speed Water Jets", Philosophical Transactions of the Royal Society of London, Series A, Vol. 260, pp. 295-308, July 1966;
[4] M. C. Leu, P. Meng, E. S. Geskin, L.Tismeneskiy, "Mathematical modelling and experimental verification of stationary waterjet cleaning process", Journal of Manufacturing Science and Engineering, 120(3), 1998, pp. 571-579;
[5] Yayu Liu, Fei Ma, Hui Xie, Yong Li, "Development of Impact Test System for Waterjet Descaling Nozzles with LabVIEW", Web Information Systems and Mining (WISM), 2010 International Conference on , vol.1, no., pp. 3-7, Oct. 23-24, 2010;
[6] I L. Marcu, C. Ciupan, S, "Alternating Flow Hydraulic Generator for Water Jet Cutting Systems", "Hidraulica" (No. 1/2016) Magazine of Hydraulics, Pneumatics, Tribology, Ecology, Sensorics, Mechatronics, ISSN 1453 – 7303, pp.61-66;
[7] A. W. Momber, "Hydroblasting and Coating of Stell structures", Oxford: Elsevier Ltd, 2003;
[8] D.C. Montgomery, "Design and analysis of experiments", 8th edition, Wiley, 2013;
[9] ***http://www.enz.com., accessed in November 2016.

Pressure Setting and Control System with PWM Direction Control Valve

PhD Prof. **Mihai AVRAM**[1], PhD Teach. Assist. **Victor CONSTANTIN**[2],
PhD Assoc. Prof. **Despina DUMINICĂ**[3], PhD Prof. **Constantin BUCŞAN**[4]

[1] University POLITEHNICA of Bucharest, mavram02@yahoo.com

[2] University POLITEHNICA of Bucharest, victor.f.constantin@gmail.com

[3] University POLITEHNICA of Bucharest, despina_duminica@yahoo.com

[4] University POLITEHNICA of Bucharest, constantin_bucsan@yahoo.com

Abstract: *The paper presents a system that sets and controls pressure in a given volume. The system features an original solution of PWM direction control valve. Intelligent control algorithms are implemented and comparatively tested in order to improve system performance.*

Keywords: *Pneumatics, pressure setting and control, PWM direction control valve, fuzzy logic, PI controller*

1. Introduction

The General Union Environment Action Programme to 2020 [1] states that more action is needed to protect nature and strengthen ecological resilience, boost resource-efficient, low-carbon growth, and reduce threats to human health and wellbeing linked to pollution, chemical substances, and the impacts of climate change. In line with this strategy, the Horizon 2020 Framework Programme for 2016-2017 [2] aims to prioritize the actions which take a systemic approach to promote a more resource efficient, greener and more competitive economy as a key part of smart, inclusive and sustainable growth.
Large scale promotion of pneumatic driving systems constitutes an efficient measure towards reaching these goals. An assessment of the field of pneumatic driving [3] leads to the identification of the main tendencies and perspectives, namely:

- strong development of pneumatics in the future; intensive fundamental and applied research that aims reducing the negative effects induced by the physical properties of the working fluid (such as reduced viscosity and high compressibility) is required;
- embedment of informatics in pneumatic driving systems and equipment, leading to the development of pneutronic systems;
- increase of reliability, functional accuracy and static and dynamic performance of actual pneumatic devices, as well as development and building of new types of high performance pneumatic equipment.

In this context, the paper presents an original conception pneutronic system aimed to set and control pressure in a given volume chamber using a PWM direction control valve developed by the authors. This type of equipment was chosen due to its speed, accuracy and relatively reduced price compared to other solutions with similar performances, features that recommend it for a large range of applications, from positioning systems to biomedical engineering [4 - 11].

2. Structure of the developed system

The system aims to set the pressure in a tank chamber of fixed volume V at a target value $P_t$and to maintain it constant. The functional scheme of the system is presented in Figure 1.
The structure of the system includes the following components:

- the tank Rz;
- pneumatic 3/3 direction control valves $M_1 \ldots M_{n+1}$; the valve M_n features a special construction developed by the authors
- pressure sensor T_P;
- microcontroller μC.

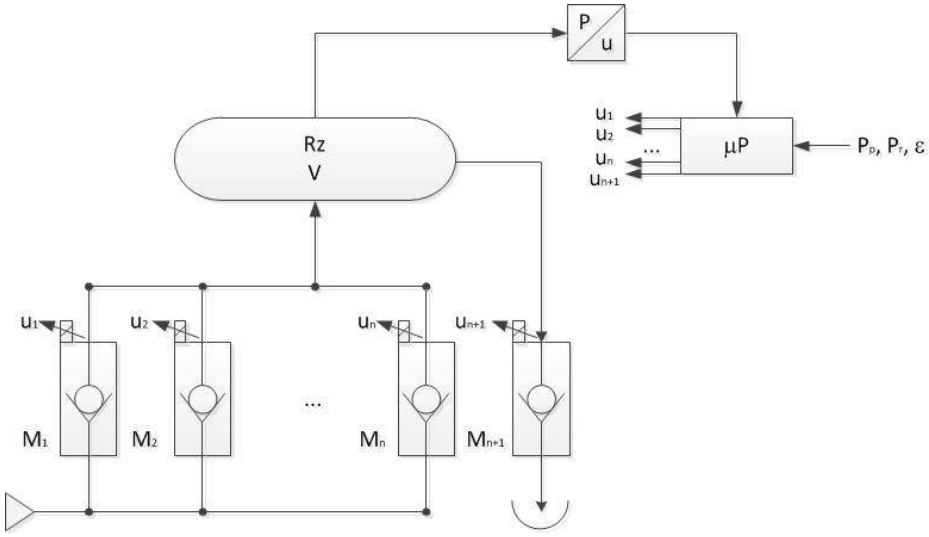

Fig. 1. Functional scheme of the system

The first (*n-1*) modules $M_1..M_{n-1}$ are controlled using PNM (Pulse Number Modulation) technique: all the modules are controlled through control signals of the same constant value ($u_1 = u_2 = u_{n-1}$); in this case, the resulted flow will be proportional to the number of controlled valves. The flow delivered by the n[th] module M_n is controlled based on the modulation of the input signal of the digital valve using the PWM technique. The module M_{n+1} is used for draining or for generating a controlled flow loss $\Delta\dot{m} = f(u_{n+1})$.

Two stages are discerned during the functioning of the system if the initial pressure in the tank is assumed equal to the atmosphere pressure P_0:

- 1[st]stage: the direction control valves$M_1..M_{n-1}$are open (in the presence of the control signals$u_1 = u_2 = u_{n-1}$); the filling of the tank occurs through a flow section equal to the flow section $S_{n1} = (n-1)\cdot S_{nm}$, S_{nm} being the flow section of a module; the pressure in the tank will consequently rise; when it equals an imposed threshold pressure P_p the control signals$u_1 \ldots u_{n-1}$ stop and the valves$M_1..M_{n-1}$ are set on preferred position;
- 2[nd] stage: if threshold pressure P_p is reached, the valve $M_n$is supplied till the target value P_r is reached; this is the moment when the PWM control signal u_n stops.

Figure 2 presents the functional scheme of the special construction PWM direction control valve developed by the authors (the valve M_n from figure 1).

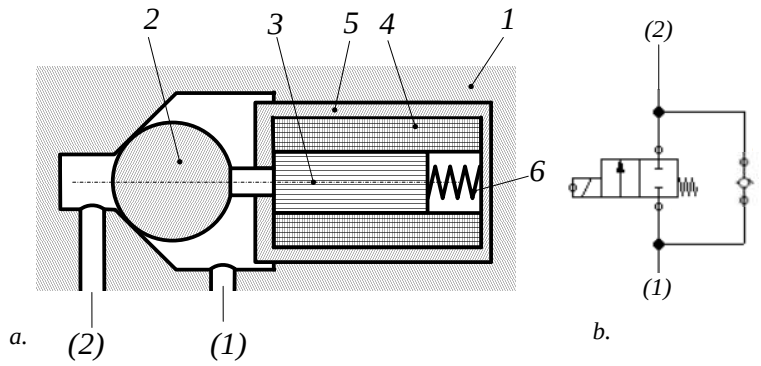

Fig. 2. Functional scheme of the PWM direction control valve. 1 – body; 2 – ball; 3 – mobile armature of the electromagnet; 4 – coil; 5 – fixed armature; 6 – spring; (1) – supply orifice; (2) – consumer orifice.

It is a small sized device (D_n = 2...3 mm) of type 2/2 or 2/3, having a preferred position, and is electrically controlled using a magnet that can function at high working frequencies (≈ 200 Hz). An airflow is obtained this way through the consumer orifice (2), corresponding to the mean value of the real flow that passes through the internal circuit of the device.

The device does not achieve a continuous control of the instantaneous flow, but controls the mean flow in direct proportion to the duty cycle. Among the advantages of the proposed solution are: reduced price compared to proportional pneumatic direction control valves, elimination of hysteresis and its bothersome effects, very good repeatability.
Various control techniques can be used [12], based on the combining of different micro direction control valves of the same type grouped together in valve arrays, as well as on the controlling of the opening and closing times of the valve section.

3. Mathematical model of the pressure setting and control system

The notations used to describe the mathematical model are presented in Table 1.

TABLE 1: Notations used to describe the mathematical model

Notation	Meaning	Notation	Meaning
V	fixed volume of the tank chamber	S_{n1}	equivalent nominal section of the first *(n-1)* modules $M_1 \ldots M_{n-1}$
P_r	the target value of the pressure to be achieved in the chamber of fixed volume V (the set pressure)	S_{nm}	nominal section of a module
P	pressure in the chamber of fixed volume V	T_a	temperature in the chamber of fixed volume V
P_a	supply pressure	χ	adiabatic constant; $\chi = 1.4$ [-]
P_p	threshold pressure; when is reached, the slide of the classical direction control valve *DC* moves back to the preferred position	$\dot{m}$	flow rate of the fluid that fills the chamber
P_0	atmosphere pressure	T	period of the pulses
R	universal gas constant; $R = 287.04$ [$m^2/(s^2 \cdot K)$]	t_a	pulse duration

The mathematical model can be suggestively described using a block structure, as presented in continuation.
The variation of pressure in the chamber of fixed volume V can be written:

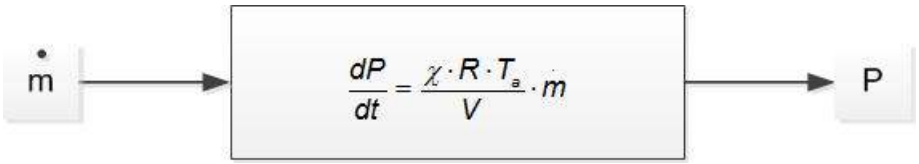

(1)

where:

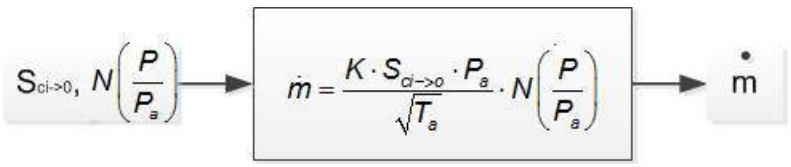

(2)

$$K = \sqrt{\frac{\chi}{R} \cdot \left(\frac{2}{\chi+1}\right)^{\frac{\chi+1}{\chi-1}}}\ ;\ K \cong 0.04042 s\sqrt{K}/m$$

$S_{ci->o}$denotes the flow section through the valve. In function of the functioning stage, it can be described as following:

$$P,\ S_{cm} \rightarrow \left\{ S_{ci->o} = \begin{cases} S_{n1} & \text{if} \quad P_0 \le P \le P_p \\ S_{cm} & \text{if} \quad P_p \le P < P_r \end{cases} \right\} \rightarrow S_{ci->0} \tag{3}$$

The flow sectionS_{cm} through the PWM controlled direction control valve can be written:

$$t \rightarrow \left\{ S_{cm} = \begin{cases} S_{nm} & \text{if} \quad rem\left(\frac{t-t_p}{T}\right) \le t_a \\ 0 & else. \end{cases} \right\} \rightarrow S_{cm} \tag{4}$$

The function *rem* denotes the remainder of the division between the two values; t_p denotes the moment of time when the pressure P_p is reached (and the PWM controlled valve is actuated).

$N\left(\frac{P}{P_a}\right)$ denotes the flow rate number.

The flow rate number $N\left(\frac{P}{P_a}\right)$ is defined as following:

$$P \rightarrow \left\{ N\left(\frac{P}{P_a}\right) = \begin{cases} 1 & if \quad 0 < \frac{P}{P_a} \le 0.528 \\ a \cdot \left[\left(\frac{P}{P_a}\right)^{2/\chi} - \left(\frac{P}{P_a}\right)^{(\chi+1)/\chi} \right]^{1/2} & if \quad 0.528 < \frac{P}{P_a} \le 1 \end{cases} \right\} \rightarrow N\left(\frac{P}{P_a}\right) \tag{5}$$

$$a = \sqrt{\frac{2}{\chi - 1} \cdot \left(\frac{\chi + 1}{2}\right)^{\frac{\chi+1}{\chi}}}\ ;\ a = 2.6143[-].$$

The mathematical model based on these relations is depicted in Figure 3.

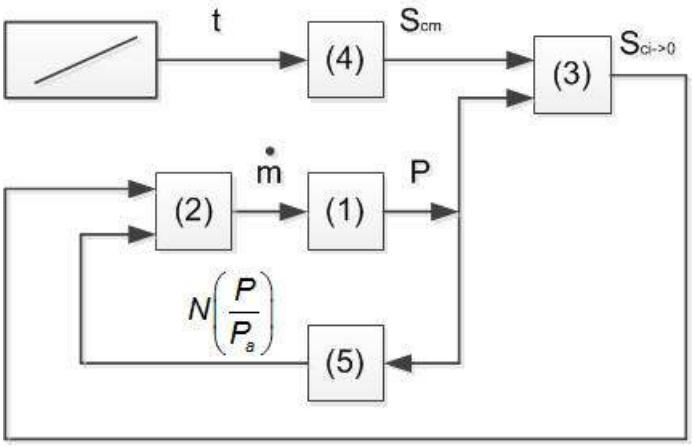

Fig. 3. The block structure that describes the mathematical model of the system.

The analysis of the functioning of the automated system for pressure setting and control can be performed analytically as well as numerically [13].

4. The control algorithm

A series of control algorithms were tested in order to improve system performance:
- the use of a constant duty cyclet_a/T=50% (classical work algorithm);
- dynamic variation of the pulse duration t_a using fuzzy logic;
- implementation of a PID controller.

The three cases were numerically simulated using SIMULINK. The two controllers (fuzzy and PID) were implemented with the help of predefined blocks chosen from the software libraries. The choice of the method that allowed the filling of the tank in the shorter time and with the smallest error constituted the purpose of the simulation.
Three triangular sets of inputs, respectively outputs, directly connected, were used in the case of the fuzzy controller. The physical setting of the input and output values was possible also due to the existence of an experimental set-up in an incipient phase.
The ideal control law was used in the case of the PID controller [14]:

$$u(t) = K_R \cdot \varepsilon(t) + K_I \cdot \int \varepsilon(t)dt + T_d \cdot \frac{d\varepsilon}{dt} \tag{6}$$

Figure 4 presents the results of the simulations, obtained for a target pressure P_r=3bar, using a threshold pressure P_p=2bar. The frequency of the PWM signal was fixed at a value of 10Hz in all three cases in order to be able to compare results.

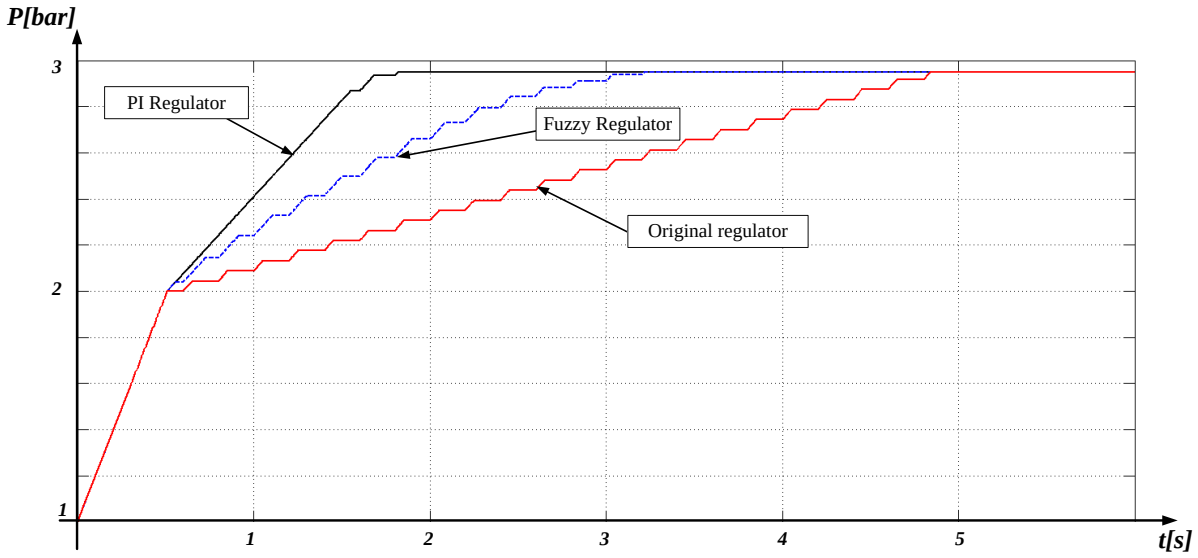

Fig. 4. Comparison between the performances of the three control algorithms

It can be noticed that the classical work algorithm (which implies a fixed duty cycle of t_a/T=50%) leads to the filling of the tank in the range [P_p...P_r] in a time that is twice the time required when the fuzzy algorithm is used. In the case of the latest, a decrease of the pulse duration was noticed in the proximity of the target pressure. The target pressure can be more rapidly reached in the case of the classical algorithm if the duty cycle is increased, but the error will also increase.
In the case of PID control, proportional, integrative and derivative gains were chosen according to Ziegler-Nichols method. It implies the initial setting of all values to 0, followed by the increase of the proportional component till obtaining constant oscillations of the system. The absence of overshoot, as well as of a physical way of compensating its occurrence led to the removal of the derivative gain, finally resulting a PI controller.

According to simulation results, the use of the PI algorithm leads to the rapid filling of the tank till an intermediary pressureP_{int}>P_p, behaviour corresponding to a duty cycle of 100%. The decrease of the duty cycle as result of the controller intervention can be noticed in the range [P_{int}…P_r].

5. Testing and validation of simulation results

A test set-up was developed in order to validate the simulation results. It includes an electronic control unit based on an Atmel microcontroller, as well as the electronics needed in order to amplify the control signals from the TTL level to the level required for driving the valve electromagnets (24V/0.3A, respectively 7V/2A). Signals were amplified using MOSFET (IRF510) and BJT(BD139) transistors, according to system requirements. Voltage regulators (LM78XX, respectiv LM338) were also used due to the various levels of stabilised voltage needed in the system (5V, 7V, 12V si 24V) in order to obtain an unified supply of the electronic unit. The system works in closed loop, the current pressure at the valve level being read by an analog voltage output pressure sensor. The principle scheme of the set-up is presented in Figure 5.

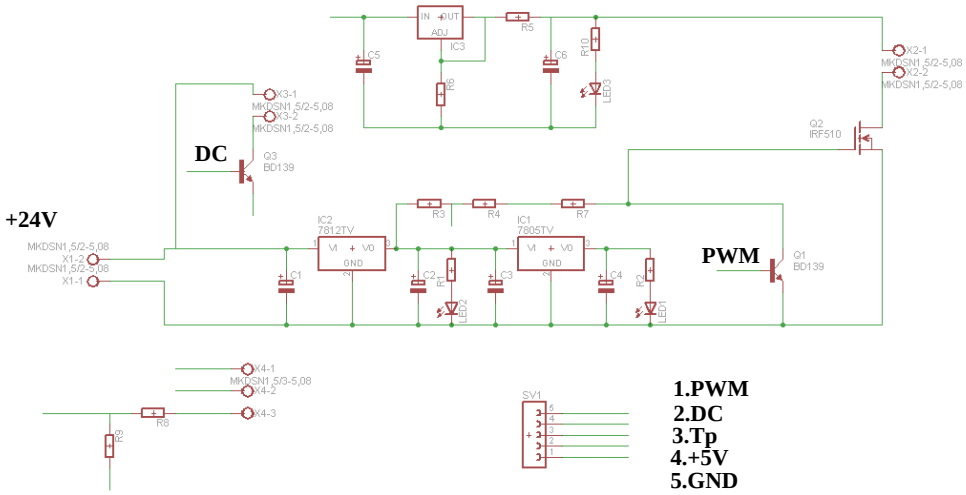

Fig. 5. The electronic scheme of the control unit

The Atmega328 microcontroller is programmed in the C language and contains the code needed for the control of the pressure setting system, including the control algorithms. The system contains also a FTDI interface that allows the collection and storage of data regarding the system performance on a PC for further processing and interpretation.
The experimental research validated the simulation results.

6. Conclusions

The research proves that the proposed system allows the setting of a target pressure in a tank with an imposed error. The system is easy to configure, being mostly composed of standard equipment. An important functional role is played by the original conception PWM direction control valve. The construction of the device is simple and does not require sophisticated manufacturing and mounting technologies. The implementation of intelligent control algorithms increases the system performance, the best results being obtained when a PI controller is used.

References

[1] 7th EAP — The new general Union Environment Action Programme to 2020 "Living well, within the limits of our planet", available at: http://eur-lex.europa.eu/legal-content/EN/TXT/?uri=CELEX:32013D1386
[2] HORIZON 2020 - Work Programme 2016 - 2017 "Climate action, environment, resource efficiency and raw materials", available at: http://ec.europa.eu/research/participants/data/ref/h2020/wp/2016_2017/main/h2020-wp1617-climate_en.pdf

[3] G.Vogel, E. Mühlberger, „L'univers fascinant de la pneumatique", Würzburg, Germany, 2001;
[4] G. Belforte, S. Mauro, G. Mattiazzo, "A method for increasing the dynamic performance of pneumatic servosystems with digital valves", Mechatronics, Vol. 14, pp. 1105-1120, 2004;
[5] K. Ahn, S. Yokota, "Intelligent switching control of pneumatic actuator using on/off solenoid valves", Mechatronics, Vol. 15, pp. 683-702, 2005;
[6] H.E. Fawaz, M. Abdul Aziz, „Position control of a pneumatic actuator using digital valves and fuzzy PI controller", International Journal of Mechanical and Mechatronics Engineering, Vol. 16, Iss.1, pp. 10-22, 2016;
[7] M. Shiee et al., „An experimental comparison of PWM schemes to improve positioning of servo pneumatic systems", The International Journal of Advanced Manufacturing Technology, Vol. 82, Iss.9, pp. 1765-1779, 2016;
[8] S. Hodgson, M. Tavakoli, M.T. Pham, A. Leleve, „Dynamical model averaging and PWM based control for pneumatic actuators", Proceedings of 2014 IEEE International Conference on Robotics and Automation ICRA 2014, Hong Kong, pp. 4798 – 4804, 2014;
[9] G. Figliolini, P. Rea, „Mechatronic design and experimental validation of a novel robotic hand", Industrial Robot: An International Journal, Vol. 41, Iss. 1, pp. 98 – 108, 2014;
[10] V.T. Jouppila et al., „Sliding mode control of a pneumatic muscle actuator system with a PWM strategy", International Journal of Fluid Power, Vol. 15, Iss. 1, pp. 19-31, 2014;
[11] K. Takanaka, T. Nakamura, "Development of pneumatic control system for walking assist using dual On/Off valves", 2013 IEEE International Conference on Mechatronics, Vicenza, Italy, pp. 138-143, 2013;
[12] M. Avram, "Acţionări hidraulice şi pneumatice. Echipamente şi sisteme clasice şi mecatronice", Editura Universitară, Bucureşti, 2005;
[13] M. Avram, D. Duminică, L.A. Cartal, "Theoretical analysis of a pressure setting and control system with PWM direction control valve", Proceedings of the ACME 2016 Conference, Iaşi, Romania, 2016;
[14] I. Dumitrache, „Ingineria reglării automate", Politehnica Press, Bucureşti, 2010.

Role of Engine Design in Combustion Process

Sanjay SINGH[1]

[1] Indus University, India, ssd776776@gmail.com

Abstract: *Structural design of engines plays an important role in combustion based noise in engines. In this work the attenuation of engines has been overviewed.*

Keywords: *combustion process, combustion noise, structural design*

1. Introduction

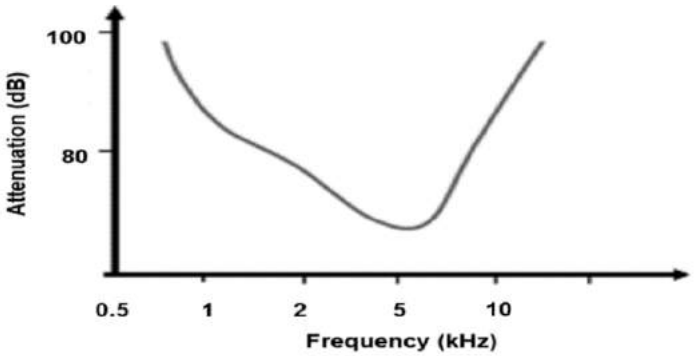

Fig. 1. Attenuation curve of engine[1-10]

This curve can be divided into three distinct regions:
a) Below 2000Hz-in this range the attenuation is very high as most of engine parts have high stiffness with their natural frequencies in low or mid ranges.
b) In mid frequency ranges of 2000Hz-5000Hz, the attenuation is small as most of natural frequencies of engine parts fall in this range.
c) Above 5000Hz- natural frequencies of most of the parts are above the natural frequencies of most of the parts, hence attenuation is quite high.

2. Background

Controlling the rate of pressure is the key to control combustion noise which mainly depends upon the ignition delay and quantities of combustion gas formed during delay period. A shorter delay period means lesser amount of combustible gas formed in the cylinder and hence lesser combustion noise. Hence delay period must be reduced as much as possible to reduce combustion noise. Structure and layout of engine also plays an important role.
Increase in compression ratio and chamber temperature also shortens the delay period. However increase in compression ratio may cause rise in the piston slap noise. Various parameters of fuel injection system like angle of fuel injection, injection pressure, number of nozzles and fuel supply rate also affect the combustion noise in engines. An increase in the injector pressure leads to an increase in the amount of fuel accumulated in the ignition delay period and hence an increase in the combustion noise.
If other factors remain unchanged, an increase in engine speed increases the fuel injection rate and hence greater quantity of fuel is injected in the period of combustion delay which leads to an increase in combustion noise.
There are many approaches to control combustion noise. One of these includes reducing cylinder pressure spectrum typically in middle and high frequency ranges. Other include reducing ignition delay period or amount of combustible gases formed during this period. Increasing the stiffness of

parts, use of turbo charging process and use of split injection methods in engine cycle have also approved to be effective methods [11-20].

3. Factors affecting

The analysis of in cylinder pressure is one of the most common way to examine the combustion noise in diesel engines. Anderton and Priede were first to observe that abrupt combustion led to high frequency contents of in cylinder pressure spectrum [14].Crocker suggested that frequency contents up to 300 Hz were related to maximum cylinder pressure [15]. Between 300Hz-2000Hz they were related to first derivative of in cylinder pressure, whereas above 2000Hz were related to second derivative of cylinder pressure.
Previous works have shown a relationship between peak of combustion noise and overall heat release rate[16].Rusell has developed a technique based on block attenuation curve which is still most reliable one for study of combustion noise[17].It was observed that higher slopes of rate of heat release curves led to higher combustion noise irrespective of fuel injection timings[18].There is a tradeoff between combustion efficiency and noise generated due to combustion[19].Efficient combustion leads to higher heat release rate near top dead center which gives rise to high frequency components in noise spectrum. Late heat release rates leads to lower in cylinder pressures and hence low frequencies in combustion noise.

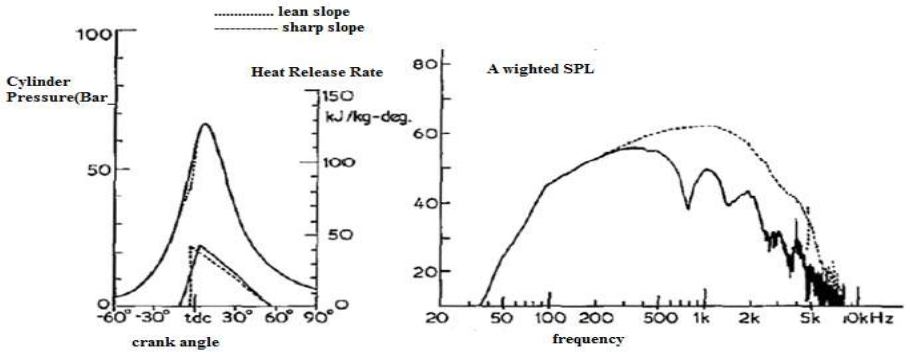

Fig. 2. Effects of heat release rate on combustion noise

It was observed that a 10dB reduction in sound pressure levels was possible without change in fuel consumption. However, there is a fall in efficiency of cycle and smoke emissions increase if ROHR is not terminated 50° BTDC [17].Combustion process in diesel engines vary with cycle which leads to variations in combustion noise [10].These variations may be attributed due to different fuel injection rates, compression ratios as well as difference in fuel spray process, mixture formation and flame propagation. Torregrosa has studied cyclic variations in combustion noise as given by figure no 2[11]. Variations may be attributed to resonance phenomenon occurring in combustion chamber.

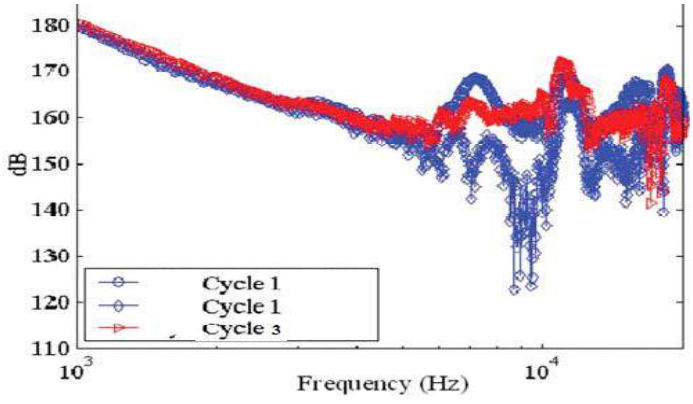

Fig. 3. Cyclic variations in combustion noise

4. Resonance phenomenon

Resonance process taking place in the combustion chamber effects the noise radiated from engines. Grover has observed high peaks in noise spectrum which may be attributed to this phenomenon [12].
Previous works have shown effects of gas temperature and effects of resonant frequency on high amplitude combustion chamber oscillations [13]. Hickling has observed several peaks in cylinder pressure spectrum by filtering data with cutoff frequencies in range 20Hz- 1500Hz which increase in amplitude with increase of load [14]. The frequencies of these peaks varied inversely with cylinder bore diameter. The resonant frequency (f_r) may be defined in terms of cylinder bore(B),axial length(L) and speed of sound(C) as:

$$fr=\sqrt{(\frac{K}{2L})^2+(\frac{q_{m,n}}{B})^2} \quad (1)$$

Where m,m,k determine circumfencial, axial and radial modes.

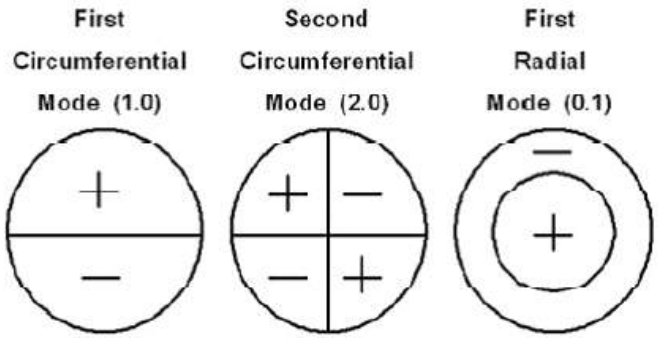

Fig. 4. Various modes of combustion chamber cavity

5. In cylinder pressure decomposition method

The signal processing methodology to decompose cylinder pressure signals was first proposed by Payri [15].In this methodology the cylinder pressure signals were decomposed into three parts namely-Combustion pressure, resonance pressure and compression pressure. The combustion art which is strongly dependent on rate of heat release is defined by injection strategy in engines. Using suitable cutoff frequencies motored part of pressure signal was isolated from excessive pressure signals. Figure no 4.78 shows results of such a methodology adopted for a cylinder pressure signal.

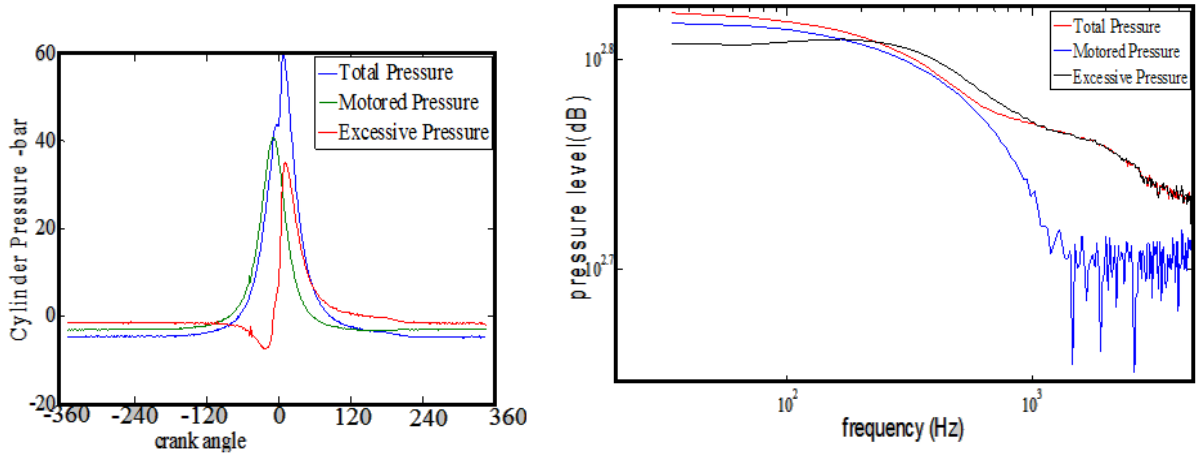

Fig. 5. Time and frequency decomposition of Cylinder pressure signal

As evident from these figures, motored pressure signal dominates the pressure spectra at low frequency ranges. By subtracting the motored pressure signal from total pressure signal, the excessive part of signal can be obtained. The resulting signal has contributions due to both resonance as well as combustion pressures. Resonance portion is clearly visible with fluctuating peaks in pressure spectra. Hence it can be isolated by filtering excessive pressure signal using high pass filter. The resulting resonance signal can be subtracted from excessive portion to obtain contribution due to combustion process. Figure no 4 shows total decomposition of cylinder pressure signal. It is evident from the lot that contribution due to combustion portion dominates in mid frequency range whereas the resonance phenomenon dominates at high frequency ranges [16].

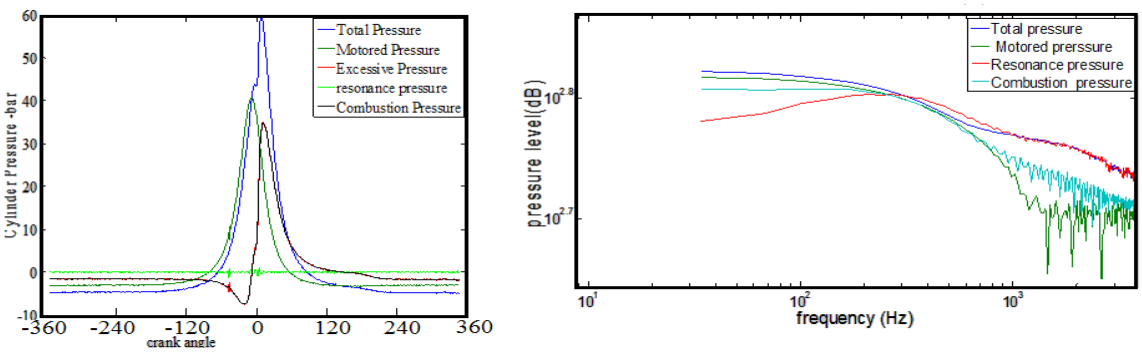

Fig. 6. Total decomposition of Cylinder pressure signal

The decomposed signals can be used to calculate noise indices defined in terms of ideal engine speed as:

$$I_n = n\log[\frac{N}{N_{ideal}}] \quad (2)$$

$$I_1 = [\frac{N}{N_{ideal}}]\ [\frac{(\frac{dp}{dt})_{pilot} + (\frac{dp}{dt})_{main}}{(\frac{dp}{dt})_{motored}}] \quad (3)$$

$$I_2 = 10\log(10^6 \int (\frac{P_{residual}{}^2}{P_{motored}{}^2})dt \quad (4)$$

Where $(\frac{dP}{dt})_{pilot}$ is maximum pressure gradient during pilot injection period , $(\frac{dP}{dt})_{main}$ is maximum pressure gradient during main injection, $P_{residual}$ is residual pressure and $(\frac{dP}{dt})_{motored}$ is maximum pressure gradient in motored pressure signal.

These indices can be further used to find overall noise (ON) emitted from engine as:

$$ON = C_0 + C_1 I_1 + C_2 I_2 + C_n I_n \quad (5)$$

Where constants C_0, C_1, C_2 and C_n depend upon size of engine

6. Mathematical Model of Generation of Combustion Noise

In wavelet transformation complex morlet wavelet can be used as mother wavelet. A morlet wavelet may be defined in terms of central frequency f_c and bandwidth f_b as:

$$\psi(t) = \frac{1}{\sqrt{\pi f_b}} e^{i2\pi f_c t}\ e^{\frac{-t^2}{f_b}} \quad (6)$$

Figure no 6 shows real and imaginary parts of such a morlet wavelet having $f_b = 1.5$ and $f_c = 1$

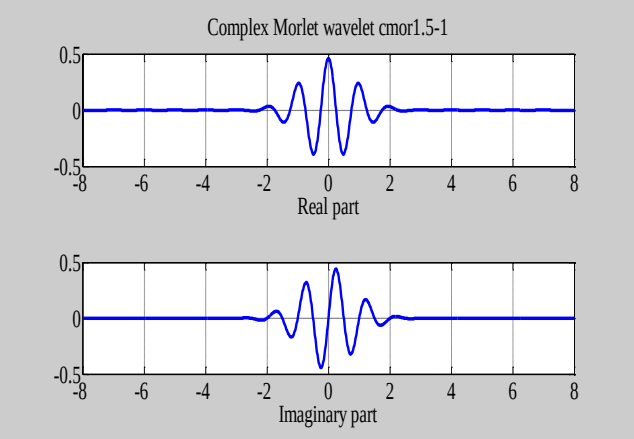

Fig. 7. Complex Morlet Wavelet

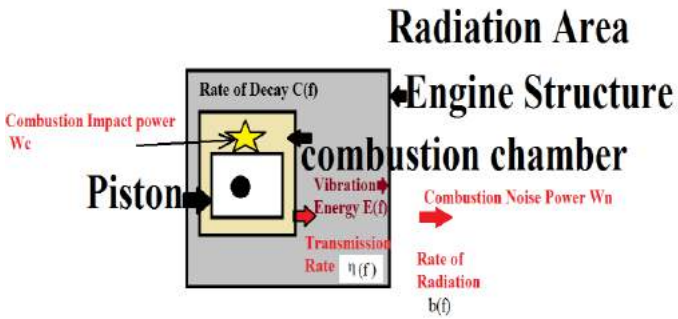

Fig. 8. Noise Generation Model

Figure no 7 shows a transient model of combustion noise generation in engines. This model can be analyzed by following three processes: generation of vibrational energy in combustion chamber due to combustion process, decay of energy in the engine structure and finally radiation of energy around engine surface.
The combustion process in engine generates combustion impact power (Wc) which can be expressed in terms of in cylinder pressure (p), impedance of medium (ρc) and cylinder surface area (A) as:

$$Wc = \frac{p^2}{\rho c} A \tag{7}$$

The available energy at engine surface can be expressed in terms of transmission rate coefficient η(f) as:

$$E(f) = \eta(f) \int_0^t W_c dt \tag{8}$$

Differentiating both sides of this equation we have:

$$\frac{d}{dt}\left(E(f)\right) = \eta(f) W_c \tag{9}$$

Taking into account the decay rate this equation gets modified as:

$$\frac{d}{dt}(E(f)) = \eta(f) W_c - C(f)E(f) \tag{10}$$

Where the decay constant C(f) may be defined as :

$$C(f) = -\frac{d[\log(Wn))]}{dt} \tag{11}$$

$$\frac{d}{dt}(W_n) = b(f)\eta(f) W_c - C(f)\, W_n(f) \tag{12}$$

Figure no 4.85-4.89 shows the plots of combustion impact power plotted for tests enlisted in table no 4.1 using reference value of W_0 as 10^{-12} Watts.

As clear from these results, the impact power had higher value at lower frequencies over a long crank angle duration. There was a fall in value of impact power with delay in injection period of fuel.

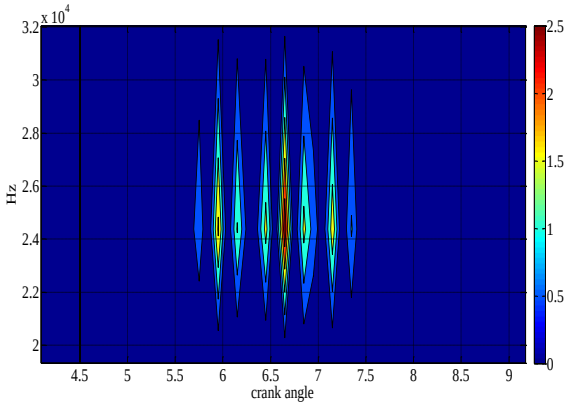

Fig. 9. Combustion Impact power (Case1)

7. Evaluation of Combustion Noise methods

A combustion noise measurement technique has been proposed by Lucas [7]. Austin & Priede have shown that combustion noise was most dominant in the frequency range 800Hz- 4kHz. Acoustic measurements of noise outside the engine may be used for combustion noise analysis only when the engine is operated in such a way that contribution of combustion events towards the noise emissions is maximum. This can be achieved without changing mechanical noise either by either operating the engine with advanced injection timing or by changing Cetane number of fuel used. Russell has used alkyl blended fuel to maximize in cylinder pressure so that combustion noise becomes dominant [7].

Structural attenuation of engine structure also plays a vital role in determination of combustion noise. Austin and Priede were able to determine this function by subtracting spectrum of in cylinder pressure level from the spectrum of noise emissions recorded at a distance of 0.9 m from engine structure [7]. Value of structure response functions fell by 10dBA in 500Hz to 5kHz range [7]. More recently AVL has developed a combustion noise meter which based on analysis of engine indicator diagram on frequency domain. Good correlation was observed when the data from this noise meter has been compared with that computed results from computer programming. Figure no 4.95 shows structural response functions of a group of 9 engines as recorded by AVL noise meter. The response of direct injection high speed diesel engines falls by 12dB over 5kHz frequency range [7].

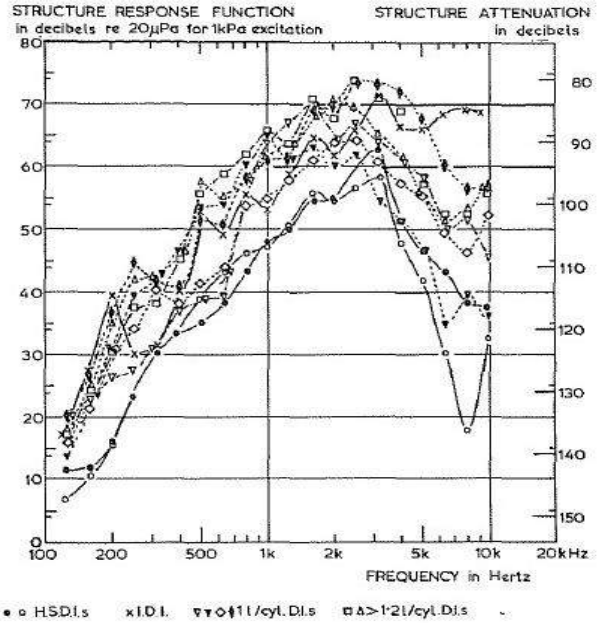

Fig. 10. AVL Structural response function and structural attenuation

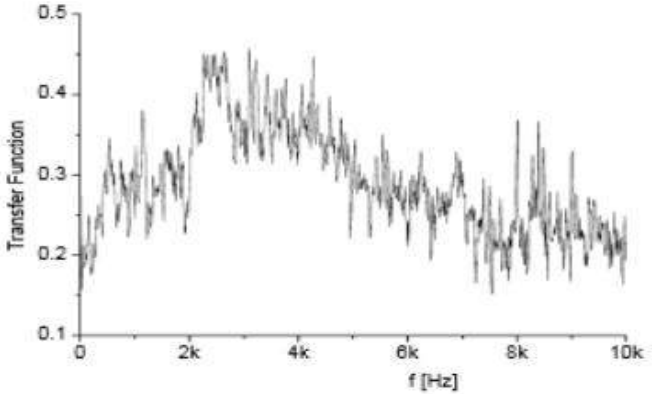

Fig. 11. Transfer function obtained by explosive charge

Shu has predicted this transfer function by setting an explosive charge in cylinder at a locked crank angle position as seen from figure no 11. Different functions for various designs of combustion chambers and different explosion charges were compared.
All the above discussed methods use expensive and time consuming methodology to analyze the transfer function of combustion noise, consequently an alternative method of analysis has been studied which evolves use of which include Cepstrum analysis.
The aim of this part is to provide an overview of combustion noise generation process. This was done by analyzing the methodology provided in previous works done. Engine combustion noise originates from combustion process taking place in cylinder. When fuel is injected inside the combustion chamber where high pressure air is present, then part of ignitable gas starts to burn causing a rapid rise in pressure as well as temperatures inside combustion chamber. The pressure wave thus generated also strikes the walls of combustion chamber causing resonance of structure. The vibrations are radiated in air through engine structure and are perceived as combustion noise.
In actual practice it is difficult to distinguish between combustion noise and piston slap as both coincide near top dead center positions. For sake of convenience it is assumed that combustion noise originates due to pressure vibrations inside engine cylinder and is transmitted to cylinder cover, piston, connecting rod, crank shaft and engine surroundings. Mechanical noise includes noise from piston-liner impact, valve operations, pump operations, injector operations as well as operation of various accessories and valve trains. Generally for indirect injection diesel engines and gasoline engines, the combustion process is less severe as compared with diesel engines; hence the combustion noise is lesser as compared with mechanical noise [20-24].

References

[1] C. Tung Simon, M.L. McMillan, "Automotive tribology overview of current advances and challenges for the future", Tribology International 2004; 37:517–35;
[2] D.F. Li, S.M. Rhode, H.A. Ezzat, "An automotive piston lubrication model", ASLE Transactions 1983; 26(2):151–60 ;
[3] V.W. Wong, T. Tian, H. Lang, J.P. Ryan, Y. Sekiya, Y. Kobayashi, et al., "A numerical model of piston secondary motion and piston slap in partially flooded elasto hydrodynamic skirt lubrication", SAE paper no. 940696, 1994;
[4] S. Jiang, J. Cho, "Effects of skirt profiles on the piston secondary movements by the lubrication behaviors", International Journal of Automotive Technology 2004; 5(1):23–31;
[5] A. Gupta, S. Narayan, "Electrical Analogy of Liquid Piston Stirling Engines", Hidraulica Magazine no 2 (2016): 58;
[6] S. Narayan, V. Gupta, "Overview of Working of Striling Engines", Journal of Engineering Studies and Research, 21.4 (2015): 45;
[7] A. Gupta, S. Narayan, "A Review of Heat Engines, Hidraulica Magazine no 1 (2016): 67;
[8] S. Narayan, "Analysis of noise emitted from diesel engines", Journal of Physics: Conference Series, Vol. 662, no. 1. IOP Publishing, 2015;
[9] A. Gupta, S. Narayan, "Effects of turbo charging of spark ignition engines", Hidraulica Magazine no 4 (2015): 62;

[10] S. Narayan, "Designing of liquid piston fluidyne engines", Hidraulica Magazine no 2 (2015): 18;
[11] S. Narayan, “Effects of Various Parameters on Piston Secondary Motion”, No. 2015-01-0079, SAE Technical Paper, 2015;
[12] S. Narayan, "Analysis of Noise Radiated from Common Rail Diesel Engine", Tehnički glasnik 8.3 (2014): 210-213;
[13] S. Narayan, "Time-Frequency Analysis of Diesel Engine Noise", Acta Technica Corviniensis-Bulletin of Engineering 7.3 (2014): 133;
[14] S. Narayan, A. Gupta, R. Rana, "Performance analysis of liquid piston fluidyne systems", Mechanical Testing and Diagnosis, 5.2 (2015): 12;
[15] S. Narayan, V. Gupta, "Motion analysis of liquid piston engines", Journal of Engineering Studies and Research, 21.2 (2015): 71;
[16] S. Narayan, “Modeling of Noise Radiated from Engines”, No. 2015-01-0107. SAE Technical Paper, 2015;
[17] I. Sfarlea, L. Marcu, D. Banyai, "Flow through Command Hydraulic Resistance", Hidraulica Magazine no 3 (2015): 59;
[18] V. Gupta, S. Sharma, S. Narayan, "Review of working of Stirling engines", Acta Technica Corviniensis-Bulletin of Engineering, 9.1 (2016): 55;
[19] A. Singh, S. Bharadwaj, S. Narayan, "Review of how aero engines work", Tehnički glasnik 9.4 (2015): 381-387;
[20] S. Narayan, "A review of diesel engine acoustics", FME Transactions, 42.2 (2014): 150-154;
[21] S. Narayan, "Noise Optimization in Diesel Engines", Journal of Engineering Science and Technology Review, 7.1 (2014): 37-40;
[22] A. Singh, S. Bharadwaj, S. Narayan, "Analysis of Various NHV Sources of a Combustion Engine", Tehnički glasnik, 10.1-2 (2016): 29-37;
[23] X. Meng, Y. Xie, "A new numerical analysis for piston skirt–liner system lubrication considering the effects of connecting rod inertia", Tribology International, 47 (2012): 235-243;
[24] S. Narayan, et al., "A priority based exploration algorithm for path planning of an unmanned ground vehicle", Embedded Systems (ICES), 2014 International Conference IEEE, 2014.

Approaches of the Best Maintenance Strategies Applied to Hydraulic Drive Systems

PhD. stud. eng. **Alexandru-Daniel MARINESCU[1],** PhD. eng. **Teodor Costinel POPESCU[1],**
Dipl. eng. **Alina-Iolanda POPESCU[1],** Prof. PhD. eng. **Carmen-Anca SAFTA[2]**

[1] Hydraulics and Pneumatics Research Institute INOE 2000 – IHP, Bucharest, marinescu.ihp@fluidas.ro

[2] University POLITEHNICA of Bucharest, Power Engineering Faculty

Abstract: *As a consequence of global competition priority measures are necessary for a total elimination of losses and failures of hydraulic drive systems. This is the reason why the maintenance activity must be continuously improved. So, the maintenance activity must be understood more than a periodic revision to remove the damages that may occur. Many companies are not underestimating the maintenance activity and large amounts of funds are invested in maintenance management. The research activity is encouraged to develop new design methods in the reliability of hydraulic systems and in preventive and predictive maintenance. The paper extends a careful review of all maintenance strategies capable of ensuring the smooth running of hydraulic drive systems with a case study applied to an agricultural tractor.*

Keywords: *Maintenance, hydraulic system, equipment importance, total productive maintenance, environment, European directives*

1. Introduction

A hydraulic drive system can be analyzed as a black box, without knowing what it is inside but knowing who are the inputs and the outputs. Any change in the system operation is observed as a change of output parameters or the occurrence of other undesirable sizes which will oblige us to check firstly the input parameters. If the inputs do not register deviations from the operation rules of the system then the causes of mal functioning must be search in the structure of the black box system. Because a hydraulic system has a structural integrity, the system reliability is dependent on the each element reliability. These considerations must take into account when we want to manage the maintenance activity of a hydraulic system.
In our days maintenance is not a simple troubleshooting activity.
Maintenance is the act of maintaining the technical integrity and the functionality of a system as long as possible, [1, 2, and 3]. For a hydraulic system, maintenance is as an act of defence which prevents component failure and improves system reliability, [1].
There are two basic maintenance approaches: a corrective maintenance (or reactive maintenance, the mostly used to minimize the troubleshooting time response) and a preventive maintenance (or proactive maintenance suitable the best maintenance practice for hydraulic systems), [1]. The corrective maintenance performed the tasks of identification, isolation and rectification of a fault so that the failed hydraulic system can be restored to its normal operable state. The preventive maintenance is oriented to performance in order to prevent all hydraulic system failure before it occurs.
In practice there are some combinations of basic approaches that it will be discussed in the paper as a case study of the hydraulic driving mechanisms of a 90 HP agricultural tractor having the hydraulic block diagram plotted in Figure 1, [4].
The hydraulic system contains an A1VO axial piston pump with variable capacity, a steering, a steering cylinder, a priority valve, a battery of directional valves (working hydraulics) and two hydraulic cylinders. Other components are: a hitch control, a 3 point hitch, a controller, a draft sensor, a position sensor, and a control panel.

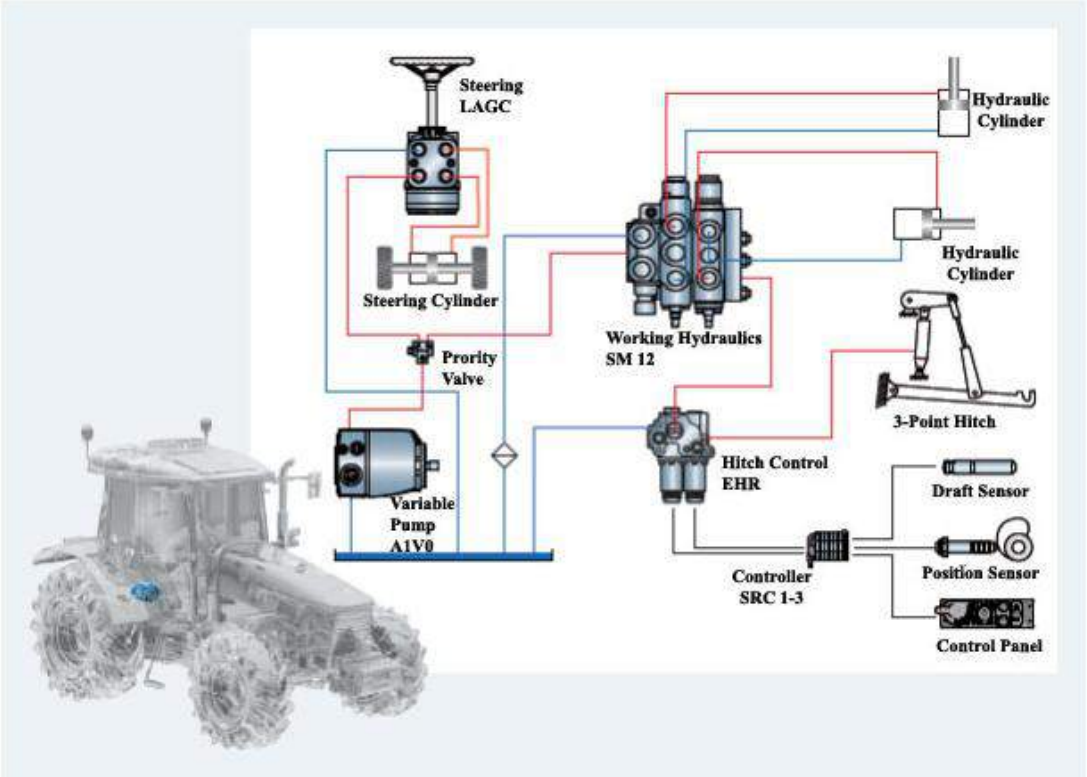

Fig. 1. Block diagram of a 90 HP agricultural tractor, [4]

In the paper maintenance types and how to choose the proper type of maintenance is presented for the 90 HP agricultural tractors. A decision tree for the maintenance strategy is presented, too, in correlation with the equipment importance factor, I.

2. Maintenance types

In Figure 2 are presented a simplified classification of maintenance types, [5]. The scheduled and unscheduled maintenance activities are the core of this classification. It is observed that even the corrective maintenance is a scheduled activity.

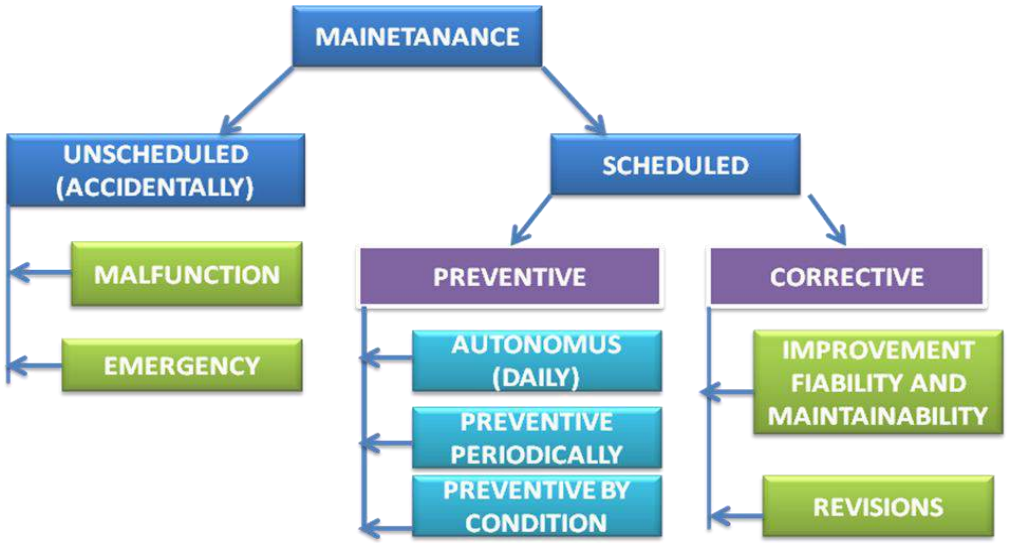

Fig. 2. Maintenance types, [5].

The unscheduled - (accidentally) maintenance are at fault, or in emergency case. The operators begin repairs after an unforeseen defect and shall restore the facility or its components in acceptable working conditions. Accidentally maintenance may be required as a result of a specific choice of the company or unscheduled, as attitude like "wait and see", [5].

The scheduled maintenance is preventive or corrective.

Preventive maintenance should be performed after predetermined criteria covering the following issues:

- ✓ defect prevention by the identification and measurement of one or more parameters;
- ✓ extrapolating the remaining time before failure, using appropriate models. The probability that the hydraulic system or a part of the system is not in acceptable operational conditions is reduced. Preventive maintenance can be done at different time periods: at regular intervals, at safe intervals, at irregular intervals, at constant time intervals, at a constant date, as a routine operation or an extraordinary one, [5].

From this point of view, ***the predictive maintenance (also called conditional maintenance)*** is performed as routine checks or continuous checks and is based on the following concepts:

- ✓ many defects do not occur instantly proper functioning;
- ✓ it is possible to identify the emergence and the evolution of defects.

In other words the plants give some warning signals before the crash. These warning signals can be defined as a potential faults. Knowing the real state of the system components, the operator will proceed by applying a rational preventive action, [5].

Corrective maintenance is a concept based by intervention on equipment after it has crashed (for example repair, partial or total change of defective equipment). Corrective maintenance is "all actions taken after the failure of equipment or after his office degradation unexpectedly", [4].

Reliability centered maintenance can be defined as a process used to determine the steps to be taken to make sure the equipment performs its function in its operational context. This maintenance concept appeals to effective methods of maintenance that helps to prevent critical failures appearance, [4].

3. The choice of maintenance type

A careful review of all maintenance strategies applied to hydraulic drive systems will follow a decision tree like in Figure 3, [4].

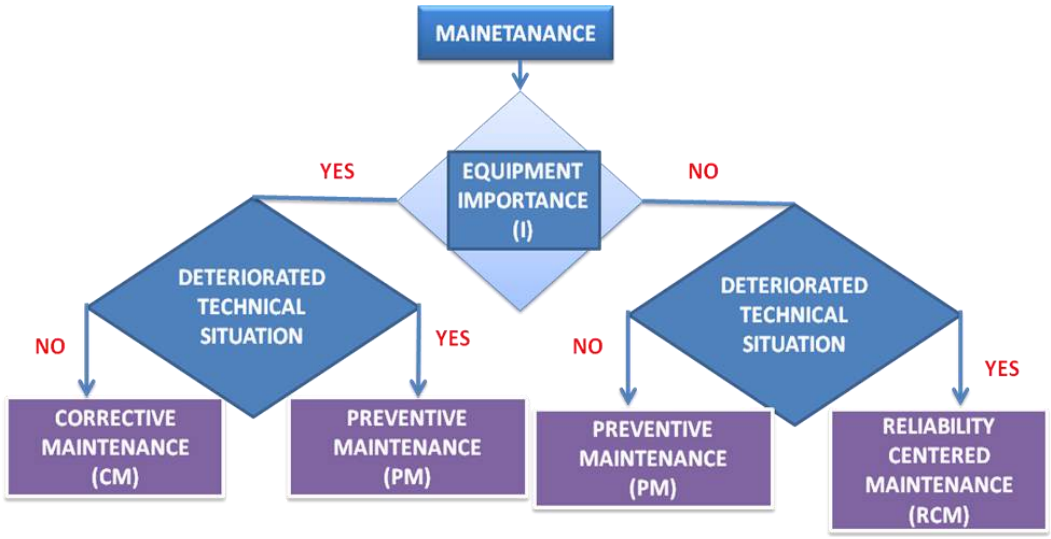

Fig. 3. Decision tree for election of the maintenace strategies

From this perspective, for the hydraulic equipment of 90 HP agricultural tractor, shown in Figure 1, the following choices are available, as in Table 1.

TABLE 1: Maintenance choices

Apparatus class	**Apparatus**	**Equipment Importance I**		**Applied type of maintenance**
		%	**Qtr (see fig. 4)**	
Execution	**Steering cylinder**	**10**	**1st**	PM, RCM
Command	**Steering**	**10**	**2nd**	PM, RCM
Execution	**Hydraulic cylinders**	**5**	**3rd**	PM, RCM
Power	**Axial piston pump with variable capacity**	**60**	**4th**	CM, PrM
Safety and distribution	**Battery of directional valves**	**10**	**5th**	PM, RCM
Safety and distribution	**Priority valve**	**5**	**6th**	PM, RCM

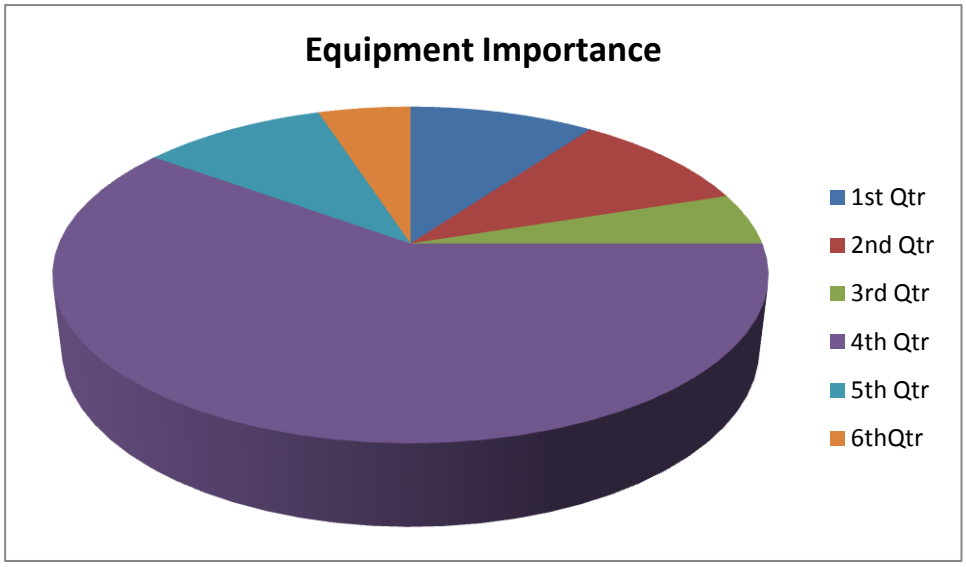

Fig. 4. Equipment importance

Each element of the hydraulic system is quantifying as function of the equipment importance (I) in the maintenance scheme and operation rules. In Figure 4 is plotted the equipment importance as percent average from the whole.

4. Total productive maintenance, an innovative concept

Total productive maintenance, TPM, is an innovative Japanese concept. The origin of TPM can be traced back to 1951 when preventive maintenance was introduced in Japan, [6].
The hydraulic drive installations are component part of many technological systems from different industries of production. Therefore, the total productive maintenance model can be successfully applied in this case.
Total productive maintenance is based on the "5S" (Sort, Set, Shine, Standardize, Sustain), [2]. The support activities of this maintenance model, and recognized as the eight pillars of total productive maintenance, "eight pillars of TPM" are presented in Figure 5 [TPM].

Fig. 5. The eight pillars of TPM, [1]

The total productive maintenance targets are available not only in machines manufactured production, [1, 7] but in hydraulic system, too. The TPM targets are, [7]:

- ✓ to obtain minimum 80% OPE, (Overall Process Effectiveness);
- ✓ to obtain minimum 90% OEE (Overall Equipment Efficiency);
- ✓ to run the machines even during lunch;
- ✓ to operate in a manner, so that there are no customer complaints;
- ✓ to reduce the manufacturing cost by 30%;
- ✓ to achieve 100% success in delivering the goods as required by the customer;
- ✓ to maintain an accident free environment;
- ✓ to develop multi-skilled and flexible workers.

5. Maintenance of work fluid and environmental protection

The maintenance of hydraulic systems of different machineries means not only the maintenance of relevant apparatus but also the maintenance of hydraulic oil, the working fluid in the system. It is estimated that about 70% of the breakdown of hydrostatic drive systems have as main cause the used hydraulic oil. The working fluid maintenance means firstly to monitor the contamination of the hydraulic used oil and the fluid leakage control, too. The importance of this maintenance transcends its purely technical aspect, it having too by produced effects a strong environmentally character. The oil leaks of fluid are not only unsightly, they are hazardous. It makes workplace floors slippery and dangerous and can also contaminate the environment. In fact, as little as a quart of oil can pollute up to 250,000 gallons of water, and it is estimated that 100 million gallons of oil are leaking annually from hydraulic systems, [8]. For this reason oil leakage occurring in plants must be removed as quickly as possible by gathering connections and/or replacing the defective seals.

Because of the work environment conditions and additives used in the hydraulic oil, after an operation period of time, any hydraulic oil loses its purity through contamination with small solid particles. Because of the hydraulic oil contamination the hydraulic system performance will decrease.

Used oil must be carefully replaced from the system and stored in special containers for recycling, compliance with environmental standards. Solid particles are highlighted with specific laboratory equipment. At INOE 2000 – IHP Bucharest, there are concerns in this regard since 2005, through the purchase of a machine type CM Laser, manufactured by Parker Company. Tests made on samples of oil may indicate the existence of impurities solid particles of different diameters.

6. European Directives and international standard protection

The maintenance activity brings together elements concerning to safety and health at work (see the last TPM pillar). For this reason, Framework Directive 89/391 /EEC, take into account the introduction of measures for the safety and health of workers at work improvement promotion. Directive 89/391/EEC fixes the basic legal and legislative framework for the adoption of special directives on minimum health and safety requirements at using by operators of protective equipment at work place, and is republished in consolidated text by Directive 2009/104/EC.
In the field of Hydraulics, we can mention "Machinery Directive 2006/42/EC", "Electromagnetic Compatibility Directive EMC 2004/108/EC", "Low Voltage Directive - 2006/95/EC", "Guidelines for explosive atmospheres ATEX 94/9/EC and IECEx Certification Scheme for Explosive atmospheres", "Pressure Equipment Directive PED 97/23 / EC ", [1]. For waste oils it was been adopted Directive 75/439/EEC.
In the year, 2007 once Romania joined to European Union, it was passed to implement the international quality standards from ISO 9000 to ISO 9004. The Romanian harmonized version ISO 9000 can be found in the standards SR EN ISO 9000.

7. Conclusions

Establishing the correct maintenance strategies are imperative when it is desired an optimal functioning of a technical system. For hydraulic drive systems, the type of maintenance can be determined depending of the component equipments importance. Besides a good knowledge of support and repair techniques by multi-skilled and flexible workers for these activities, is recommended the implementation of EU directives and international standards in the field. The direct benefits arising here are those relating to environmental protection and health of workers by ensuring the safety and reducing the number of accidents at work.

References

[1] R. Smith, K. R. Mobley, "Rules of thumb for maintenance and reliability engineers", Ed. Elsevier, 2008;
[2] S. Nakajima, „Introduction to TPM: Total Productive Maintenance", Productivity Press; 1988;
[3] S. Costinaş, "Managementul mentenanţei staţiilor electrice", Editura Electra, Bucureşti 2005;
[4] Rexroth, "A1VO Variable Axial Piston Pump: Economical load-sensing now for the smaller power classes". On: http://www.livhaven.com/pdf/A1VO-Overview.pdf;
[5] http://cefran.altervista.org/formazione/Archivio/POLITICHE_DI_MANUTENZIONE.pdf;
[6] http://reliabilityweb.com/articles/entry/total_productive_maintenance/;
[7] J. Venkatesh, "An Introduction to Total Productive Maintenance (TPM)", Plant Maintenance Resource Center, 2015, http://www.plant-maintenance.com/articles/tpm_intro.shtml;
[8] https://www.gates.com/~/media/files/gates/industrial/fluid-power/manuals/gates_fluid_power_ebook.pdf.

An Introduction to Combustion Engines

Sunny NARAYAN[1], Aman GUPTA[2]

[1] Indus University, India, sn2008@rediffmail.com

[2] Indus University, India

Abstract: *A numerical model for the skirt is studied to consider the effects of the connecting rod inertia on the piston skirt–liner system lubrication. The piston motion, the oil film lubrication model and the friction losses of the system have been studied and compared. The results on a dual cylinder diesel engine show that inertia of connecting rod also affects system lubrication as well as the piston motion, especially at higher speeds.*

Keywords: *Combustion engines*

1. Introduction

Most of the very earliest internal combustion engines of the 17th and 18th centuries can be classified as atmospheric engines. These were large engines with a single piston and cylinder, the cylinder being open on the end. Combustion was initiated in the open cylinder using any of the various fuels which were available. Gunpowder was often used as the fuel. Immediately after combustion, the cylinder would be full of hot exhaust gas at atmospheric pressure. At this time, the cylinder end was closed and the trapped gas was allowed to cool. As the gas cooled, it created a vacuum within the cylinder. This caused a pressure differential across the piston, atmospheric pressure on one side and a vacuum on the other. As the piston moved because of this pressure differential, it would do work by being connected to an external system, such as raising a weight [1]. Some early steam engines also were atmospheric engines. Instead of combustion, the open cylinder was filled with hot steam. The end was then closed and the steam was allowed to cool and condense [2]. This created the necessary vacuum. In addition to a great amount of experimentation and development in Europe and the United States during the middle and latter half of the 1800s [3], two other technological occurrences during this time stimulated the emergence of the internal combustion engine.

In 1859, the discovery of crude oil in Pennsylvania finally made available the development of reliable fuels which could be used in these newly developed engines. Up to this time, the lack of good, consistent fuels was a major drawback in engine development [4]. Fuels like whale oil, coal gas, mineral oils, coal, and gun powder which were available before this time were less than ideal for engine use and development. It still took many years before products of the petroleum industry evolved from the first crude oil to gasoline, the automobile fuel of the 20th century [5]. However, improved hydrocarbon products began to appear as early as the 1860s and gasoline, lubricating oils, and the internal combustion engine evolved together [6]. The second technological invention that stimulated the development of the internal combustion engine was the pneumatic rubber tire, which was first marketed by John B. Dunlop in 1888 [7]. This invention made the automobile much more practical and desirable and thus generated a large market for propulsion systems, including the internal combustion engine [8]. During the early years of the automobile, the internal combustion engine competed with electricity and steam engines as the basic means of propulsion. Early in the 20th century, electricity and steam faded from the automobile picture—electricity because of the limited range it provided, and steam because of the long start-up time needed.

Thus, the 20th century is the period of the internal combustion engine and the automobile powered by the internal combustion engine as shown in figures no 1,2,3 [9]. At the end of the century, the internal combustion engine was again being challenged by electricity and other forms of propulsion systems for automobiles and other applications [10].

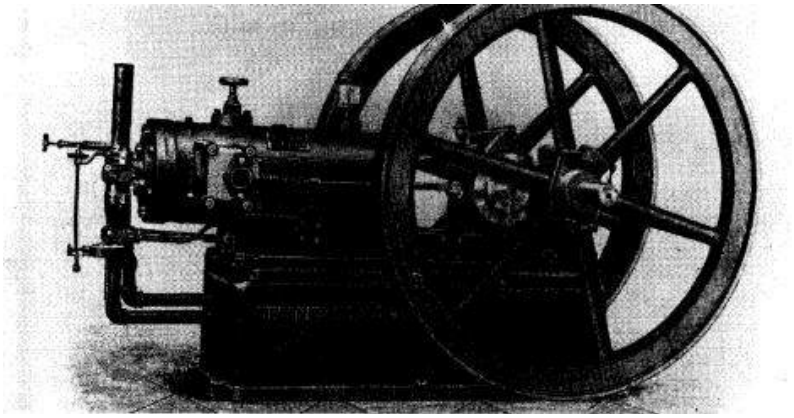

Fig. 1. Charter Engine

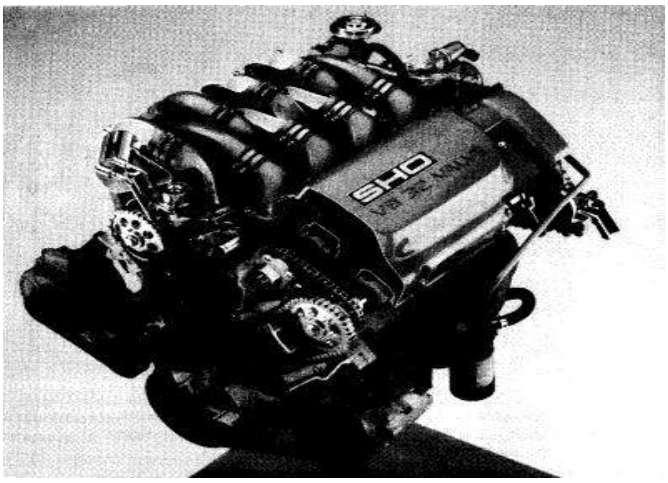

Fig. 2. Ford Engine

During the second half of the 19th century, many different styles of internal combustion engines were built and tested [11]. These engines operated with variable success and dependability using many different mechanical systems and engine cycles. The first fairly practical engine was invented by J. J. E. Lenoir [12]. During the next decade, several hundred of these engines were built with power up to about 4.5 kW (6 hp) and mechanical efficiency up to 5%.

In 1867, the Otto-Langen engine, with efficiency improved to about 11%, was first introduced, and several thousand of these were produced during the next decade. This was a type of atmospheric engine with the power stroke propelled by atmospheric pressure acting against a vacuum [13]. During this time, engines operating on the same basic four-stroke cycle as the modern automobile engine began to evolve as the best design. Although many people were working on four-stroke cycle design, Otto was given credit when his prototype engine was built in 1876 [14]. In the 1880s the internal combustion engine first appeared in automobiles [15].

Also in this decade the two-stroke cycle engine became practical and was manufactured in large numbers. By 1892, Rudolf Diesel had perfected his compression ignition engine into basically the same diesel engine known today. This was after years of development work which included the use of solid fuel in his early experimental engines [16].

Early compression ignition engines were noisy, large, slow, single-cylinder engines. They were, however, generally more efficient than spark ignition engines. It was not until the 1920s that multi-cylinder compression ignition engines were made small enough to be used with automobiles and trucks [17].

2. Classifications [18]

Internal combustion engines can be classified in a number of different ways:

1. Types of Ignition (a) Spark Ignition (SI). An SI engine starts the combustion process in each cycle by use of a spark plug. The spark plug gives a high-voltage electrical discharge between two electrodes which ignites the air-fuel mixture in the combustion chamber surrounding the plug. In early engine development, before the invention of the electric spark plug, many forms of torch holes were used to initiate combustion from an external flame. (b) Compression Ignition (CI). The combustion process in a CI engine starts when the air-fuel mixture self-ignites due to high temperature in the combustion chamber caused by high compression.

2. Engine Cycle (a) Four-Stroke Cycle. A four-stroke cycle experiences four piston movements over two engine revolutions for each cycle. (b) Two-Stroke Cycle. A two-stroke cycle has two piston movements over one revolution for each cycle.

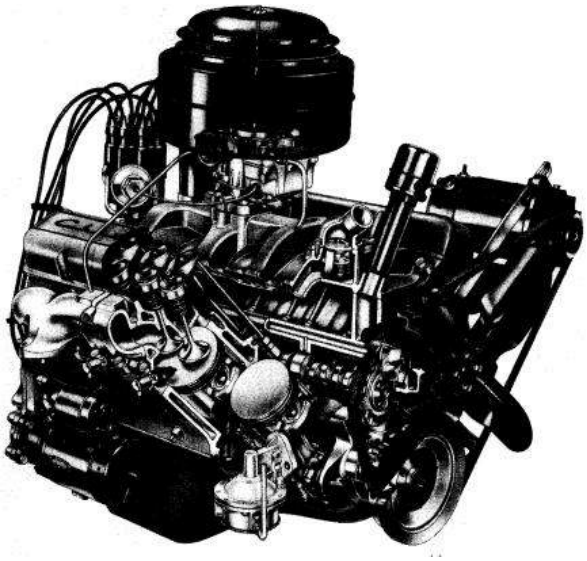

Fig. 3. Chevrlot Engine

Three-stroke cycles and six-stroke cycles were also tried in early engine development [19].

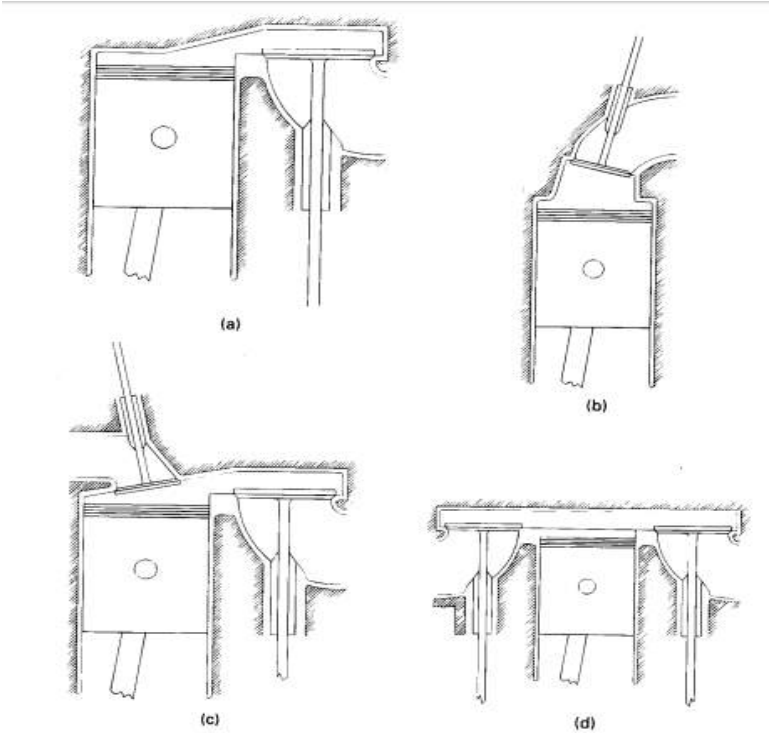

Fig. 4. Engine classification by valve location

3. Valve Location [20] – As seen from figure no 4, (a) Valves in head (overhead valve), also called I Head engine. (b) Valves in block (flat head), also called L Head engine. Some historic engines with valves in block had the intake valve on one side of the cylinder and the exhaust valve on the other side. These were called T Head engines. (c) One valve in head (usually intake) and one in block, also called F Head engine; this is much less common.
4. Design of Engine [21] – (a) Reciprocating. Engine has one or more cylinders in which pistons reciprocate back and forth. The combustion chamber is located in the closed end of each cylinder. Power is delivered to a rotating output crankshaft by mechanical linkage with the pistons. (b) Rotary-Engine is made of a block (stator) built around a large nonconcentric rotor and crankshaft. The combustion chambers are built into the nonrotating block.
5. Position and Number of Cylinders of Reciprocating Engines [18] – As seen from figure no 5 various systems can be:
(a) Single Cylinder. Engine has one cylinder and piston connected to the crankshaft.
(b) In-Line-Cylinders are positioned in a straight line, one behind the other along the length of the crankshaft. They can consist of 2 to 11 cylinders or possibly more. In-line four-cylinder engines are very common for automobile and other applications. In-line six and eight cylinders are historically common automobile engines. In-line engines are sometimes called straight (e.g., straight six or straight eight).
(c) V Engine – Two banks of cylinders at an angle with each other along a single crankshaft. The angle between the banks of cylinders can be anywhere from 15° to 120°, with 60°-90° being common. V engines have even numbers of cylinders from 2 to 20 or more. V6s and V8s are common automobile engines, with V12s and V16s (historic) found in some luxury and high-performance vehicles.
(d) Opposed Cylinder Engine – Two banks of cylinders opposite each other on a single crankshaft (a V engine with a 180°V). These are common on small aircraft and some automobiles with an even number of cylinders from two to eight or more. These engines are often called flat engines (e.g., flat four).

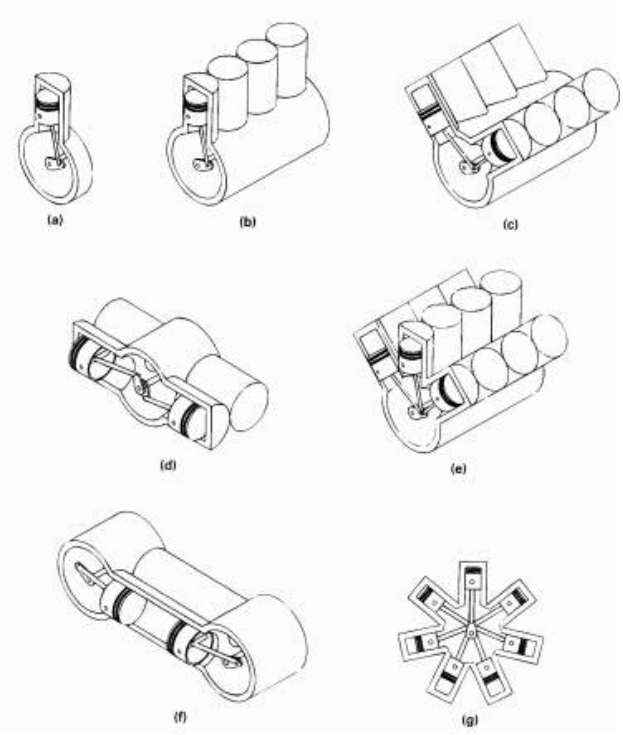

Fig. 5. Various engine arrangements a-Single, b-In line, c-V block, d-Opposed cylinder, e-W type, f-opposed piston, g-Radial

(e) W Engine-Same as a V engine except with three banks of cylinders on the same crankshaft. These are not common, but some have been developed for racing automobiles, both modern and historic. Usually 12 cylinders with about a 60° angle between each bank.
(f) Opposed Piston Engine – Two pistons in each cylinder with the combustion chamber in the center between the pistons. A single-combustion process causes two power strokes at the same time, with each piston being pushed away from the center and delivering power to a separate crankshaft at each end of the cylinder. Engine output is either on two rotating crankshafts or on one crankshaft incorporating complex mechanical linkage.
(g) Radial Engine – Engine with pistons positioned in a circular plane around the central crankshaft. The connecting rods of the pistons are connected to a master rod which, in turn, is connected to the crankshaft. A bank of cylinders on a radial engine always has an odd number of cylinders ranging from 3 to 13 or more. Operating on a four-stroke cycle, every other cylinder fires and has a power stroke as the crankshaft rotates, giving a smooth operation. Many medium- and large-size propeller-driven aircraft use radial engines. For large aircraft, two or more banks of cylinders are mounted together, one behind the other on a single crankshaft, making one powerful, smooth engine. Very large ship engines exist with up to 54 cylinders, six banks of 9 cylinders each.

3. Engine components [22]

The following is a list of major components found in most reciprocating internal combustion engines, as shown in figure no 6.
a. Block – Body of engine containing the cylinders, made of cast iron or aluminum. In many older engines, the valves and valve ports were contained in the block. The block of water-cooled engines includes a water jacket cast around the cylinders. On air-cooled engines, the exterior surface of the block has cooling fins.
b. Camshaft [22] – Rotating shaft used to push open valves at the proper time in the engine cycle, either directly or through mechanical or hydraulic linkage (push rods, rocker arms, tappets). Most modern automobile engines have one or more camshafts mounted in the engine head (overhead cam). Most older engines had camshafts in the crankcase. Camshafts are generally made of forged steel or cast iron and are driven off the crankshaft by means of a belt or chain (timing chain). To reduce weight, some cams are made from a hollow shaft with the cam lobes press-fit on. In four-stroke cycle engines, the camshaft rotates at half engine speed.
c. Carburetor [24] – Venturi flow device which meters the proper amount of fuel into the air flow by means of a pressure differential. For many decades it was the basic fuel metering system on all automobile (and other) engines. It is still used on low-cost small engines like lawn mowers but is uncommon on new automobiles. Catalytic converter Chamber mounted in exhaust flow containing catalytic material that promotes reduction of emissions by chemical reaction.
d. Combustion chamber [25] – The end of the cylinder between the head and the piston face where combustion occurs. The size of the combustion chamber continuously changes from a minimum volume when the piston is at TDC to a maximum when the piston is at BDC. The term "cylinder" is sometimes synonymous with "combustion chamber" (e.g., "the engine was firing on all cylinders"). Some engines have open combustion chambers which consist of one chamber for each cylinder. Other engines have divided chambers which consist of dual chambers on each cylinder connected by an orifice passage. Connecting rod – Rod connecting the piston with the rotating crankshaft, usually made of steel or alloy forging in most engines but may be aluminum in some small engines.
e. Connecting rod bearing [26] – Bearing where connecting rod fastens to crankshaft. Cooling fins – Metal fins on the outside surfaces of cylinders and head of an air cooled engine. These extended surfaces cool the cylinders by conduction and convection.
f. Crankcase [27] – Part of the engine block surrounding the rotating crankshaft. In many engines, the oil pan makes up part of the crankcase housing. Crankshaft – Rotating shaft through which engine work output is supplied to external systems. The crankshaft is connected to the engine block with the main bearings. It is rotated by the reciprocating pistons through connecting rods connected to the crankshaft, offset from the axis of rotation. This offset is sometimes called

crank throw or crank radius. Most crankshafts are made of forged steel, while some are made of cast iron.

g. Cylinders [28] – The circular cylinders in the engine block in which the pistons reciprocate back and forth. The walls of the cylinder have highly polished hard surfaces. Cylinders may be machined directly in the engine block, or a hard metal (drawn steel) sleeve may be pressed into the softer metal block. Sleeves may be dry sleeves, which do not contact the liquid in the water jacket, or wet sleeves, which form part of the water jacket. In a few engines, the cylinder walls are given a knurled surface to help hold a lubricant film on the walls. In some very rare cases, the cross section of the cylinder is not round.

h. Exhaust manifold [29] – Piping system which carries exhaust gases away from the engine cylinders, usually made of cast iron. Exhaust system – Flow system for removing exhaust gases from the cylinders, treating them, and exhausting them to the surroundings. It consists of an exhaust manifold which carries the exhaust gases away from the engine, a thermal or catalytic converter to reduce emissions, a muffler to reduce engine noise, and a tailpipe to carry the exhaust gases away from the passenger compartment.

i. Fan [31] – Most engines have an engine-driven fan to increase air flow through the radiator and through the engine compartment, which increases waste heat removal from the engine. Fans can be driven mechanically or electrically, and can run continuously or be used only when needed.

j. Flywheel [30] – Rotating mass with a large moment of inertia connected to the crankshaft of the engine. The purpose of the flywheel is to store energy and furnish a large angular momentum that keeps the engine rotating between power strokes and smooths out engine operation. On some aircraft engines the propeller serves as the flywheel, as does the rotating blade on many lawn mowers.

k. Fuel injector [31] – A pressurized nozzle that sprays fuel into the incoming air on SI engines or into the cylinder on CI engines. On SI engines, fuel injectors are located at the intake valve ports on multipoint port injector systems and upstream at the intake manifold inlet on throttle body injector systems. In a few SI engines, injectors spray directly into the combustion chamber. Fuel pump – Electrically or mechanically driven pump to supply fuel from the fuel tank (reservoir) to the engine. Many modern automobiles have an electric fuel pump mounted submerged in the fuel tank. Some small engines and early automobiles had no fuel pump, relying on gravity feed.

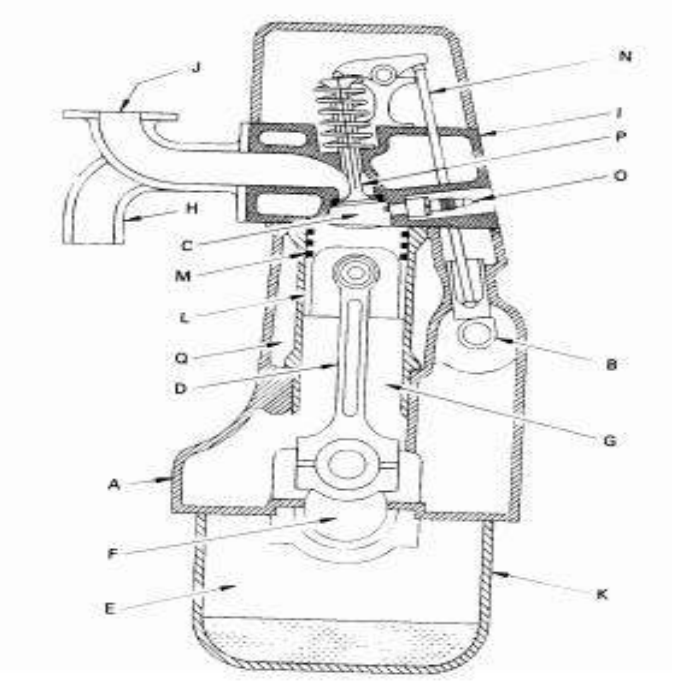

Fig. 6. Parts of Engine – Cross section of four-stroke cycle S1 engine showing engine components; (A) block, (B) camshaft, (C) combustion chamber, (D) connecting rod, (E) crankcase, (F) crankshaft, (G) cylinder, (H) exhaust manifold, (I) head, (J) intake manifold, (K) oil pan, (L) piston, (M) piston rings, (N) push rod, (0) spark plug, (P) valve, (Q) water jacket.

l. Glow plug – Small electrical resistance heater mounted inside the combustion chamber of many CI engines, used to preheat the chamber enough so that combustion will occur when first starting a cold engine. The glow plug is turned off after the engine is started.

m. Head – The piece which closes the end of the cylinders, usually containing part of the clearance volume of the combustion chamber. The head is usually cast iron or aluminum, and bolts to the engine block. In some less common engines, the head is one piece with the block. The head contains the spark plugs in SI engines and the fuel injectors in CI engines and some SI engines. Most modern engines have the valves in the head, and many have the camshaft(s) positioned there also (overhead valves and overhead cam).

n. Head gasket – Gasket which serves as a sealant between the engine block and head where they bolt together. They are usually made in sandwich construction of metal and composite materials. Some engines use liquid head gaskets. Intake manifold – Piping system which delivers incoming air to the cylinders, usually made of cast metal, plastic, or composite material. In most SI engines, fuel is added to the air in the intake manifold system either by fuel injectors or with a carburetor. Some intake manifolds are heated to enhance fuel evaporation. The individual pipe to a single cylinder is called a runner.

o. Main bearing– The bearings connected to the engine block in which the crankshaft rotates. The maximum number of main bearings would be equal to the number of pistons plus one, or one between each set of pistons plus the two ends. On some less powerful engines, the number of main bearings is less than this maximum.

p. Oil pan – Oil reservoir usually bolted to the bottom of the engine block, making up part of the crankcase. Acts as the oil sump for most engines.

q. Oil pump – Pump used to distribute oil from the oil sump to required lubrication points. The oil pump can be electrically driven, but is most commonly mechanically driven by the engine. Some small engines do not have an oil pump and are lubricated by splash distribution. Oil sump – Reservoir for the oil system of the engine, commonly part of the crankcase. Some engines (aircraft) have a separate closed reservoir called a dry sump.

r. Piston – The cylindrical-shaped mass that reciprocates back and forth in the cylinder, transmitting the pressure forces in the combustion chamber to the rotating crankshaft. The top of the piston is called the crown and the sides are called the skirt. The face on the crown makes up one wall of the combustion chamber and may be a flat or highly contoured surface. Some pistons contain an indented bowl in the crown, which makes up a large percentage of the clearance volume. Pistons are made of cast iron, steel, or aluminum. Iron and steel pistons can have sharper corners because of their higher strength. They also have lower thermal expansion, which allows for tighter tolerances and less crevice volume.

Aluminum pistons are lighter and have less mass inertia. Sometimes synthetic or composite materials are used for the body of the piston, with only the crown made of metal. Some pistons have a ceramic coating on the face.

s. Piston rings – Metal rings that fit into circumferential grooves around the piston and form a sliding surface against the cylinder walls. Near the top of the p usually two or more compression rings made of highly polished hard chrome steel. The purpose of these is to form a seal between the piston and cylinder walls and to restrict the high-pressure gases in the combustion chamber from leaking past the piston into the crankcase (blowby). Below the compression rings on the piston is at least one oil ring, which assists in lubricating the cylinder walls and scrapes away excess oil to reduce oil consumption.

t. Push rods – Mechanical linkage between the camshaft and valves on overhead valve engines with the camshaft in the crankcase. Many push rods have oil passages through their length as part of a pressurized lubrication system. Radiator – Liquid-to-air heat exchanger of honeycomb construction used to remove heat from the engine coolant after the engine has been cooled.

The radiator is usually mounted in front of the engine in the flow of air as the automobile moves forward. An engine-driven fan is often used to increase air flow through the radiator.

u. Spark plug – Electrical device used to initiate combustion in an SI engine by creating a high-voltage discharge across an electrode gap. Spark plugs are usually made of metal

surrounded with ceramic insulation. Some modern spark plugs have built-in pressure sensors which supply one of the inputs into engine control. Speed control; cruise control – Automatic electric-mechanical control system that keeps the automobile operating at a constant speed by controlling engine speed. Starter – Several methods are used to start IC engines. Most are started by use of an electric motor (starter) geared to the engine flywheel. Energy is supplied from an electric battery. On some very large engines, such as those found in large tractors and construction equipment, electric starters have inadequate power, and small IC engines are used as starters for the large IC engines. First the small engine is started with the normal electric motor, and then the small engine engages gearing on the flywheel of the large engine, turning it until the large engine starts. Early aircraft engines were often started by hand spinning the propeller, which also served as the engine flywheel. Many small engines on lawn mowers and similar equipment are hand started by pulling a rope wrapped around a pulley connected to the crankshaft. Compressed air is used to start some large engines. Cylinder release valves are opened, which keeps the pressure from increasing in the compression strokes. Compressed air is then introduced into the cylinders, which rotates the engine in a free-wheeling mode. When rotating inertia is established, the release valves are closed and the engine is fired.

v. Supercharger– Mechanical compressor powered off of the crankshaft, used to compress incoming air of the engine. Valve is mounted at the upstream end of the intake system, used to control the amount of air flow into an SI engine. Some small engines and stationary constant-speed engines have no throttle.

w. Turbocharger Turbine – Compressor used to compress incoming air into the engine. The turbine is powered by the exhaust flow of the engine and thus takes very little useful work from the engine.

x. Valves – Used to allow flow into and out of the cylinder at the proper time in the cycle. Most engines use poppet valves, which are spring loaded closed and pushed open by camshaft action. Valves are mostly made of forged steel. Surfaces against which valves close are called valve seats and are made of hardened steel or ceramic. Rotary valves and sleeve valves are sometimes used, but are much less common. Many two-stroke cycle engines have ports (slots) in the side of the cylinder walls instead of mechanical valves.

y. Water jacket – System of liquid flow passages surrounding the cylinders, usually constructed as part of the engine block and head. Engine coolant flows through the water jacket and keeps the cylinder walls from overheating. The coolant is usually a water-ethylene glycol mixture.

z. Water pump – Pump used to circulate engine coolant through the engine and radiator. It is usually mechanically run off of the engine. Wrist pin – Pin fastening the connecting rod to the piston (also called the piston pin).

References

[1] C. Tung Simon, M.L. McMillan, "Automotive tribology overview of current advances and challenges for the future", Tribology International 2004; 37:517–35;

[2] D.F. Li, S.M. Rhode, H.A. Ezzat, "An automotive piston lubrication model", ASLE Transactions 1983; 26(2):151–60 ;

[3] V.W. Wong, T. Tian, H. Lang, J.P. Ryan, Y. Sekiya, Y. Kobayashi, et al., "A numerical model of piston secondary motion and piston slap in partially flooded elasto hydrodynamic skirt lubrication", SAE paper no. 940696, 1994;

[4] S. Jiang, J. Cho, "Effects of skirt profiles on the piston secondary movements by the lubrication behaviors", International Journal of Automotive Technology 2004; 5(1):23–31;

[5] A. Gupta, S. Narayan, "Electrical Analogy of Liquid Piston Stirling Engines", Hidraulica Magazine no 2 (2016): 58;

[6] S. Narayan, V. Gupta, "Overview of Working of Striling Engines", Journal of Engineering Studies and Research, 21.4 (2015): 45;

[7] A. Gupta, S. Narayan, "A Review of Heat Engines, Hidraulica Magazine no 1 (2016): 67;

[8] S. Narayan, "Analysis of noise emitted from diesel engines", Journal of Physics: Conference Series, Vol. 662, no. 1. IOP Publishing, 2015;

[9] A. Gupta, S. Narayan, "Effects of turbo charging of spark ignition engines", Hidraulica Magazine no 4 (2015): 62;

[10] S. Narayan, "Designing of liquid piston fluidyne engines", Hidraulica Magazine no 2 (2015): 18;

[11] S. Narayan, “Effects of Various Parameters on Piston Secondary Motion”, No. 2015-01-0079, SAE Technical Paper, 2015;
[12] S. Narayan, "Analysis of Noise Radiated from Common Rail Diesel Engine", Tehnički glasnik 8.3 (2014): 210-213;
[13] S. Narayan, "Time-Frequency Analysis of Diesel Engine Noise", Acta Technica Corviniensis-Bulletin of Engineering 7.3 (2014): 133;
[14] S. Narayan, "Wavelet Analysis of Diesel Engine Noise", Journal of Engineering and Applied Sciences 8.8 (2013): 255-259;
[15] S. Narayan, V. Gupta, "Motion analysis of liquid piston engines", Journal of Engineering Studies and Research 21.2 (2015): 71;
[16] S. Narayan, “Modeling of Noise Radiated from Engines”, No. 2015-01-0107. SAE Technical Paper, 2015;
[17] S. Narayan, A. Gupta, R. Rana, "Performance analysis of liquid piston fluidyne systems", Mechanical Testing and Diagnosis, 5.2 (2015): 12;
[18] V. Gupta, S. Sharma, S. Narayan, "Review of working of Stirling engines", Acta Technica Corviniensis-Bulletin of Engineering, 9.1 (2016): 55;
[19] A. Singh, S. Bharadwaj, S. Narayan, "Review of how aero engines work", Tehnički glasnik 9.4 (2015): 381-387;
[20] S. Narayan, "A review of diesel engine acoustics", FME Transactions, 42.2 (2014): 150-154;
[21] S. Narayan, "Noise Optimization in Diesel Engines", Journal of Engineering Science and Technology Review, 7.1 (2014): 37-40;
[22] A. Singh, S. Bharadwaj, S. Narayan, "Prikaz rada motora zrakoplova", Tehnički glasnik 9.4 (2015): 381-387;
[23] X. Meng, Y. Xie, "A new numerical analysis for piston skirt–liner system lubrication considering the effects of connecting rod inertia", Tribology International, 47 (2012): 235-243;
[24] S. Narayan, A. Gupta, "A geometrical model of piston-liner system", Hidraulica Magazine no. 3 (2016): 52-59;
[25] A. Gupta, S. Narayan, "Electrical Analogy of Liquid Piston Stirling Engines", Hidraulica Magazine no. 2 (2016): 58;
[26] S. Bharadwaj, A. Gupta, S. Narayan, "A Review of Various NVH Sources of Combustion Engines", International Journal of Mechanical Engineering and Automation 3.6 (2016): 249-261;
[27] A. Gupta, S. Narayan, "A Review of Heat Engines", Hidraulica Magazine no. 1 (2016): 67;
[28] A. Singh, S. Bharadwaj, S. Narayan, "Analysis of Various NHV Sources of a Combustion Engine", Tehnički glasnik, 10.1-2 (2016): 29-37;
[29] A. Gupta, S. Sharma, S. Narayan, "Liquid Piston Engines" (2016): 300. [31];
[30] A. Gupta, S. Sharma, S. Narayan, "Combustion Engines. An Introduction to Their Design, Performance, and Selection" (2016): 272;
[31] S. Bharadwaj, A. Gupta S. Narayan, "Effects of Turbocharging in a S.I. Engine", International Journal of Mechanical Engineering and Automation 3.3 (2016): 107-113.